TÉCNICO LISBOA

Bone Remodeling Analysis After Total Ankle Arthroplasty

Ana Margarida Martins Barata

Thesis to obtain the Master of Science Degree in

Biomedical Engineering

Supervisors: Prof. Paulo Rui Alves Fernandes

Prof. João Orlando Marques Gameiro Folgado

Examination Committee

Chairperson: Prof. Cláudia Alexandra Martins Lobato da Silva

Supervisor: Prof. Paulo Rui Alves Fernandes

Member of the Committee: Prof. José Arnaldo Pereira Leite Miranda Guedes

December 2014

Abstract

To treat arthrodesis, in the ankle joint, there are several treatments, and one of these procedures is the total ankle arthroplasty (TAA), which does not demonstrate the same success rate of the arthroplasties performed in other joints, such as the knee, shoulder and, more frequently, the hip joints. This way, the main goal of the present work is the analysis of bone remodeling, after the introduction of two prostheses, the Agility™ and S.T.A.R.™, thanks to a bone remodeling model, developed in IDMEC/IST. To use the bone remodeling model, a finite element (FE) model of the ankle joint complex (AJC) is developed. The bone remodeling analysis is performed for three models: the intact model of the AJC, and for two combined models, the TAA+Agility™ and the TAA+S.T.A.R.™.

To achieve the goal of this work, the three FE modeling are performed. Then, the bone density distribution was obtained thanks to the mentioned bone remodeling model. The bone remodeling was analysed in two bones, the tibia and talus, and using different input parameters, that were tested.

Observing the results, the bone remodeling analysis allowed to conclude that the insertion of both prostheses leads to the occurrence of stress shielding effect. That was also obtained information about the effects of the values of two parameters, k and m, thanks to the analyses of bone mass volume and compliance. The optimal solutions were achiever, since the minimization of compliance was verified. The prostheses have some unverified characteristics and the optimal configuration is not found yet.

Keywords: Agility™, Ankle joint complex, Bone remodeling, Finite element method, S.T.A.R.™, Total ankle arthroplasty.

Resumo

Para tratar a artrodese, na articulação do tornozelo, existem vários tratamentos, e um desses procedimentos é a artroplastia total do tornozelo (AAT), que não demonstra a taxa de sucesso das artroplastias realizadas em outras articulações, como o joelho, ombro e, mais frequentemente, as articulações do quadril. Assim, o principal objetivo do presente trabalho é a análise da remodelação óssea, após a introdução de duas próteses, Agility™ e STAR™, graças ao modelo desenvolvido no IDMEC/IST. Para usar o modelo de remodelação óssea, um modelo de elementos finitos do complexo articular do tornozelo é desenvolvido. A análise de remodelação óssea é realizada em três modelos: no modelo intacto do referido complexo, e nos dois modelos combinados, AAT+Agility™ e AAT+STAR™.

Para atingir o objetivo deste trabalho, a modelação de três modelos de elementos finitos é executada. Em seguida, a distribuição da densidade óssea foi obtida graças ao modelo remodelação óssea. A remodelação óssea foi analisada em dois ossos, tíbia e tálus, e utilizando diferentes parâmetros de entrada, que foram testados.

Observando os resultados, concluiu-se que a inserção das duas próteses leva à ocorrência do efeito de blindagem. Também foi obtida informação sobre os efeitos dos valores de dois parâmetros, *k* e *m*, graças às análises do volume da massa óssea e do trabalho das forças aplicadas. As soluções óptimas foram obtidas, pois verificou-se a minimização do trabalho das forças aplicadas. As próteses ainda têm características não verificadas e a configuração ideal das mesmas ainda não foi encontrada.

Palavras-chave: Agility™, Artroplastia total do tornozelo, Complexo articular do tornozelo, Método de elementos finitos, Remodelação óssea, S.T.A.R.™.

Acknowledgments

Firstly, I would like to thank my supervisors, Prof. Paulo Fernandes and Prof. João Folgado.

Prof. Paulo Fernandes has helped me every time that I asked for something, suggesting approaches and always given a background of everything, to clarify and foment my interest. His lessons promoted my interest in this area, unknown for me until them.

Regarding the Prof. João Folgado, he gave me guidance when the doubts appeared, contributing for the understanding of the operation of several issues.

I am very grateful to Daniela, who was also available for me, and is the prove that girls are not measured by feet.

I want to thank to Carlos Quental, for his patient and for the sharing of his knowledge, which was very helpful.

I am grateful to my parents, for their friendship and companionship during all my life, doing every thing for my happiness. I want to thank to Mariana too, for being my other half, more than a sister.

I am also grateful to my best friend for more than 10 years, Helena that knows me like nobody and also supports me in everything.

I want to thanks to Teresa, Carolina and Marília, for the companionship through these months, with a certain that we created a friendship for life.

I am grateful to Priscilla, for supporting me during the last months. Her friendship helped to overcome the last difficulties.

Finally, I also want to thank to Rini, Mafalda, Beta and Grandma. Without you, life was not so funny.

Content

List of figures

List of tables

List of symbols

$\boldsymbol{a}$, $\boldsymbol{a_i}$	Microstructure parameters
$\boldsymbol{a_i^e}$	Microstructure parameters of the finite node *e*
$(\boldsymbol{a_i^e})^{\boldsymbol{k}}$	Microstructure parameters of the finite node *e* at the *k*th iteration
$\boldsymbol{d}$	Step length of the optimization process
$\boldsymbol{e_{ij}}$, $\boldsymbol{e_{kl}}$	Strain field
$\boldsymbol{E}$	Young's modulus
E_{ijkl}^H	Homogenized material properties tensor
$\boldsymbol{k}$	Biologic parameter, metabolic cost of maintaining bone tissue
K	Iteration number
m	Biologic parameter, corrective factor for the preservation of the intermediate densities
NC	Number of load cases
P	Index of load case
u^P, u_i^P	Displacement for load case *P*
v^P, v_i^P	Virtual displacement for load case *P*
α^P	Weight factor of the load *P*
$\boldsymbol{v}$	Poisson's coefficient
Γ	Surface of the body
Γ_u	Surface where the body is fixed
μ	Relative density
$\boldsymbol{\theta}, \boldsymbol{\theta_i}$	Euler angles
Ω	Volume of the body (domain)

List of acronyms

AJC	Ankle Joint Complex
ATaFi	Anterior Talofibular
ATiFi	Anterior or Anteroinferior Tibiofibular
BMU	Basic Multicellular Unit
BW	Body Weight
CaFi	Calcaneofibular
Co-Cr	Cobalt-Chromium
Co-Cr-Mo	Cobalt-Chromium-Molybdenum
CT	Computed Tomography
DATiTa	Deep Anterior Tibiotalar
DPTiTa	Deep Posterior Tibiotalar
FE	Finite Element
FEA	Finite Element Analysis
FEM	Finite Element Method
FDA	Food and Drug Administration
GRF	Ground Reaction Forces
ITiFi	Interosseous Tibiofibular
LCL	Lateral Collateral Ligaments
MCL	Medial Collateral Ligaments
OA	Osteoarthritis
PTaFi	Posterior Talofibular
PTiFi	Posterior or Posteroinferior Tibiofibular
PTA	Post-Traumatic Arthritis
RP	Reference Point
SS	Stainless Steel
SPTiTa	Superficial Posterior Tibiotalar

SLC	Syndesmotic Ligament Complex
3-D	Three-Dimensional
TiCa	Tibiocalcaneal
TiNa	Tibionavicular
TiS	Tibiospring
Ti	Titanium
TAA	Total Ankle Arthroplasty
UHMWPE	Ultra-High-Molecular-Weight Polyethylene

1. Introduction

1.1. Motivation

Despite most of the times the foot not being considered a central part of the body, it has a great importance, allowing all movements that characterize our day-to-day, such as walk, jump, run, among others. The foot is considered the basis of the body and has a fundamental role in the balance of the body. One of the main joints existent on the foot is the ankle joint, playing a hinge role between the leg and foot. This region of meeting between the leg and foot enables the transference of load among these two components of the lower limb. The ankle joint is a complex structure, due to many factors, such as its anatomy, its mechanics, the materials that a characterize it (the cartilage), and so on. These characteristics make the ankle serve various functions, beyond those mentioned: it absorbs the impact promoted for each step during the movement, and withstands, also during the movement, the high mechanical strains and stresses [1].

The greatest part of the problems associated with the disruption of the ankle's function are related to the arthritis. Like it will be exposed below, this pathology is related with the destruction of the articular cartilage, that convers the articular surfaces of bones, and which good condition is central to protect the joint and enable the smooth movement between bones, despising the friction associated to the contact among bones [2]. The arthritis manifests itself in different types, due to different causes [3], as it is possible to see below:

- Osteoarthritis (OA) is one of the two most common types of arthritis, it is also known as primary OA [2] and it will be explained below;
- Rheumatoid arthritis is the other most common type of arthritis and it is a disorder in systemic level. When it is verified, the immune system of the body incorrectly attacks healthy tissue, leading to the possible inflammation of membranes, cartilage and bone [2, 4];
- Post-traumatic arthritis (PTA) is also known as secondary OA. It happens when fracture, ligament injury or severe sprain are verified [2].

Arthritis is the term given to a set of more than one hundred of diseases and affects millions of people. It involves the joint inflammation and swelling as well as around the joint and surrounding soft tissues. Some of the consequences of this inflammation are the felt pain and stiffness. It is verified in many types of arthritis the progressive joint deterioration and the cartilage in joints is gradually lost. These events lead to the rubbing and wearing between bones and the soft tissues existent in the joint also may start to suffer wearing. This clinical condition can be painful and promote limited movement, deformities in the joints, and the loss of the joint function. [2] Nowadays, the arthritis is more prevalent, as a cause of activity limitations, than cancer, diabetes or heart disease. Some of the injuries that affect the ankle joint complex (AJC) are due to the extreme sport activity [5], others are due to the evolution of lateral ligament injuries to chronic instability [6]. Currently, there are two types of solutions/treatments for arthritis, which

are classified by if it is surgical or not. The first type mentioned, the surgical solution, is the most effective and comprises the total ankle arthroplasty (TAA) and the ankle arthrodesis. The other type is not very effective and it is common to fail, because it does not reduce the pain [7].

OA is the most common type of arthritis. It is also known as "wear-and-tear" arthritis, degenerative joint disease or age-related arthritis. Like it was possible to verify by the last denomination, this is a condition which is more likely to happen in elderly people, and the modifications due to it occur slowly and over the years, although there are exceptions. OA is due to the inflammation and injury of the joint, in this case, the ankle joint, which causes the breaking of cartilage tissues, promoting deformity, pain and swelling. There are some data from scientific studies and clinical experiments about the treatment of ankle OA that mention that secondary ankle OA is the type with more prevalence, resultant from ankle fractures or ligamentous injury, while the primary ankle OA is rare. Although the ankle joint is the one subjected to greater weight bearing force (per cm^2), and consequently the more frequently injured, it is important to established that the predominance of symptomatic arthritis, in the mentioned joint, is about nine times lower than in the hip and knee. Between 6% and 13% of all cases of OA are related to the ankle joint and, relatively to the frequency of the ankle arthroplasty and arthrodesis combined, it is possible to say that is not very common, when compared to the total knee arthroplasty: the total knee arthroplasty happens 24 times more than the ankle arthroplasty. The degenerative changes are due to many different causes, some more common than others: trauma or abnormal ankle mechanics are the most common causes; causes, such as tumor, infection, hemochromatosis, neuropathic and inflammatory arthropathies, are the less common. Despite the low incidence of severe ankle arthritis, when compared with the knee or hip, the effects of symptomatic end stage ankle arthritis are significant, for patient quality of life. The mental and physical disability associated with end-stage of both ankle and hip arthrosis are very severe [4].

Ankle arthrodesis is the denomination given to the artificial induction of joint ossification between two bones via surgery. The main objective of this technique is the relief of the patient pain and it has been chosen among other treatments as the preferred one [9]. Some experiments and scientific articles, about the ankle arthrodesis, have shown good results. Some techniques have been used in this surgical procedure, such as plate fixation, cannulated screws, external fixation and retrograde nail. However, this procedure has a main drawback: the high rate of later arthrosis in adjacent joints in about 10% to 60% of the cases, which makes this technique far from the perfection, due to the elimination of the joint and its associated mobility (which causes discomfort, increases the stresses on the neighbouring joints, leading to the occurrence of the arthritis and promoting a conditioning movement) [10]. The mentioned failures are due to high subtalar fusion rate at 5 years (2.8%) when compared the 0.7% of TAA. The ankle arthrodesis fails due to other factors, such as malalignment, wound infection (3% to 25%) and non-union (10% to 20%) [11].

The arthroplasty, in this case the TAA, has the purpose of relief the patient pain, through the substitution of the arthritic or injured ankle joint with a prosthesis (artificial ankle joint). Other purposes of the arthroplasty are to restore the stability and integrity of the joint, without forget the main function for the patient, the restoring of the mobility. Due to its characteristics, the arthroplasty became, through

the years, a competitor of the arthrodesis in the treatment of ankle arthritis. The history of the ankle prostheses started in the seventies and, after that, it showed some negative periods, when they – the first generation of prostheses - fell into disuse, due to the bad results demonstrated, such as instability, impingement, malalignment, loosening, and stiffness and wound complications. Later, another family of prostheses (uncemented prostheses, with two or three modular components) appeared, the second generation, which tried, successfully, to overcome the negative aspects of the first generation prostheses. Thanks to that, it was possible to understand more deeply the behaviour and biomechanics of the ankle joint, which led to improvement/creation of new total ankle prostheses. Nowadays, the TAA is still evolving but has the potential advantage to preserve range of motion, restore gait, and, thus, protect adjacent articulations. Also, the results obtained after the TAA have been improved: for instance, it was verified a situation of 89% survival from 7942 TAAs at 10 years and a study showed that in 1105 TAAs, they were verified about 10% failure rate at 5 years with residual pain in 27% to 60% of cases [12].

Currently, some studies report that the TAA may be preferred to the arthrodesis, due to the results shown by it and its demonstrated viability. The use of TAA has increased over the years and it is possible that, in the future, its use will further increase [12]. However, like in many other scientific fields, the opinions differ from investigators to investigators. Some of them do not consider the TAA a good choice due to the fact of it does not show a higher success rate when compared to the hip and knee arthroplasties [13]. This failure may be it is due to many factors that are listed below:

- The existence of large forces acting through the ankle joint [14-16],
- The small surface area for prosthetic support [17],
- Wound problems [17],
- The mismatch between the anatomical component shape and physiological ankle biomechanics [18],
- The weak bone support (caused by the larger resection required by the low thickness necessary for the polyethylene component of the prosthesis to avoid wear and failure) [17].

Other situation that promotes the disuse of the TAA compared with the total hip and knee arthroplasty is the lack of information about TAA, due to the poor research made, until now, in this area – the biomechanical researchers have lost more time in the other joints: the hip and knee [19].

Through the times, it was verified the necessity of improved prostheses without being based solely on clinical reports. This way, the creation of physical and mathematical models to demonstrate, respectively, real constructions and conceptual representations have been taken into account more recently, a situation that is common in biomechanics. With the help of these models, the design of new prostheses became more accurate and reliable [20]. Finite element method (FEM) is a numerical model that has been used through the years, with great satisfaction, contributing for the enrichment of orthopaedics, thanks to the information provided for it. Due to the FEM, it is possible to investigate the bone remodeling, osteoporosis, fracture healing, stress and strain conditions of bones, cartilage and ligaments [21]. Thanks to these information, the design of prostheses was facilitated. However, like it

was said before, the ankle joint has not been target of a deep research, so there are not many finite elements (FE) models, for this joint. The models that exist, for the ankle joint, demonstrate some failures: some of them do not have bones, others do not have prostheses, there are some that just have part of the bones, others miss the ligaments and cartilage, and so on [20]. In addition, that are used real models. They are difficult to obtain, they do not allow to obtain many information, their use is dependent on the time spent in the preparation and the available material to procedure to the analysis, and they can be used only once. This way, it is preferred to use the FE models, whose validation is performed through the comparison between their conclusions and the clinical results described in scientific articles, for instance, due to the fact that the real models cannot perform all the predictions made by FE models. Other contribute of the FE models is the investigation of processes that occur in biological tissues and are dependent on time [21]. One of them, and also the main issue of this work, is the bone remodeling process. Like it is easily understood, this process cannot be investigated just with the recurrence to FEM. Besides the FEM, other specific algorithms are used to perform computational simulations that reproduce the phenomenon of tissue adaptation in response to biomechanical factors. The study of the bone remodeling process allows the access to precious information: thanks to it, information about the bone adaptation is obtained. If the mentioned information is compared, before and after the colocation of the prosthesis in the bone, it is possible to assess the amount of bone resorption (explained below) associated to a given prosthesis design. Loosening, subsidence and the possible failure of the prosthesis are sceneries that can be predicted due to the information obtained about the amount of bone resorption. Other valence of the mentioned models, the bone adaptation models, is the possibility of study the orthopaedic devices. If the modifications, in mechanical and biological terms, observed in bone tissue, after the insertion of prostheses, are understood, the performance of the orthopaedic devices is tested and optimized, which allows the correct choice of the right prosthesis for each patient, by the clinicians, and the optimization of the geometry of the prosthesis, by the industry. Until now, the study of the bone remodeling process in the ankle joint is very poor [22].

Bone remodeling consists in a process that occurs during all life of the individual. In this process, the old and microdamaged bone is removed from the skeleton – *bone resorption* – and the new bone is added – *bone formation* or *ossification*. Bone remodeling is a continuous process that removes discrete packets of old bone, which are replaced by newly synthesized proteinaceous matrix, and subsequent mineralization of the matrix: this allows the formation of the new and healthier bone. One of the characteristics of the bone remodeling is the control that it enables over the reshaping/replacement of bone, during growth and injuries. These injuries can be of two types: fractures or microdamage, and can occur during the normal activity of the individual. Bone remodeling also prevents the accumulation of microdamages by substituting the old bone with the new one. This process occurs in response to the mechanical loads that act over the bone and, due to this, the bone is removed from the places where it is not necessary and added where it is needed. In addition, the bone remodeling is fundamental to maintain two important necessities: the mineral homeostasis and bone mechanical strength. Like it was said before, the skeleton suffers continuous remodeling during lifetime, due to the fact of being a metabolically active organ. Maintain the structural integrity of the skeleton through the balanced activities of its constituent cell types) and support its metabolic functions (for instance, a storehouse of

ions, such as calcium and phosphorus, the most associated to the bone tissue), are other occurrences promoted by the bone remodeling. Like many processes in the human body, the bone remodeling is also characterized for cycles, which request a coordination between the two main phenomena, the bone resorption and bone formation. This coordination is dependent on the orderly development and activation of osteoclasts (responsible for bone resorption) and osteoblasts (responsible for bone formation). The main function of osteoclasts is related to the changes of pH. This type of cells presents, around their membrane, highly active ion channels, whose function is to pump protons into the extracellular space, which leads to the decrease of the pH in their own microenvironment. This decrease leads promotes de dissolution of the bone mineral. Due to what was mentioned, bone consists in a very dynamic tissue, where constantly occurs the resorption of the old bone and the formation of the new one. This dynamic nature allows the reparation of damaged tissue, the maintenance of bone tissue, and the homeostasis of the metabolism responsible for the phosphorus and calcium. There are verified interactions between two cell lineages (the hematopoietic osteoclastic and the mesenchymal osteoblastic lineages), that control series of highly regulated and sequential steps (coupling of bone formation and bone resorption), which, in turn, constitute the bone remodeling cycle. Periosteal bone balance is softly positive, while trabecular and endosteal bones balance is softly negative, which causes the thinning of trabecular and cortical bones with aging. This alteration occurs due to the fact of the endosteal resorption being greater than the periosteal formation. As was given to understand above, osteoclasts and osteoblasts, the two main cell types, determine the balance between bone resorption and bone formation/deposition. The mentioned two types of cells, when coupled together via paracrine cell signaling, are considered bone remodeling units [22].

Bone remodeling is a balanced process, connected in both time and space, under normal conditions. It is referred to as a balance process because, in a young individual, its skeleton presents an amount of resorbed bone proportional to the newly one formed; the difference between these two quantities is called bone balance. Each remodeled unit, in human body, presents an average lifetime of 2-8 months, and most of this time, it is used for bone formation. Like it was said, bone remodeling is a process that happens during the lifetime, and after the thirties, the mentioned balance becomes positive. This happens because this is when the bone mass achieves its maximum, which is maintained until the age of 50, just showing small variations. After the age of 50, the bone resorption predominates and, consequently, the bone mass starts to decreasing. For instance, relatively to what happens in women, the bone remodeling increases in two situations of life: in perimenopause and early postmenopause. On the other hand, after the early postmenopause, the bone remodeling retards with further aging but continues at a faster rate than in women suffering premenopause. The cortical bone consists in about 75% of the total volume; however, in trabecular bone, it is verified a metabolic rate ten times higher (the cortical bone turnover, in an adult, is between 2% and 3%, per year – enough for the maintenance of the biomechanical strength of bone), which is due to the fact of the surface area-to-volume ratio being much greater, because the surface of the trabecular bone represents about 60% of the total. This higher rate of trabecular bone turnover is more than the required for maintenance of mechanical strength, which indicates that this turnover is more important for mineral metabolism. This way, the renewal of total bone, per year, is about 5-10% [22].

Finally, and after the exposure, it is easily understandable that the TAA should suffer a deep investigation, with more incidence in the bone remodeling process associated.

1.2. Approach and objectives

The purpose of the present work is to study the bone remodeling of the ankle joint after a TAA. To achieve this purpose, it is used a FE model of the AJC. In this model, two prostheses are introduced, the Agility™ and S.T.A.R.™, and the study is performed for each of them. In particular, the main objective of this work is to relate the prostheses geometry with their effect over the host bone, in terms of bone remodeling, changing the appropriated parameters. It has major importance due to the fact of the ankle joint is one of the joints that are subjected to a higher loading, which combined with the required mobility and with the anatomy of the involved bones, leads to a higher failure rate of the TAA, when compared to the hip and knee arthroplasties. Thanks to the processes mentioned, the deepening of the formation in the Biomechanics area and the knowledge in FEM is possible.

The commercial software ABAQUS® v6.10 (Hibbitt, Karlsson and Sorensen, Inc., Pawtucket, Rhode Island, USA) is used to enable the access to the FEM. For the performing of bone remodeling, the model of bone remodeling developed in IDMEC/IST is used [23-28]. Regarding to the FEM, it is possible to say that it consists in a numerical analysis technique, as it was mentioned before, which purpose is to estimate solutions that are close to the differential equations that try to describe a wide range of non- and physical problems. Synthetically, the FEM consists in a domain that is divided into sub-domains, which are smaller, the FEs, originating the FE mesh – it is called the FE discretization. To associate the FEs, there are discrete node points, which are more or less, according to the type of the element chosen. It is developed an approximation to the solution over each FE and, to obtain the global solution (the solution of the whole domain), the assembly of all the FEs are made. The solution consists in the set of nodal displacements, which allows the admeasurement of the strain and stress [21]. Relatively to the model of bone remodeling, it follows a topology optimization criterion. Wolff [29] established that some mathematical rules could describe the adaptation of the trabecular bone to the mechanical environment, and that is verified a dependence of bone structure and morphology upon applied loading. Although the first step was taken by Wolff, other authors decided to develop several mathematical models used for the study of bone remodeling. Some of these authors are Fernandes *et al.* [26] and Folgado *et al.* [27, 28]. The first team developed the computational model used for the bone remodeling and the second one introduced in the existent model the equilibrium equation expressed for the contact problem. Since the bone is a porous material that adjusts itself in response to the applied loads, which makes its structure more stiffer, and the mentioned model studies the case as if the material is porous, with the purpose of, for different load situations, achieve the stiffest structure, it is understandable the use of the topology optimization problem to develop the bone remodeling process [23, 28]. Below, it is possible to see the relation between the applied loads and the reaction of the bone tissue.

- ↑ applied load → ↑ stress → ↑ bone mass/density (bone formation is verified) → ↑ stiffness
- ↓ applied load → ↓ stress → ↓ bone mass/density (bone resorption is verified) → ↑ weakness of the bone structure.

For a full description of the model see [23, 25-28].

The development of the three-dimensional (3-D) components of the intact AJC and both prostheses (the Agility™ and S.T.A.R.™) were made with the aid of the commercial software SolidWorks® v2012 (SolidWorks Corporation, Massachusetts, USA). The intact AJC consists in cartilages, ligaments, interosseous membrane [20] and, of course, four bones: the tibia, talus, fibula and calcaneus. Also in the SolidWorks®, the assembly of the AJC with each prosthesis was performed. The composition of the AJC with a prosthesis is sufficient to simulate a TAA. Everything that was mentioned in the last sentences, the construction of the parts and the assembly, was performed by Daniela Rodrigues, in her Master Thesis [30]. Through the commercial software ABAQUS®, it was possible to create the FE meshes, to proceed to the finite element analysis (FEA). Actions like the establishment of the materials properties, the interactions between the parts constituent of the models, the conditions of loading and boundary, and, finally, the mesh generation, were also performed by ABAQUS®. The mentioned software is very user-friendly and intuitive, enabling the achievement of very good and noticeable results, which are possible to characterize according a wide range of options (different colours, views of different planes, positions, among others). Finally, the FEM was introduced in the model responsible for the bone remodeling, which allowed the achievement of the distribution of the bone density. This distribution is considered the real solution of the bone remodeling process.

1.3. Contributions

Due to the lack of information about the TAA and the bone remodeling after it, this thesis promotes the clarification of the biological and mechanical changes induced in bone tissue by total ankle prostheses, to possibly allow implant companies to optimize the geometry of the total ankle prosthesis and, more important, orthopaedic surgeons to adopt the best solution for each patient.

1.4. Organization

The present thesis is divided in five parts, if the Acknowledgments, the Abstract, the organizing lists, the Content, the Bibliography and the Annexes are neglected.

The first chapter is an Introduction that comprises the motivation of this work, the approach used, the objectives and contributions of the work and how it is organized.

The second chapter, called Background, contextualizes the anatomy and biomechanics involved in this work, describes the total ankle prosthesis and the principles of the bone remodeling.

The third chapter, the Computational modeling, describes how the things were made/achieved, since the geometric models to the obtainment of the results from the bone remodeling analysis.

In the fourth chapter, the Results and Discussion, it is possible to access the images and graphics that illustrated the results obtained and their discussion.

Finally, the fifth chapter, the Conclusions and Future Directions, provide not only a brief description of what was made, concluded and which could be improved, but also a list of future directions that could guide someone in the next works.

2. Background

2.1. The skeletal system

The skeletal system is one of the most important corporal systems: without it, it is impossible to move, and the body does not have neither form nor configuration. This system includes all of the bones, joints, ligaments and cartilages in the body. The bones are complex living organs, made up of minerals (calcium), protein fibers and many cells (bone matrix). The bones are connected by joints, with the help of ligaments. Joints and ligaments allow or restrict the movement, depending on the direction. The cartilages are an elastic form of conjunctive tissue and constitute skeleton parts in which the movement occurs. These components do not have their own blood supply and their cells obtain oxygen and nutrients through long range diffusion. The skeletal system is divided into two distinct divisions: the first one is the axial skeleton, which comprises the skull, the vertebral column, twelve ribs and the sternum; the second one, the appendicular skeleton, is formed by the upper and the lower limbs, the pectoral girdles and the pelvic girdle [31].

2.1.1. Human foot: its articulations

The ankle joint is created by the meeting of four bones, the tibia (the shin bone), the fibula (the thinner bone running next to the tibia), the talus (a foot bone that sits above the heel bone) and the calcaneus (the heel bone), and by the articulations among these ones. These articulations are the subtalar joint, known as talocalcaneal joint, the ankle joint or talocrural joint, and the midtarsal joint, which are formed by talonavicular and cubocalcaneal articulations [32]. There are more articulations in this area but they just allow small motions whereby they do not have extensive medical attention. The subtalar joint occurs at the meeting point of the calcaneus and the talus, while the ankle joint is created by the distal ends of the fibula and tibia, and the proximal end of talus [33]. Finally, and like it was mentioned, the midtarsal joint is created by the articulation of the cuboid with the calcaneus – the cubocalcaneal articulation, and the articulation of the talus with the navicular – talonavicular articulation [32].

2.1.2. Ankle joint complex (AJC)

Like in many other things, there are two different definitions of AJC, from author to author. Many of them say that the AJC is formed by both ankle and subtalar joints; the other part, add to this complex the distal/inferior tibiofibular joint. This last joint is constituted by the inferior extremities of the tibia and fibula. Here, it was take into account that the AJC is composed by three joints: ankle (the more important for the present work), subtalar and distal tibiofibular joints. These three joints are involved by nerves, arteries, veins, muscles, tendons and syndesmotic and collateral ligaments. The subtalar and the distal tibiofibular joints are both composed by two bones: the first one by talus and calcaneus and the second one by fibula and tibia [34]. The ankle joint is constituted by three bones, tibia, fibula and talus [31].

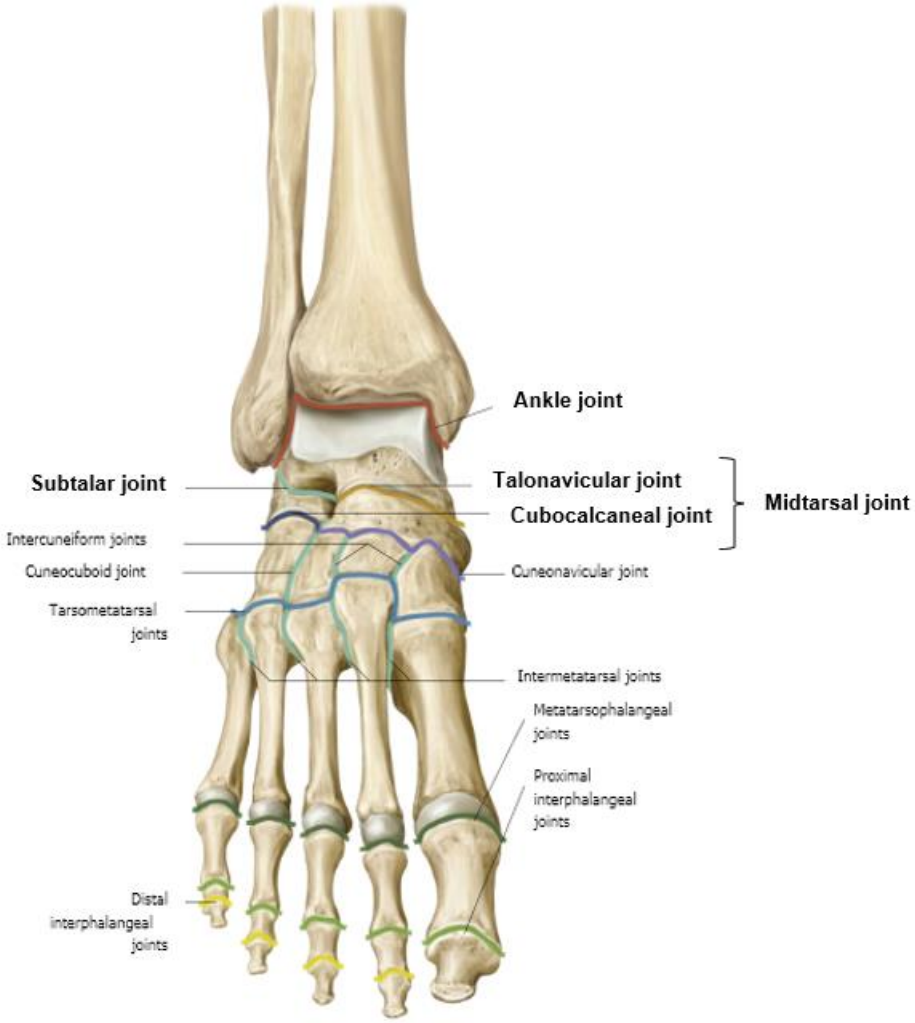

Figure 2.1 - Representation of the three more important joints of the foot, for its motion [8].

2.1.3. Constitution in terms of bones

The tibia, the fibula, the talus and the calcaneus are four of the major bones in the lower limb. The tibia and the fibula are long bones and constitute the leg, one of the three anatomic segments that composed the lower limb, which are, from top to bottom: the thigh, leg and foot. The talus and calcaneus are short bones and constitute the foot [31].

The tibia is the second longest bone of the skeleton and it is located between the femur and the talus, at the medial side of leg. It carries most of the load in the leg and it has two extremities and a body [20]. The tibia has, in its lower end, the medial *malleolus*, a bony prominence on the inner side of the ankle. This prominence provides a larger surface area to the ankle joint and promotes the asymmetry of the tibia's articular surface, also known as tibial plafond or tibial pilon. Another term that should be taken into account is the ankle mortise, which is an arch composed by the the tibial plafond and the medial and lateral *malleoli*. Finally, an interesting characteristic of the tibia is the fact of its superior extremity being much bigger than the inferior [36].

Connected to the tibia, by the interosseous membrane [20], is the fibula. This one has two extremities and a body, is the most slender of all the long bones and it is situated on the lateral side of the tibia. The fibula is related with another prominence on the lateral side of the ankle, the lateral *malleolus*, which has pyramidal form, is somewhat flattened from side to side and descends to a lower level than the medial *malleolus.* This prominence results from the slightly forward inclination of the inferior extremity of the fibula, which is on a plane anterior to that of the superior extremity, and below to the tibia. Finally, the fibula makes articulation with two other bones, like it was said, the tibia and talus [36].

Apart from calcaneus, the talus, also known as astragalus or the ankle bone, is the largest bone of the foot, it articulates with tibia, navicular, fibula and calcaneus, and it is a part of a collection of bones that constitutes the foot named the tarsus [36]. The tarsus builds the lower zone of the ankle joint through its articulations with the *malleoli* of the tibia and fibula. Because of its irregular shape, the talus is mainly divided in three parts: a head, which is slightly round, a neck and a cuboidal body [20]. Relatively to the cuboidal body, it is possible to say that it presents some articular surfaces which are prominent. Regarding to one of this surfaces, the superior one, it is important to mention that it is composed by two adjacent crests (in terms of the frontal plane). This surface features the trochlea, which is used with the purpose of articulate with the tibia and has this name because of its soft trochlear surface. The talus is wedge-shaped due to the fact of the trochlea being wider in its anterior part than in its posterior one [37]. The part of the talus which is more susceptible to fracture is the connection between the trochlea and the superior surface of the neck [36], due to its narrow cross section, when compared to the head [36]. To conclude, and relatively to the cartilage, it is verified a difference between the thickness of the articular cartilage that covers the talus and the one that covers the knee, for instance: the first one is less thick than the last one, having an average thickness prowling 1.6 mm, while the knee is cover by articular cartilage with a thickness between 6 mm and 8 mm. About 60% of the talus is covered by the mentioned cartilage [32].

Like it was mentioned, the calcaneus, also known as the heel bone, is not only the largest but also the strongest bone of the foot. This bone is the most responsible for the transmission of the weight of the human body to the ground and it is situated at the back and lower part of the foot. The calcaneus connects with the cuboid and talus, forming a powerful handle for the muscles [36].

2.1.4. Configuration of ligaments

In terms of ligaments, it can be said that the AJC has a huge number of ligaments that are divided in different categories according their anatomic position. More specifically, the ligaments that surround the AJC can be split into three groups: the lateral collateral ligaments (LCL), at the distal tibiofibular joint, there is the syndesmotic ligament complex (SLC), and forming the medial part of the ankle joint, attaching the medical *malleolous* to multiple tarsal bones, there is the deltoid ligament or medial collateral ligaments (MCL) [38-40].

The first group mentioned, the LCL, is composed by three different types of ligaments: the calcaneofibular (CaFi), the anterior talofibular (ATaFi), and the posterior talofibular (PTaFi) ligaments.

The LCL group just has one type of ligaments, the CaFi, which connects the ankle and subtalar joints [38].

Ankle sprain is the most frequent way of injury to the ankle ligaments. This mechanism promotes, in particular, the lesion of the ATaFi ligament, the type of ligament which more frequently suffers injury.

The SLC group is composed by three ligaments. They are the posteroinferior tibiofibular (PTiFi), the interosseous tibiofibular (ITiFi), and the anteroinferior tibiofibular (ATiFi) ligaments. Looking for the first one mentioned, the PTiFi, it can be said that it has two components: the deep, also known as the transverse ligament, and the superficial or PTiFi ligament [41].

Finally, the MCL group has many anatomical aspects that should be referred. This type of ligaments has many fascicles in its constitution, so it is called a multifascicular group and it is constituted by two layers, one more superficial and other more deep. This group comes from the medial *malleolus* and it is related to three bones: the navicular, calcaneus, and talus. The MCL is composed by six components: the deep anterior tibiotalar (DATiTa), deep posterior tibiotalar (DPTiTa), superficial posterior tibiotalar (SPTiTa), tibiocalcaneal (TiCa), tibionavicular (TiNa), and tibiospring (TiS) ligaments. Like some names may suggest, the DPTiTa, SPTiTa and DATiTa ligaments constitute the deep layer, and the TiCa, TiS and TiNa ligaments belong to the superficial layer [42-45].

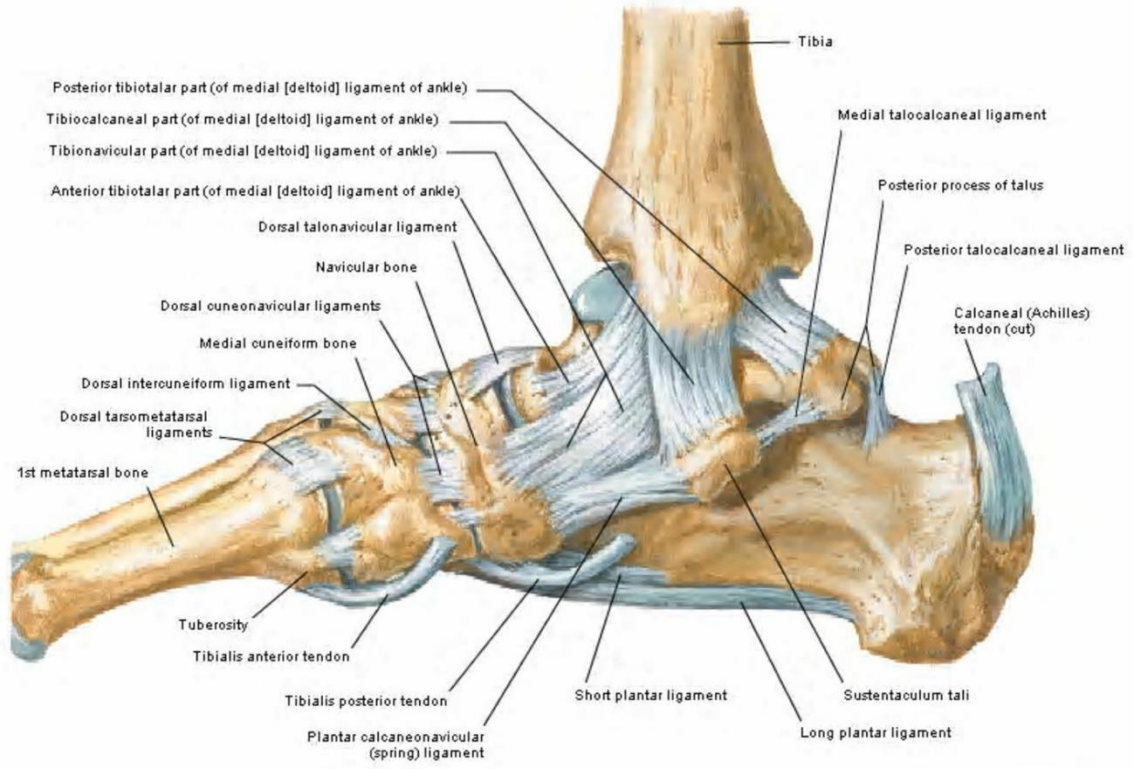

Figure 2.2 - Representation of the ligaments of the foot and some associated bones [8].

2.2. The biomechanics

Like every subject, the description of the direction and position of a biomechanical system also needs a specific terminology, which should be accepted by a large population, to simplify the scientific communication about biomechanical issues. This terminology is fundamental to describe motions of joints and, in this particular case, the AJC motion.

2.2.1. Anatomical reference position

The anatomical reference position allows the documentation of where a body part is, comparatively other part, regardless of the human body is stand up, lying or in other position. This specific position is characterized by the erect body, the feet slightly separated, in parallel, laterally suspended arms, and hands palms facing forward. Below, it is possible to see the nomenclature used to describe, relatively to the direction, the relative position of the components that constitute the AJC [46].

Table 2.1 – Terminology of comparison and interrelation and examples [46].

Position	Description	Example
Anterior	Toward the front of the body	The patella is anterior to the knee joint.
Posterior	Toward the back of the body	The scapula is posterior to the clavicle.
Superior	Closer to the head	The heart is superior to the stomach.
Inferior	Farther away from the head	The trunk is inferior to the neck.
Medial	Closer to the midline of the body	The big toe is medial surface to the other.
Lateral	Further from the midline of the body	The thumb is on the lateral side of the hand.
Superficial	Closer to the surface of the body	The skin is superficial to the muscles.
Deep	The opposite of superficial; further into the body	The lungs are deeper than the ribs.
Proximal	Closer to the trunk	The knee is proximal relative to the ankle.
Distal	Further from the trunk	The wrist is distal relative to the elbow.

2.2.2. Reference planes and axes to anatomic descriptions

There are three anatomical reference planes also known as cardinal plans, which have a purpose of help in the description of large amplitude movements, and for the definition of specific terminology of

the movement types of the human body. These planes divide the body into two halves of equal mass, and have as intersection common point, the mass center of the body or the center of gravity (when the body is in the anatomical reference position). The anatomical reference planes are perpendicular (or orthogonal) between them, and they are: the sagittal plane, which divide the body vertically, in their right and left halves, the frontal or coronal plane, which divide the body vertically, in their anterior and posterior halves, and the transverse or axial plane, which divide the body horizontally, in their superior and inferior halves [46]. Each plane has its type of movements, which occur along or parallel to them: the sagittal plane has movements like running, march, or bicycle, the coronal plane comprises movements such as lateral jumps, wheel, or side kicks in martial arts, and finally, the transverse plane is connected to a movements like dance, gymnastic, or artistic jumps. It is important to note that these three anatomical reference planes can also be applied to specific body parts, and not only to the whole body. Taking this into account, it can be verified that these three planes can be used in position descriptions of the foot (the body part of interest in this work) and that its midline axis goes from its posterior to anterior sections [47]. Finally, it is curious to refer that there are many movements of human body that do not be oriented according to these planes. In these situations, oblique planes are used [46].

Besides the planes, there are three anatomical reference axes and each of them is perpendicular to one of the three planes. These axes are imaginary and pass through a joint, so when a part of the body moves, it has a rotation around an axis. The anteroposterior axis is perpendicular to the coronal plane, the mediolateral axis is perpendicular to the sagittal plane, and finally the longitudinal axis is perpendicular to transverse plane, which means that the rotation in each of the planes occurs around the respective axis. So, it can be associated types of motions to each axis: eversion/inversion motions occur around the anteroposterior axis, dorsi/plantarflexion motions occur around the mediolateral axis, and abduction/adduction motions occur around the longitudinal axis. In the next figure, it is possible to observe a scheme of the information presented above [46].

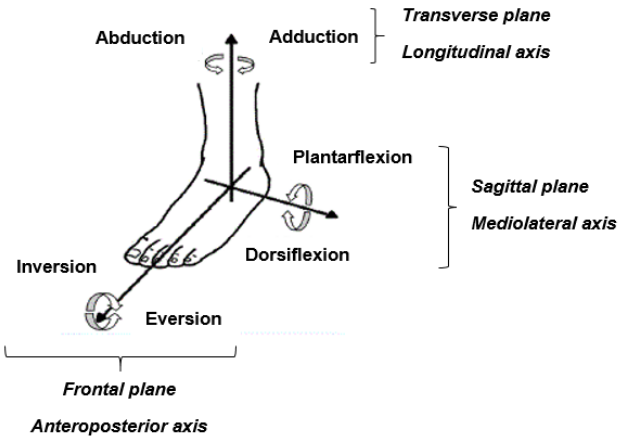

Figure 2.3 - Foot motions and their associated planes and axis (adapted from [48]).

2.2.3. Nomenclature of articulation motion

There are two important things that should be referred, to start this topic: like it was said, it is considered the anatomical reference position, for the human body, where all the segments are positioned at zero degrees, and the joint that was studied here is the ankle joint, in the foot. The human motions are considered general movements, because they are a combination of two types of movements: linear movements, that comprises the translation movements, and angular movements, that are rotational. It is important to stablish that the rotation of a body segment away from anatomical reference is quantitatively measured by the measure of the angle located between the anatomical reference plane and the position of the body segment. Other aspect is that the rotation of a body component or segment away from anatomical reference position is nominated thanks to the direction of movement [46]. The movement of the foot is made in three anatomical planes: in the frontal plane inversion/eversion motions occur (they are rotary motions and happen thanks to the subtalar and midtarsal joints), dorsi/plantarflexion motions occur in the sagittal plane, and in the transverse plane abduction/adduction motions are verified [49]. If something leads to the loss of eversion or inversion, like disease or wear, the foot cannot adjust to walking on irregular areas, resulting in disability. The subtalar joint does not have any influence in dorsiflexion and plantarflexion of the foot. The midtarsal joint allows the more extensive movement, compared with the other tarsal joints. The three joints mentioned above, the subtalar, ankle and midtarsal joints, have a simultaneously movement so that it is possible, when the foot everts in subtalar and midtarsal joints, it suffers dorsiflexion in the ankle joint. This synchronization results in pronation, a complex motion. Contrary, exists a complex motion, named supination. It occurs when the foot suffers adduction, plantarflexion and inversion. Pronation and supination are called tri-plane motion because they occur simultaneously in the three planes: frontal, sagittal and transverse. Below, it is possible to see the description of each motion [46].

Table 2.2 - Motions of the foot: their descriptions and illustrations (adapted from [27, 32, 46, 48]).

Motion	Description of motion	Illustration
Inversion	Internal rotation of the foot while it is rolling over towards the medial side of the body.	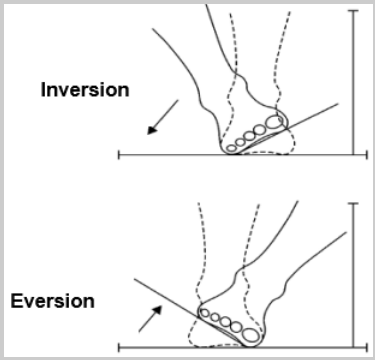
Eversion	External rotation of the foot while it is rolling over towards the lateral side of the body.	
Dorsiflexion	Movement of the foot when the toes are lifted off the ground.	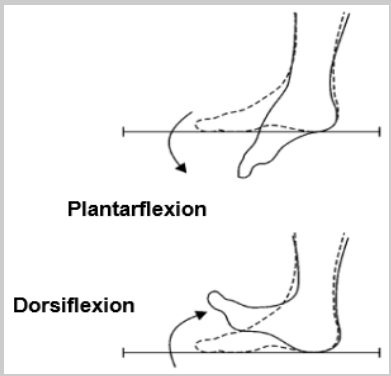
Plantar-flexion	Movement of the foot when the toes are pushed down towards the ground.	
Abduction	The motion of bringing something away from the midline of the body (lateral rotation).	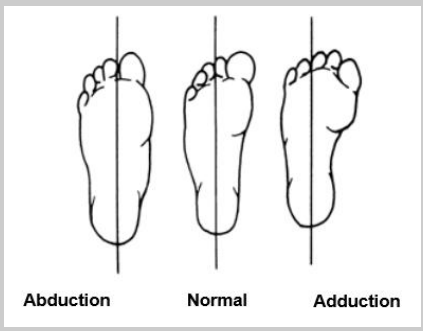
Adduction	The motion of bringing something towards the midline of the body (medial rotation).	
Pronation	Combination of abduction, eversion, and dorsiflexion. Movement of the foot up and away from the center of the body (the plantar surface faces laterally).	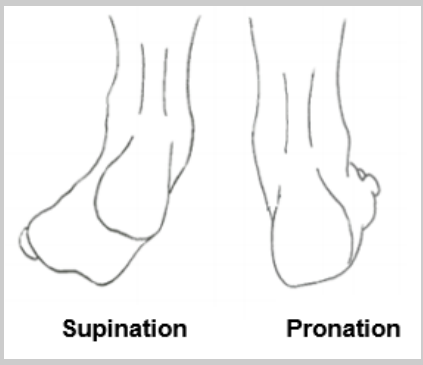
Supination	Combination of adduction, inversion, and plantarflexion. Movement of the foot down and towards the center of the body (the plantar surface faces medially).	

2.2.4. Evolution of the comprehension of the rotation axis

There was a background history behind the axis of rotation of the ankle joint. This joint is very complex so, over time, the definition of its axis of rotation has changed. Above, it is possible to see what it is thought over years and by who.

- **Hippocrates (B. C.), Bromfield (in 1773) and Fick (in 1911)** → the ankle joint is like a hinge joint; the rotation occurs only in sagittal plane [50, 51].
- **Lazarus (in 1896)** → the ankle joint is like a screw joint; with this type of joint, it occurs the rotation and shifting along the axis – lateral motion [52].
- **Barnett and Napier (in 1952) and Cunningham (in 1943)** → the ankle has not a horizontal fixed axis but a changing one, and the ankle joint is not a hinge joint. There was some facts that supported this theory: different lateral and medial radii of curvature, the medial profile is a composition of arcs of two circles of different radii and the lateral profile is an arc of a circle which allows the axis of rotation to pass through the center of this circle (for any position of the talus and every time). The observation made relatively to the medial profile would lead to a changing axis of rotation. With respect to the different medial and lateral radii of curvature (studied thanks to the examination of the profiles of the trochela), they could not be maintained as well as the wedge-shaped talus, which implie the verified tibiotalar congruency, in the motion made in the sagittal plane. This preservation would be possible only if the talus featured coupled axial rotation. In the plantarflexion motion, they observed that the axis of rotation was inclined medially and downwards, on other hand, in the dorsiflexion motion, the same axis was inclined downwards too but laterally, which supports their theory. Other fact that is important to mention relatively to these axes is that the changes between them occur extremely close to the neutral position, in where the axis is practically horizontal [37, 53].
- **Hicks (in 1953)** → establish that the ankle joint has two main axes – at dorsiflexion and plantarflexion positions, according to Barnett and Napier and other investigators, both in vitro and in vivo [54].
- **Kapandji (in 1974) and Inman (in 1976)** → establish that the ankle joint has just an axis. The experiments of the more recent one, Inman, showed that, since the medial radii is small and the lateral radii is large, the trochlea, from talus, can be illustrated by a slice (section) of the frustum of a cone, which tip should be pointing in medial terms. Other thing that he conclude was the perpendicularity between the axis of rotation and the lateral surface and the fact that the medial surface had an inclination of 6 degree. So, the surfaces were illustrated in different ways: the medial surface were illustrated as ellipsoid and the lateral one as a circle. Finally, Inman observed that the ankle joint axis passed in different places, from plane to plane: in the transverse plane it passed in the centers of the *malleoli* and the inclination was posterolateral; in the frontal one, the axis passed below the extremities of the *malleoli*, which promote a laterally and downward inclination [55, 56].
- **Sammarco (in 1977)** → the ankle joint is a multi-axial joint. He established this characteristic due to the observation of the motion between the talus and tibia, in the sagittal plane. He

observed that this motion happened around not one but multiple centers of rotation, which leaded to the idea of the existence of a changing axis of rotation. Nevertheless, his obtained results showed some discrepancies when compared to the previous ones. The changes between the mentioned axes occurred in a gradual way, not suddenly: contrarily to what was established by Hicks, and Barnett and Napier, Sammarco observed that the plantarflexion axes, when compared to the dorsiflexion axes and in the frontal plane, were inclined medially and downward, and more horizontal. However, Sammarco's studies agreed with the evidences of Inman, Mann and Morrissy (the studies from the last two will be possible to see below): the ankle joint axis in the frontal plane and in 10º to 30º of dorsiflexion crossed near the tips of the *malleoli* and the same axis, when projected onto the transverse plane, passed near to the centers of the *malleoli* [57].

- **Mann (in 1985)** → define that the ankle joint has just an axis. This idea was supported thanks to the existence of a 80 degree angle defining the axis which was created by the center of the longitudinal axis of the tibia, the ankle joins axis and a line that passed in the tips of the *malleoli*, in the frontal plane, and a 84 degree angle created in the transverse plane from the midline axis of the foot, which also defined the axis [47].
- **Lundberg *et al.* (in 1989)** → The ankle joint uses different axes for plantarflexion and dorsiflexion. This affirmation was supported by the 3-D analysis of the ankle joint in 8 healthy subjects and through the use of roentgen stereophotogrammetry [58].
- **Morrissy (in 1990)** → establish that the ankle joint axis, in the transverse plane, is the same axis that crosses the centers of the *malleoli*. His experiments showed that the ankle joint axis is an inclined axis of rotation, which explains the occurrence of the ankle motion simultaneously in the three anatomical planes and, relatively to the axes, it shows the existence of an interation between the three. His results presented some differences when compared with the previous ones found in the frontal plane (Inman established 8º and Mann 8º), however, they encouraged and validated the experiments of Inman. In geometric terms, these results putted the ankle joint axis within of the mediolateral axis in the three planes, specifically: between 8º and 10º in the transverse plane, 6º in the frontal plane and, finally, 84º in the sagittal one [59].
- **Leardini *et al.* (in 1999)** → Like other studies and authors, they used precise techniques with the purpose of observe slight motions in 3-D structures and, this way, prove that the ankle joint axis is not constant during the motion but it changes in a continuous way. So, Leardini and his group developed a mathematical model which described the dorsiflexion and plantarflexion in the AJC during the passive motion. Here are some of their observations: the AJC acts as a system of a single degree of freedom, when the foot moves from plantarflexion to dorsiflexion positions (in this case, the subtalar joint demonstrates a flexible structure and the ankle joint works with a mechanism defined by a single degree of freedom), and the ankle is an incongruent joint which rotates around multiple centers of rotation (verified due to the translation of the instant center of rotation from the posteroinferior to anterosuperior positions and in the mentioned motion, this is from plantarflexion to dorsiflexion positions). As Sammarco, also the

Leardini team supported some results of Barnett and Napier by established that the trochlea is polyradial and polycentric [33].

- **Hintermann (in 2005)** → the orientation with oblique nature of the ankle joint axis originates the occurrence of inversion from plantarflexion and eversion from dorsiflexion [34].

In the above points, it has been described different studies/experiments/assumptions that do not complement each other, having many discrepancies. This way, nowadays, it is difficult to choose what is the best idea/definition of the axis of rotation. Like it was observed, the explanation of the different studies about the axis of rotation was very extensive, which is easily comprehensible due to the importance of the axis of rotation in some situations, such as, in the design of total ankle prostheses, and in the positioning of the prosthesis in the ankle joint, during the ankle replacement surgery. Thus, anatomy books and scientific articles compare this axis of rotation to the empirical axis [20] of the ankle joint. In general parameters, the current empirical axis of the ankle joint agrees with the fundaments established by three of the investigators that study this case, Inman [56], Mann [47] and Morrissy [59], which, for example, helps the surgeons in the identification of the empirical axis by touching with the fingers on the tips of the *malleoli*. Nevertheless, there are many aspects that should be understandable and, then, enlightened. To conclude, the importance of clarifying these aspects lies on the fact that the the ankle joint axis being dynamic, which leads to bad results in TAA [34]. To overcome these results, it would be necessary designing new total ankle prostheses with the information in mind about the dynamic position of the ankle joint. These new designs would lead to the simulation of the real behaviour of the ankle joint axis and, consequently, the real behaviour of the ankle joint.

2.2.5. Gait cycle

The gait cycle is the name that is given to the time interval that separate the repetitive events of walking, events that are exactly alike. Frequently, it is established that the beginning of the gait cycle is the moment when one of the feet contacts the ground. The gait cycle continues until the moment when the same foot re-contacts the ground [60]. The gait cycle can be split into different phases, namely two periods. The first and the one that comprises the most of the cycle (about 60%) is the stance phase [16, 49]. This phase starts at the moment when the foot contacts the ground and it ends up when the swing phase begins, or, in other words, when the foot is in the air. This last phase comprises about 40% of the gait cycle [49, 60, 61]. Below, it is possible to observe the division of the two mentioned phases into subphases. However, there is no widely accepted nomenclature to describe both phases of the gait cycle, and the below designations are based on the movement and position of the foot [49].

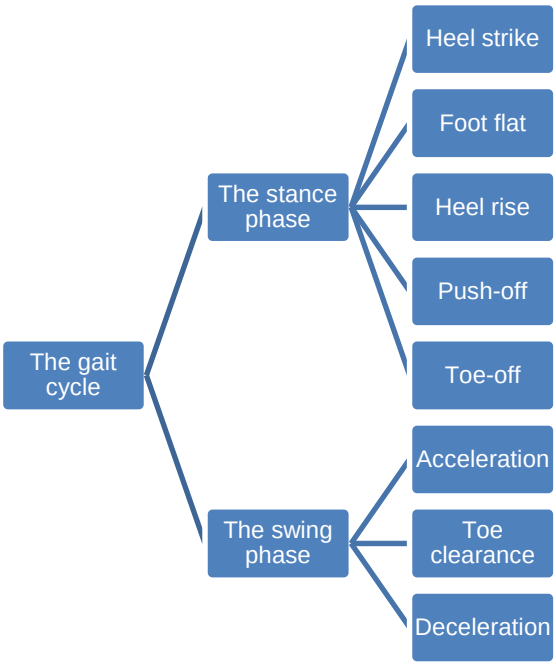

Figure 2.4 - The gait cycle: its phases and subphases [49].

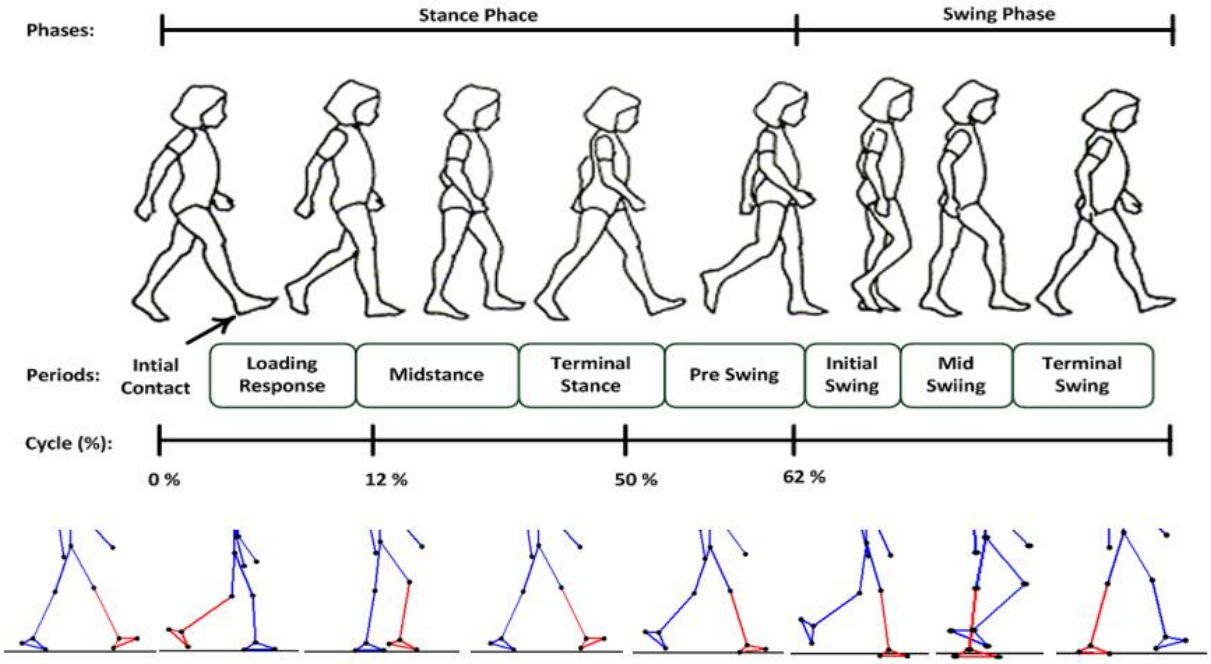

Figure 2.5 - The gait cycle.

It is important to describe why the subphases have the above designations and how the foot moves. The *heel strike* is the subphase where the heel contacts with the ground but contrary to what is expected, the contact is not made in the center of the ankle joint [32, 49]. This contact is offset laterally from the center of the ankle joint, and, this way the subtalar joint suffers eversion from *heel strike* to *foot flat*, where the maximal eversion occurs. In *foot flat* the foot gains flexibility to absorb the shocks that it is subject and it gains the capability of adaptation to the existing irregularities in the surface of the ground floor. These advantages acquired in this subphase are due to the internal rotation of the tibia conjugated with the pronation of the foot. Next subphase is *toe-off* and in this one it is possible to verify the maximal

inversion of the subtalar joint. In turn, the external rotation of the tibia occurs at *heel rise* and *push-off* [32, 49]. One of the main functions of the foot is to propel the body forward and to do that it is necessary that the foot has the right rigidity. This rigidity is provided by the conjugation of the inversion of the subtalar joint and supination of the foot [32, 62].

In a normal, correct and entire gait cycle two motions of dorsiflexion and two of plantarflexion are expected: both motions of plantarflexion and one of dorsiflexion happen during the stance phase, while the other event of dorsiflexion is located in the swing phase. Despite what was mentioned, there is another moment of dorsiflexion which is quickly, soft and insignificant. It happens thanks to the load response, and due to the contact of the heel with the ground, at *heel strike* subphase. After that, the first motion of plantarflexion happens, followed by the first event of dorsiflexion, where just the tibia shows movement. The neutral position happens in the *foot flat* subphase, followed by dorsiflexion. The maximum dorsiflexion is about 10º and occurs more or less in the middle of the gait cycle (about 48%). After this event, it is verified a quickly plantarflexion (about 15º), with which the stance phase ends, at the *toe-off*. Then, there is a dorsiflexion, which is the last one of this cycle and that starts the swing phase. Finally, the ankle stays in the neutral position since the *toe clearance* subphase until the end of the cycle, despite the verification of events of soft plantarflexion (between 3º and 5º) and the end of the swing phase [61].

2.2.6. The understanding of forces in the ankle joint through the years

The internal forces are of a kind that is very hard to measure *in vivo* whereby computational methodologies are used to make that measurements. These type of forces are generated by the ligaments and muscles existents at the local and that some way or another influenced the AJC. The external forces that act in the ankle joint can be measured thanks to a force platform in an experimental way and during the gait cycle. These forces are generated due to the contact between the body and ground and are called ground reaction forces (GRF). Then, the forces that are transmitted through the AJC consist in a mix/combination of the two mentioned types of forces: the internal and external [20]. Returning to the internal forces, it is important to refer that through the times a development of biomechanical models [15, 16, 63] has been verified with the purpose of calculate and measure the mentioned forces. However, they are not completely clarified because the AJC study is not very thorough especially when compared with other joints, like the knee and hip joints, which are extremely investigated. Nowadays, there are a broad set of techniques and methods that help in the acquirement of kinematic data from joints, such as telemeterized prosthesis (used for *in vivo* measurement of forces), computational and optimized models with the inclusion of muscle forces (to characterized the reality with more reliability), models of inverse dynamic, studies of gait cycle with the aid of fluoroscopy. Like it was said, other joints receive more importance than the AJC but lately it has been a target of greater curiosity, whereby there are, through the years, a development in the studies to calculate and measure the internal forces in the mentioned joint. Below, it is possible to see some of the referred studies [64-67].

- **Seireg and Arkvikar (in 1975)** → they calculated the joint reactions at the three joints, ankle, knee and hip. It is possible due to the introduction of a simple GRF as the input for the 3-D model of the lower limb. Thanks to a technique, focused in optimization, the sum of the muscle forces is minimized: relatively to the tangential forces, their maximum in x direction (anterior-posterior) and y direction (medial-lateral) are respectively the twice of body weight (BW) and the BW; relatively to the compressive force in z direction it is about five times the BW, specifically 5.2 times [64].
- **Stauffer *et al.* (in 1977)** → they created a model in two dimensions which simulates the ankle joint in a specific plane, the sagittal plane. The model utilized used an inverse dynamics and measured the reaction forces at the ankle joint in three types of subjects: patients with disabling joint disease, diseased patients retested after undergoing TAA, and healthy subjects [16]. In terms of results, it is possible to say that the maximum compressive forces (observed at the stance phase of gait) for healthy individuals was about five times the BW (between 4.5 and 5.5 times the BW). Another conclusion obtained was related to the patients with disabling joint disease (and showing good clinical results): the decrease of the joint load was about three times the BW and it was not verified a meaningful increase of it at post-operative level [20].
- **Procter and Paul (in 1982)** → they obtained a maximum torque of 40 N.m, which come from external and internal rotation of the foot, and a maximum compressive force, in average, about four times the BW (specifically 3.9 times the BW), which oscillated between 2.9 and 4.7 times the BW. These results were obtained due to an analysis in three dimensions of the ankle joint, realized in a force platform and during the stance phase of the gait cycle [15, 68, 20].
- **Reggiani *et al.* (in 2006)** → this team based their work in the information obtained from the mentioned works developed by Seireg and Arkvikar (the compressive and anterior-posterior tangential forces) and Procter and Paul (the internal-external torque and plantar-dorsiflexion rotation). Their model is in two-dimensions and with finite elements. It investigates many subjects, such as the kinematics, the forces of ligaments, and the contact pressures of the ankle joint [54]. Like it was said, they based their work in previous information, so they compared their own results with the previous ones (the results of Seireg and Arkvikar [64]) and concluded that the first data (namely, the hip joint contact forces) was 2.25 times bigger than their own data. This way, the force determined by the first group were properly dimensioned so the maximum compressive force is now 2.3 times the BW.

However, the opinion about internal forces in the ankle joint were not the only aspect that changes through the years. The weight-bearing capacity of the fibula has been a theme of discuss through over the time: before the seventies, it was accept that the fibula just stabilized the ankle joint and the transference of loads was made through the talus and tibia; after that, some evidences stablished that the fibula was responsible for the support of a percentage of the total load that acts in the ankle joint [20]. The evidences were from three groups of investigation: Lambert [68], Takebe *et al.* [69] and Wang *et al.* [70]. The first one used strain gages to observe that the fibula transferred 17% of the total load.

The second group mentioned showed that the first percentage obtained was a very high value. They inserted force transducers into parts of the bones that were resected with the purpose of measure the weight-bearing capacity of the bone of this issue, the fibula. Thanks to this measure, it was possible to understand that the fibula just carried a little percentage of the total load, between 6% and 7%. Other aspect that they understood was about the positions of the foot: when the foot suffers eversion and dorsiflexion, the fibula supports more quantity of load and when it suffers inversion and plantarflexion, the fibula carries less load, always compared with the neutral position of the foot. Finally, the last group of investigators, composed by Wang *et al.*, established that when loads of higher intensity are transferred in the leg, the percentage of the load supported by the fibula is higher.

2.3. Total ankle prostheses

There are many groups where total ankle prostheses can be inserted, according a specific classification that focuses some features.

Table 2.3 - Methods of classification of the total ankle prostheses [71].

Classification according to…	**Characteristics of each classification**
Number of components	Two or three components
Fixation type	Cemented and uncemented
Bearing type	Fixed and mobile
Component shape	With and without anatomic shape
Constraint type	Constrained, semiconstrained, and unconstrained
Congruency/conformity type	Fully congruent, partially congruent, and incongruent

Some of the terms mentioned in the table 2.3 are not completely clear. It is important to clarify concepts that lead to two different types of classifications, such as constraint and congruency/conformity. Constraint is the term attributed to the capacity of resistance of prosthesis to a particular degree of freedom. A prosthesis lightly constrained is a good choice because it simulates the normal joint range of motion, reducing the shear forces at bone-prosthesis interface. In other hand, when an excessive constraint is verified, it promotes high shear forces at the mentioned interface, leading to the lost, subsidence and, finally, to the failure of the prosthesis [19, 72-74]. The other group of terms is congruency/conformity. They constitute a type of prosthesis classification that is related to the geometric measure of closeness of fit between the articular surfaces of a joint/prosthesis. Incongruent or partially congruent prostheses have higher wear rates and reduced stability (depending on the ligaments to

provide the stability). These two characteristics are due to, respectively, the higher local stresses and the smaller contacting surfaces. In other hand, prostheses that are called fully congruent have full articular contact thanks to the fact that the articular surfaces have the same sagittal radii of curvature. Contrarily to the first type of prosthesis mentioned, these ones have low wear rates and great stability, thanks to, respectively, the lower local stresses and the larger contacting surfaces [71].

In the next sections, it is possible to understand the differences between the two major families of total ankle prostheses: the first and the second generations. More specifically, it will be explained the characteristics of two particular prostheses, that were chosen for the present study: the Agility™ (DePuy Orthopaedics, Inc., Warsaw, Indiana, USA) and S.T.A.R.™ (Waldemar-Link, Hamburg, Germany; acquired by Small Bone Innovations, Inc., Morrisville, Pennsylvania, USA). The reasons for this choice will be explained too.

2.3.1. The first generation

This generation of prostheses, called the first generation, were discontinued, as it is possible to see below. A prosthesis of this generation had two components in its constitution and, frequently, the talar component was made of metal and the tibial one was made of polyethylene. Furthermore, the method of fixation of this generation of prosthesis use cement, which is commonly used in joint arthroplasty nowadays. Like it was mentioned before, these prostheses could be divided in two groups, constrained prostheses, which are congruent, and unconstrained prostheses, which are incongruent [19]. However, there is an exception, the spherical prosthesis. This prosthesis is an unconstrained but, at the same time, a congruent prosthesis. This special case is not appropriate for TAA due to the fact of the stability is not provided by the prosthesis but by the ligaments, in spite of being congruent in a large range of motion, which means it is of unconstrained type. The fact of the stability depends on the ligaments to limit the motion of the prosthesis can be a negative aspect, when the amount of strain disposed in the ligaments is large [75]. The mentioned characteristics reinforce the idea that the unconstrained prostheses are not the most suitable to use in the surgical intervention treated in the present work. So, the prosthesis considered the ideal to be used in this intervention should perform only the normal ankle joint range of motion, or just the necessary, to simulate the normal kinematics of the ankle joint.

Although in the early days, when the first generation prostheses began to be used, the results of TAA had been very good, complications began to arise later. High failure rates and complications began to be verified after the TAA [71]. Below, it is possible to see some examples of complications:

- Due to the use of bad and inadequate instrumentation and the fact of the prosthesis just have one size, fractures of the *malleoli* were verified [72];
- Inadequate positioning of the prosthesis, due to the use of incorrect surgical instruments [71];
- Problems in skin, due to the extreme traction during surgical intervention [71];
- Larger resection of bone, thanks to the use of the method of fixation with cement [19];

- The prosthesis seating on spongy bone, which leads to the incapability of support the weight of the body and to component subsidence with early loosening. This is due to the excessive bone resection [1];
- Severe osteolysis, infections and wound problems incorrections [71].

Due to the mentioned complications, the arthrodesis was the treatment chosen in the eighties to solve the present problem. The total ankle prostheses of this generation, the first generation, were interrupted, discontinued, however, in the next decade, the nineties, the TAA began to be considered and investigated [19].

2.3.2. The second generation

Like everything, if the first generation of prostheses failed and generated many complications, it was because something should be changed and improved. Following this line of thought, some investigators did not give up in TAA and tried to solve the first generation problems, designing and creating new prostheses, with the purpose of mimic and substitute the function of the ankle joint, which comprises the biomechanics and the anatomy [76]. Below it is possible to see some improvements and changes:

- To prevent the bone suffers the risk of osteolysis, most of the prostheses started to be uncemented, because the particles of cement trigger this phenomenon [71];
- In the new prostheses, the fixation started to be the press-fit [71];
- A third component was introduced between the talar and tibial components [1];
- The instrumentation was substantially developed and improved [71].

One of the mentioned changes that stands out most is the insertion of the third component [71]. It was included to surpass complications related with constrained and unconstrained prostheses. This component is considered intermediate and it has a function of a bearing [20]. The main function of this component is the absorption the forces that pass through the fibula and tibia, and also the distribution of these forces in the talus. With this action, the prosthesis mimics more faithfully the real and normal ankle motion, even after TAA. This way, the new group of prostheses, called the second generation of prostheses, is constituted by two-component and fixed-bearing prostheses, which are semiconstrained. However, in the course of time, these prostheses started to be mobile-bearing and to have three components, becoming congruent and constrained [71]. Like it is understandable, the mobile-bearing prostheses absorb the forces, during motion, in the ankle, in a different way than the fixed-bearing. One more advantage of this family of prostheses is the material that constitutes the intermediate component: it is made of polyethylene - Ultra-High-Molecular-Weight Polyethylene (UHMWPE) -, being low friction and biocompatible. However, there is an exception, the TNK ceramic/metallic prosthesis. In the present case, the intermediate component is made of the first material mentioned [77]. Other aspect that is important to refer, is that the intermediate component, in the fixed bearing prostheses, is attached to the tibial component, which makes the prostheses have just one articulation, located between the intermediate and talar components, and acting like two-component prostheses despite having three components in their constitution, like it was mentioned [71].

These prostheses are not completely conforming, just partially, and this happens to reduce the constraint, which, in turn, is achieved, by the reduction of conformity. Thanks to the referred characteristic, this type of prostheses shows higher wear rates, an observation that is possible too due to the high local stresses verified from small contact areas, and poor and weak stability. Normally, when it is verified less conformity, the wear is greater [71]. One of the prostheses analysed in the present work, the Agility™, is an example of a fixed-bearing prosthesis, as well as Salto® Talaris (Tornier, Inc., Saint Ismier, France), INBONE® (Wright Medical Technologies, Arlington, Tennessee, USA), and Eclipse (Kinetikos Medical Inc., Carlsbad, California, USA/Integra LifeSciences Corp., Plainsboro, New Jersey, USA). The other prosthesis analysed in the present work is the S.T.A.R.™ and it is an example of a mobile-bearing prostheses, as well as SALTO® (Tornier, Inc., Saint Ismier, France), and Buechel-Pappas™ (Endotec, Inc., South Orange, New Jersey, USA). This type of prostheses has the mentioned intermediate component, that like it was said it is made by polyethylene [77]. This component is mobile like a meniscus, not fixed, with the purpose of foment the stability through the maintenance of the natural and normal ankle joint kinematics. Other objective of this component is to avoid loosening, through the reduction of the impact of the shear and axial constrains in the interface between bone and prosthesis which, in turn, promotes structural integrity. The mentioned situations can be achieved thanks to the existence of two congruent articulations in the mobile-bearing prostheses that are separated. However, the existence of a second articulation does not have just good aspects: it may increase wear, though always be smaller than wear of fixed-bearing prostheses. Other negative aspect of the mobile-bearing prostheses is the possibility of occurrence of dislocation (or subluxation) of the polyethylene component [71].

In order to be applied in clinical situations, in the USA, the total ankle prostheses should be approved and accredited by the Food and Drug Administration (FDA), which the major goal is to protect and promote the society health. Nowadays, there are five total ankle prostheses approved by FDA: the Agility™, Eclipse, INBONE™, Salto® Talaris, and S.T.A.R.™. Despite of the S.T.A.R.™ has had a recent approval by the FDA, in Europe it has been used since the beginning of the eighties [78].

Relatively to the other mentioned prostheses, that are approved by FDA, it is important to say that the Eclipse is not quickly accessible to all surgeons, even though it is already approved. This fact makes that this prosthesis just participate in a few implants. The Agility™, Eclipse, INBONE™, and Salto® Talaris prostheses have fixed-bearing systems and two components in their constitutions. The only exception is the S.T.A.R.™, which have a mobile-bearing design and three components in its constitution. Nowadays, the market uses the five mentioned prostheses but like in every economic fields, there are three prostheses that dominate: the Agility™, S.T.A.R.™ and Buechel-Pappas™. Below, it is possible to see the table 2.4 that shows some characteristics and differences between the Agility™ and S.T.A.R.™, and their role in the market [7, 80, 19, 81, 82], despite the detailed information present in the next sections.

Table 2.4 - Comparison between Agility™ and S.T.A.R.™.

Agility™ *vs.* S.T.A.R.™

Agility™	S.T.A.R.™
• It was the first total ankle prosthesis approved by FDA; • It has been the most widely marketed and used total ankle prosthesis in USA; • It has published studies documenting mid- to long-term results in the USA.	• It is the most popular total ankle prosthesis in Europe; • It has published studies documenting mid- to long-term results in the USA; • It is the only prosthesis where clinical studies have been carried out by authors without a financial interest in the product, which explains the amount of available information regarding particularly this prosthesis.

Taking into account the information exposed, it is clearly obvious the choice of studying the Agility™ and S.T.A.R.™.

2.3.2.1. Agility™ prosthesis

Agility™ prosthesis has two components in its constitution and shows a fixed-bearing design. It has a component made by polyethylene which is fixed to the tibial component [22] and has a concave shape in sagittal plane, increasing the stability in anteroposterior terms. This prosthesis enables to types of motion: dorsi/plantarflexion motion and axial rotation, due to the mismatch between the talar and tibial components and the fact of being semiconstrained. The wear could increase due to the increasing of the stresses of contact in the polyethylene component, which comes from the fact that the prosthesis be partially conforming. The prosthesis is partially conforming thanks to the fact that the articular surface of the tibial component be larger than that of the talar component. This difference enables the talus to seek its own position, decreasing the shear and compressive forces at the interface between prosthesis and bone [17].

Nowadays, Agility™ is no longer like it was when it was implemented for the first time, in 1984 [83]. It has suffered some alterations, namely in its material properties and in its design. Initially, there was just one material which predominated in the construction of its two components: titanium (Ti). However, some studies showed that in the next three years after the implantation, the loss of two talar components of the prosthesis had been verified, and for that reason there was a changing in material properties, substituting the Ti, in the talar part, for cobalt-chromium (Co-Cr) alloy [23]. Through the years, the Agility™ prosthesis has been suffered alterations, like it was said and, nowadays, it has on its constitution a talar part made of Co-Cr with sintered Co-Cr beads, and a tibial component which is made of Ti and sintered Ti beads [22]. In terms of design, the talar component was firstly approximated to the

real talus, which means, its anterior part was a little bit wide than its posterior part. This anatomical fact contributes to a bigger stability during the stance phase of gait. Relatively to the tibial part, and due to the fact of had been verified two broken components in about first two dozens of TAA with this prosthesis, the tibial component was altered to become thicker, which was a solution. This alteration did not constitute totally a good choice because it did not avail all the disposable surface area [17]. In order to resolve that bad use, a new and innovative design was created and established as the new choice for the TAA. This new design makes the difference at the posterior edge, where the total maximum stresses in bone are reduced, leading to a better performance when compared to the previous design. The posterior part was increased, the designs were reviewed to became more rectangular, and the wider talar components were developed; these changes happened due to the verification, in clinic terms, that the posterior subsidence led to fail in the previous design. Of course one of the things that naturally should be modified in the prosthesis design is the contact area of the talar component that was increased. In order to compensate the geometric change in the talar component, it is necessary to shorten the sidewalls of the tibial component [84].

It is important to mention that this prosthesis promotes the resurfacing of the articular surfaces of the lateral and medial talar facets, and the ankle joint. Additionally, with the purpose to obtain a better load distribution, an arthrodesis of the distal tibiofibular joint is made using, most of the times, two screws (although it can use only one) through the distal fibula into the distal tibia. The contact area can be increased and the load distribution can be improved if a base of support for the tibial component is broad and covers almost all exposed spongy bone. Relatively to the tibial component, it is possible to say that its lateral and medial walls sit close against the cut surface of the medial and lateral *malleoli*, bridging the tibial lateral surface and the fibula medial surface. There is an option, at the end of the process, to put a plate on the fibula. This plate is placed with the purpose to enhance the fusion of bone and increase the load distribution along the mentioned bone, the fibula [85], and of course is considered in the present work. Nevertheless, and backing to the mentioned screws, before their insertion, and because it is central to withdraw some interosseous membrane, the formed space is filled with bone graft taken from talar and distal tibial bones, which were excised. There are two possibilities to fill the mentioned space: multiple cancellous chips and an individual, large, well defined block of cancellous bone, which fits correctly [86]. With the Agility™, it is verified bone resection in high amount, which leads to the existence of less bone available for support. However, the Agility™ prosthesis also presents some negative aspects, such as the increasing of the tibial component loosening, due to the lack of union (or delayed union) of tibia and fibula after the arthrodesis, the subsidence of prosthetic parts, and the radiolucency. The mentioned complications are the most common in clinical use of Agility™ prosthesis [17].

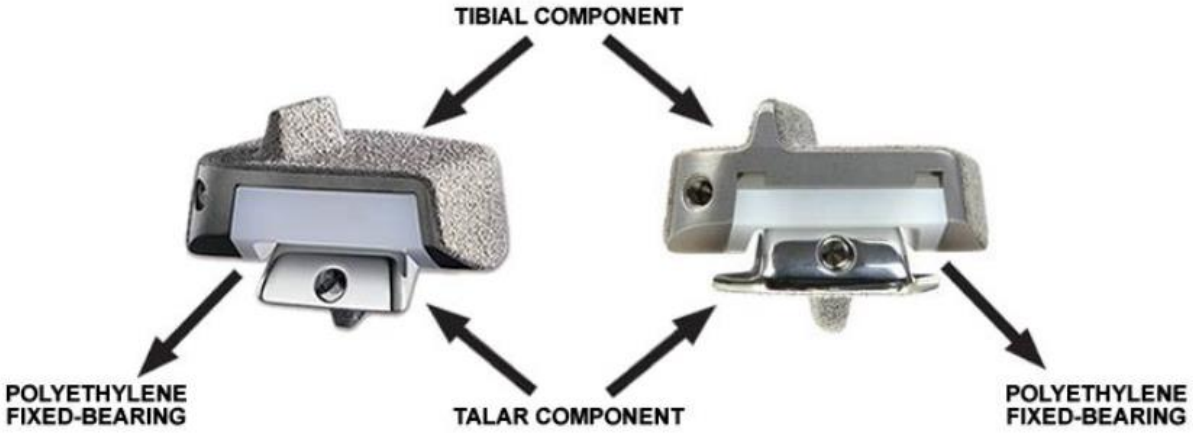

Figure 2.6 - The AgilityTM prosthesis. The first one is the old version and the second one is the new. Both have their components marked [87].

2.3.2.2. S.T.A.R.™ prosthesis

Like it was said for Agility™ prosthesis, the current S.T.A.R.™ prosthesis was not always like that. The first design of S.T.A.R.™ prosthesis had in its constitution two components, it was implanted in the eighties and was developed by a Danish orthopaedist [88]. The two components were made of different materials: the tibial component was composed by polyethylene and the talar one was made of stainless steel (SS). The method of fixation of this initial prosthesis was cement and it was fixed-bearing. This first design did not originate the expected results so it was modified. The new design of S.T.A.R.™ prosthesis is mobile-bearing, it has three components, and its method of fixation is uncemented, since the nineties [71].

The talar and the tibial components are made of the same material: cobalt-chromium-molybdenum (Co-Cr-Mo) with Ti plasma spray coating [89]. However, and like it was expected, they have anatomical differences, according their function in the AJC. The tibial component has two fixation bars with the purpose of increase the fixation to the tibia. The exposition of the ligaments to forces that they are not capable to support is due to the lower anteroposterior stability. This reduction of the anteroposterior stability is originated by the flat geometry of the tibial component. According to the talar component geometry, it is very similar to the real anatomical shape and it covers totally the dome of the talus. The polyethylene component has a medial-lateral stability regarding to the talar component. This stabilization is due to the fact of the configuration of the talar component has a longitudinal groove that agrees with a ridge in the distal surface of the polyethylene component [19]. Thanks to this characteristic, axial rotation is a motion that only occurs in the interface between the polyethylene and tibia components, and dorsiflexion and plantarflexion are motions that occur not only in the interface mentioned but also in the interface between the polyethylene and talar components [90].

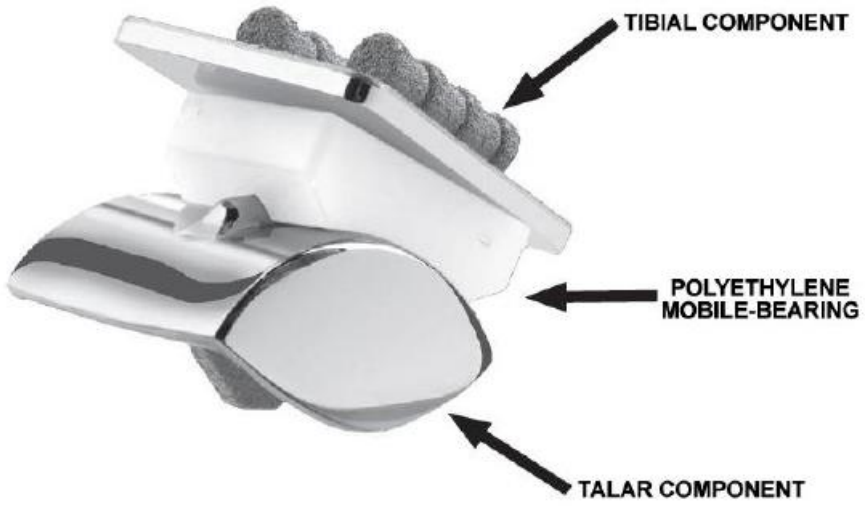

Figure 2.7 - The S.T.A.R.TM prosthesis, with its components marked [89].

2.3.2.3. Agility™ prosthesis *vs.* S.T.A.R.™ prosthesis

In terms of negative aspects, both the Agility™ and S.T.A.R.™ prostheses demonstrate problems. These prostheses, when applied, need other procedures, like secondary procedures, mainly in patients with post-traumatic amnesia and young patients, and they demonstrate elevated rates of complications. However, both prostheses satisfy in a high level the patients and confer reliable plain relief. In some aspects, namely the subsidence of prosthetic components, the rate of radiolucency, and the failure rates at greater than 10-year follow-up, the S.T.A.R.™ prosthesis presents better results than the Agility™ prosthesis [71]. Other advantage of the S.T.A.R.™ prosthesis is that it prevents from the complications associated to the delayed or non-union of arthrodesis. Finally, other characteristic of the S.T.A.R.™ prosthesis is that it resurfaces not only the surfaces of the articulation of the ankle joint but also the lateral and medial facets of the talar component, and it acts differently from the Agility™ prosthesis: while with the Agility™ prosthesis is required the arthrodesis of the joint named distal tibiofibular joint, with the S.T.A.R.™ prosthesis this procedure is not required. Consequently, due to the no requirement, there are no risks related with that process and there is significantly less bone resection [91]. The resurfacing of the lateral and medial facets is a process that creates doubts, because it has advantages and disadvantages: in a positive way, it may improve the distribution of forces and long-term stability of the talar component, but if the facets are preserved, less cortical bone is removed from the talus. It was studied and reported that the resurfacing of the facets are not fundamental and necessary, whereby this process was not included in the present work, for both prostheses. To decide which is the best choice, resurfacing or not, it is central to analyse which are the benefits that matter most for each situation and prosthesis: if the increased bone resistance and support through the preservation of the strong cortical bone of the facets, or the increased fixation and stability of the prosthesis through the resurfacing of the facets [17].

2.3.2.4. New designs of prosthesis

Nowadays, there are new designs available on the world market beside the existing total ankle prostheses, making about 20 different models. There are some aspects that they tried to improve and gave more importance in the realization of the new designs: improve the fixation, the importance/function of ligaments in the stability, minimize the resection of bone, the balance of soft tissue, options of recuperation for when the TAA fails, and correction of deformity. Below, it is possible to see the list of some of new prostheses, with new designs [81]:

- AES (BIOMET Europe, Belgium) [81];
- BOX® (MatOrtho™, Leatherhead, England): this prosthesis allows a normal ligament tensioning and re-establishes the normal kinematics at the treated joint [81];
- HINTEGRA® (Newdeal SA, Lyon, France/ Integra LifeSciences Corp., Plainsboro, New Jersey, USA): with the purpose of reduce bone resection in the treated joint, the screw fixation is used [92];
- MOBILITY™ (DePuy International, Leeds, United Kingdom) [81].

Finally, it is possible to affirm that these new designs are the perfect option to substitute the ankle joint, affirmation that is supported by the similarities verified between them, although there are no many clinical studies made [19].

2.4. Bone remodeling

2.4.1. Bone tissue

Bone tissue is a mineralized connective tissue and has many types of functions, namely biological, chemical and mechanical functions. It is a tissue completely different from the other body tissues thanks to its composite structure, which confers it special structural properties. Bone and other body tissues have different roles: bone is the tissue that determines the general structural strength and stiffness of the musculoskeletal system, and other tissues that will be mentioned below, are responsible for the transference of loads between bones. There are two important parameters to take into account when talk about bone: the stiffness and ductility [93]. These two parameters have to be in equilibrium to confer the known mechanical properties of bone: a perfect ductility to damp the impacts, and a perfect stiffness to get more efficient kinematics and lower strain [94]. The equilibrium between the stiffness and ductility in bone is reached thanks its three characteristics: anisotropy, heterogeny, and multiphase [93]. These characteristics are due to the irregular but optimized disposition and orientation of the bone components of the hierarchically organized structure. Thanks to this, different structural levels of bone demonstrate different mechanical properties: macrostructure presents cortical and trabecular bone, microstructure (10-500 μm) has both cortical and trabecular bone, in the form of osteons and single *trabecula*, respectively, sub-microstructure (1-10 μm) demonstrates lamellae, nanostructure (few hundred nm-1 μm) presents both collagen fibrils and embedded mineral, and finally, sub-nanostructure, which is

located below the last one, is characterized by collagen, mineral, glycoproteins and proteoglycans [95-98].

Like it was said, this type of tissue realizes a huge range of functions, some more known than others, such as blood cell production, storage and release of minerals, contributing to the mineral homeostasis, triglyceride storage, and more obvious, body protection and support, and an important role in movement [93]. Despite the bone being the mainly interposer in the mechanical functions, these ones are also done with the aid of others skeletal tissues, namely muscles, ligaments, tendons and cartilage. The mainly mechanical function that is done by the mentioned tissues is the transmission of forces between parts of the body, regulating the strain at the same time. These two processes mentioned, allow the protection of vital organs and the movement of the whole body [94].

2.4.2. Biology of bone

2.4.2.1. Bone cells

In percentage terms, the extracellular matrix of bone is mainly constituted by crystallized mineral salts (55%), it has about 30% of collagen fibers and, finally but not least, 15% of water. This matrix involves cells that are widely separated and together they both make bone a specialized connective tissue. These cells are known as bone cells, they have between 10 and 100 μm and can be one of the four types: osteocytes, osteoclasts, osteoblasts and osteogenic cells. The osteogenic cells are the precursors of osteoblasts. They are stem cells, with no specialization, and they can suffer cell division, leading to the origin of osteoblasts. Osteoblasts or bone-building cells are cells that synthesize extracellular matrix of bone and start the calcification. This type of cells are involved in extracellular matrix and they are caught in their own secretions: when this happens, osteoblasts transform themselves in another type of cell: the osteocytes. The major function of the mature osteocytes is the maintenance of bone daily metabolism. At last but not least, bone has osteoclasts which have a digestive role. They are fundamental in the bone resorption, digesting the organic and inorganic components of the extracellular bone matrix, thanks to the liberation of acids and enzymes. The bone resorption is the more important process that happens in bone because it is responsible by its reparation, maintenance and development [99].

2.4.2.2. Types of bone

Like it was said before, it is possible to distinguish bone in two types, macroscopically talking: the cortical bone and the trabecular bone. The first one, the cortical bone, is the most abundant bone in the skeleton, comprising about 80% of it. It is compact and dense, completely the opposite of the other type, the trabecular bone, which is cancellous and spongy and constitutes the rest of the skeleton, about 20%. Thus, the main and most notorious difference between this two types is the density or the degree of porosity [99]. Let’s see their characteristics in more detail.

2.4.2.2.1. Cortical bone

Taking into account the main difference between the two types of bones, their density, it is possible to say that the cortical bone is very dense. This type of bone is strong and heavy and it has a porosity between 5% and 10%, which is very low. This value of porosity can be translated in the measurement of the apparent density, which is the ratio between mass and total volume [99]. The apparent density of cortical bone, in the human skeleton, is assumed to be about 1.8 g/cm^3 [100]. Rings of calcified extracellular matrix, called concentric *lamellae*, are organized and disposed around a central canal – Haversian canal - to constitute osteons or Haversian systems. These osteons are structural units that when repeated form the cortical bone with its structural organization known. The Haversian canal has an important role in the nutrition and support of the cortical bone: it works like a little network of nerves, lymphatic and blood vessels. Thanks to this network, the osteocytes of the cortical bone can have access to the nutrients and oxygen, and can get rid of wastes, resultants of some processes. It is also worth mentioning that the nerves and the lymphatic and blood vessels from the fibrous layer covering all bones, the periosteum, penetrate the cortical bone. This penetration is made through the Volkmann's canals, which are transverse canals that perforate. Thanks to these canals, it is possible to say that the periosteum (the nerves and both vessels referred) is in contact with the Harversian canals and the medullary cavity, from the bone marrow. Back to the *lamellae*, it is possible to say that they are separated by small spaces – the *lacunae*, where are osteocytes and from where canaliculi radiate in all directions [99].

Like it was said, bone is a strong tissue due to many facts. One of them is the alignment of osteons with the long axis of the bone and, consequently, the increase of resistance of the axis of a long bone to bending or fracturing in many situations, such as when a strong force is submitted from either extremity. According to what was mentioned, the cortical bone appears to be thicker in zones where stresses are applied in just some directions. Thus, the cortical bone provides support, protection and resists stresses promoted by every movements and weight because it is a good material to constitute the external layer of all bones and the most part of the diaphysis of long bones [99].

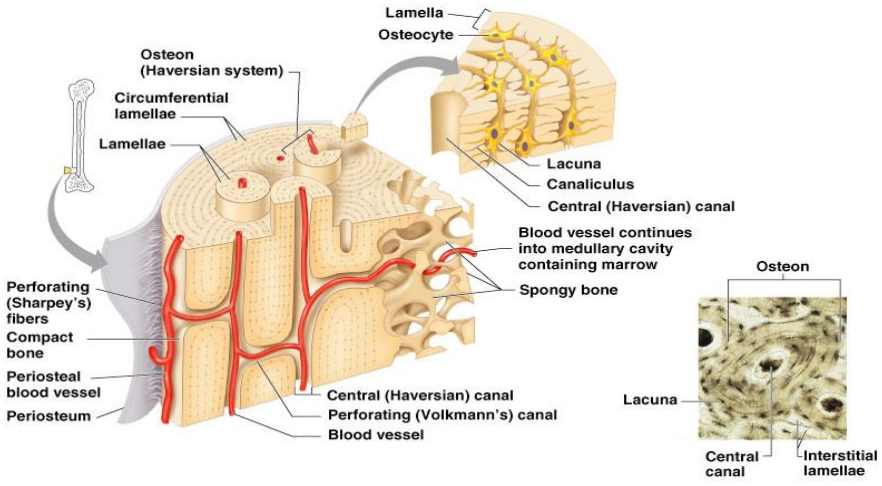

Figure 2.8 - Structure of the cortical bone [31].

2.4.2.2.2. Trabecular bone

As was said, the main differences between the two types of bones are the porosity, which in the trabecular case is between 50% and 95% [94], and the apparent density that varies from the 0.1 g/cm^3 to 1.0 g/cm^3 [100]. The mentioned values confer some characteristics to the global structure of bone, namely flexibility, elasticity and resilience. This way, it is verified an increase of the capability to absorb energy from impacts and, consequently, the adaptation to the mechanical solicitations is facilitated [99].

The trabecular bone has a hierarchical structural organization. It is composed by an irregular framework of thin columns of bone, called *trabeculae*. The *trabeculae*, in turn, is constituted by *lamellae*. The osteocytes supply (oxygen and nutrients) and waste removal are made thanks to the little blood vessels existing in both bone marrows. The bone marrows fill the spaces existing between the referred *trabeculae*, being supported and protected by the trabecular bone, and can be one of the two types: adipose tissue, which is called yellow bone marrow, and connective tissue, with the function of producing the basic blood cells and named red bone marrow [99].

The trabecular bone is localized in places where bones are not subject to stresses applied from several directions or heavy stresses, composing the most of the bone tissue of irregular shaped, short, and flat bones, and the proximal and distal extremities of long bones, called the epiphyses. These locations are possible thanks to the precise orientation of the trabecular bone along the lines of stresses, increasing its capability of resistance to stresses and transference the forces without failure [99].

2.4.2.3. Bone remodeling process

Bone remodeling can be called bone turnover and it is a process that seems not happen, when it is looked with naked eye. Thanks to the strong structure of bone, it seems to be very stable, without any change in time. However, this idea is completely wrong. Bone is a dynamic tissue that is always suffering changes over time. These changes are very subtle and can be in different categories, according to what is happening in the bone environment: they can be in composition, structure and shape and depend on whether the environmental stimuli are hormonal, physiological and mechanical. The main purpose of bone remodeling is maintain the integrity and stability of bone, in order words, is to achieve the bone homeostasis. In few words, bone remodeling happens during life and it is the continuous replacement or substitution of bone tissue which is old or damaged by new bone. Like it was said, the bone remodeling is a process that is always happen: at any moment of life, in the body, there is about 5% of the total bone mass being remodelled [99].

In terms of numbers, there is a difference between the renewal rates of the cortical and trabecular bone: the first one has a rate of 4% per year while the second one has a rate of 20% per year. In addition, it is important establish a relation between the strength of bone and the degree of stress that it is subjected: if the loads are heavy, the new bone formed will develop itself thicker and it will be stronger than its precursor [99].

Bone remodeling is a process that englobes two activities: bone formation and bone resorption. Bone formation is closely associated to the activity of osteoblasts because they add collagen fibers and

minerals to bone leading to the formation of extracellular matrix of the bone. On the other hand, bone resorption happens thanks to the activity of osteoclasts because they remove the collagen fibers and minerals from bone leading to the destruction of extracellular matrix of the bone. Synthetically, bone formation and bone resorption are opposite processes that complement each other. The basic multicellular units (BMUs) [101] are clusters of cells that function like organized units and perform the remodeling, substituting old bone by new one. They act in cortical bone, surfaces of trabecular bone, bone periosteum and endosteum [99].

There is an investigation field that conjugates mechanics and biology, the mechanobiology, and it studies the phenomena inherent to the interface between biology and engineering. Due to the fact of the bone remodeling being influenced by the mechanical loading, one of the more important studies performed by the bone mechanobiology is how the mechanical forces can be demonstrated/expressed in bone cells. Nowadays, it is known that the bone structure is commanded by a regulatory mechanism which is local [102]. The existence of a local regulatory mechanism is supported by two different ideas, established in the same century: in 1881, Roux [102], said that the bone remodeling provides, to bone, the capability of self-repairing, which make it a self-organizing process, and a decade later, in 1892, another investigator originated a law which is currently still known: the Wolff's law. Wolf [29] admitted that the structure and morphology of bone is dependent of the loads that are applied, and established his law thanks to the observation of the *trabeculae* alignment: this is characterized by the alignment with the principal stress directions and it explains the anisotropy of the bone. Anisotropy is the name given to the fact that the stiffness and strength of bone vary according to direction. This structural property allows the increase of structural efficiency, thanks to the capability of trabecular bone support a heavier load without increasing mass. Taking into account the definition of anisotropy, it is possible to say that the trabecular bone is stronger and stiffer in the direction of the alignment of the *trabeculae*, when compared with other directions. The morphology and structure of the *trabeculae* and osteons are dynamic, not static, and change in the course of time due to the physical demands that physical conditions to which the skeleton is subjected. It is related to the fact of the lines of stress in a bone are dynamic, not static, changing in life, during growth, due to fractures, physical deformity, repeated vigorous physical activity – weight training, for example, and so on [99].

Frost [102] had an important role in the study of bone adaptation, with his theories. He established that the bone mass is regulated by the local strains, this is, everything plays around a mechanical threshold: if the strain levels are below that value, it is verified bone resorption; however, if the strain values are over that threshold, bone formation happens. Although this was just a theory and in a qualitative way, it was used as a basis of many theories [103-107], either computational or mathematical, created to deepen the study and investigation of bone adaptation. In the present work, it is used a mathematical model of bone remodeling that was developed by Fernandes *et al.* [25]. This model was proposed to simulate more reliably the biomechanical behaviour of the bone. Another models, similar to this one, were created by another authors, motivated by the creation and development of innovative mathematical concepts and computational tools associated with structural optimization.

It is verified an equilibrium between the bone resorption and formation, when it is in a homeostatic equilibrium. However, the homeostatic equilibrium is not always verified: there are some situations like space flight, long term bed rest and during immobility, known as conditions of disuse, where bone is lost due the occurrence of more resorption that formation. The homeostatic equilibrium is also lost when there is an insertion of a prosthesis in bone [102]. Of course, with this insertion, the stresses gain a new distribution, thanks to the phenomenon of stress shielding, which consists in the fact that the prosthesis carries the stress significantly more than the bone, decreasing the stress in this tissue. This situation promotes the resorption more than the formation, which turns the bone more conducive to have fractures due to its weakness [25].

If the bone remodeling process and consequently the mechanical behaviour of bone are understand, the creation and design of new prosthesis and the choice of the adequate prosthesis for a given patient are benefited. It is important to value the importance of the models that describe the bone behaviour according to the load conditions, because they allow the evaluation and estimation of the quantity of the bone resorption in the case of a specific prosthesis design. The model used in the present work is one of those [25].

2.4.3. Bone remodeling model

The model used in the present work was developed by Fernandes *et al.* [71, 72], with the implementation presented in Quental *et al.* [108]. The mentioned model has as basis the Wolff's law and assumes that the bone self-adapts with the purpose of find an optimal structure to support the load to which it is subjected. To attempt to reach the microstructure of trabecular bone, it is considered an open cell unit, with rectangular holes [27]. To obtain the material properties of bone, the method of homogenization (see for instance Guedes *et al.* [109]) is used. This method allows the achievement of the effective elastic constants. The maximization of the overall stiffness of the structure is obtained thanks to the minimization of the work of the applied forces. This minimization is realized to obtain the optimal topology. The optimal topology is possible due to the use of a multiple loading criterion that considers different load conditions at different temporal instants. Regarding to the optimal bone density distribution, it is influenced by the parameter k, which is an additional term that is associated to the biological cost of the organism in maintaining bone homeostasis and controls the total bone mass. The introduction of this term in the cost function makes that the model takes into account parameters of two natures, mechanical and metabolic. Thus, the model is more truthful and approximated to physiological condition of bone. The real reason why this parameter is included in the cost function is because bone formation demands a higher energy spent by the body, which is provided by the constant vascularity in the local where the bone formation is happening [25]. The process of bone remodeling follows the node-based approach implemented by Quental *et al.* [108] in the present model, which was proposed by Jacobs *et al.* [111].

It is important to mention some aspects that characterize the mentioned model and that make it so successful. It allows the perception and the better understanding about biological mechanisms that underlying the bone remodeling. This understanding is possible thanks to the prediction of the optimal distribution of bone density. The bone adaptation is also predicted by this model, after the occurrence of the prosthesis implantation. The understanding of the bone adaptation provides the identification of the most affected areas and the demonstration of the phenomenon of stress-shielding. Thanks to the model characteristics, it is possible to understand more deeply the difference between the use of different prosthesis designs and, more important, the biomechanics of bone. Due to that, it is a good choice to use the model in tests of prostheses, before the insertion of them, called pre-clinical tests. This use should take into account different constituent materials, geometries, among others [102, 112, 113].

2.4.3.1. Material model

In this case, the bone is modeled as a linearly elastic porous material with a periodic microstructure, which is obtained by the repetition in space of a cubic cell with rectangular holes. The edges of mentioned cubic cell are represented by the dimensions a_1, a_2 and a_3 (figure 2.9).

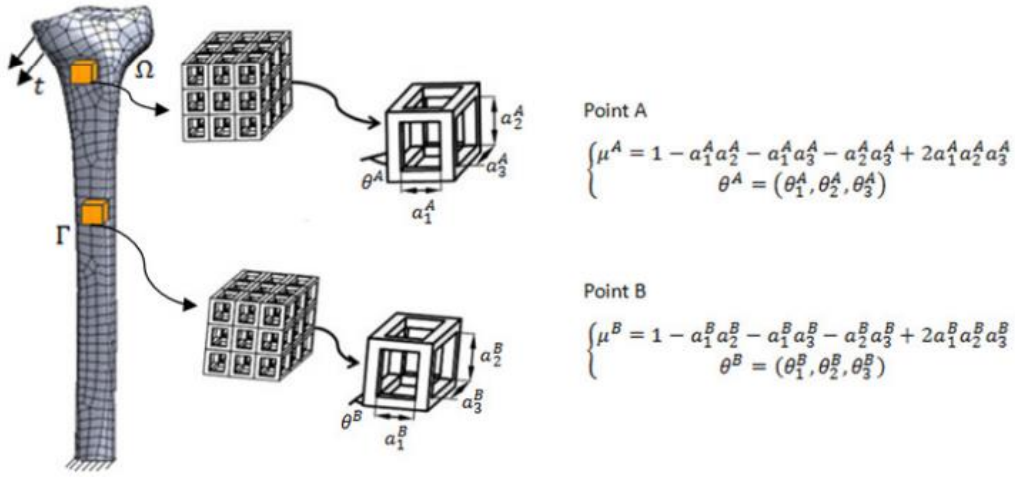

Figure 2.9 - Material model for bone (adapted from [27, 108]).

At each point, the local relative density of bone is defined by the parameters $\boldsymbol{a} = (a_1, a_2, a_3)^T$ and the orientation is characterized by the Euler angles $\boldsymbol{\theta}=[\theta_1, \theta_2, \theta_3]^T$. Considering the open unit cell, the relative density, μ, is given by:

$$\mu = 1 - a_1.a_2 - a_2.a_3 - a_1.a_3 + 2\, a_1.a_2.a_3, \text{ for } a_i \in [0,1],\ i = 1,2,3 \qquad (2.1)$$

Taking the above expression into account, it is easily understandable the below relations [108]:

- For a null value of relative density, $\mu = 0$, the a_i parameters take the value of one, $a_i = 1$ (for i =1,2,3), which in anatomic terms corresponds to the absence of bone;
- For an unitary value of relative density, $\mu = 1$ (the maximum relative density), the a_i parameters take a null value, $a_i = 0$ (for i =1,2,3), which in anatomic terms corresponds to the cortical bone;

- The intermediate values of the relative density (*0 < μ < 1)* correspond, in anatomic terms, to the trabecular bone.

Moreover, the proposed formulation considers the bone as orthotropic, allowing the simulation of bone as an oriented material.

Like it is easily comprehensible, it is hard to represent/define each individual cell of the microstructure. This way, the method of homogenization is used to obtain a homogeneous material that faithfully represents a heterogeneous material, due to the porosity verified. The main goal of this method is to achieve the equivalent elastic properties of the heterogeneous material, for the homogeneous one. They should seem equivalent to each other in the macroscopic properties. The mentioned method treats the bone as a global structure, which has much bigger dimensions than the dimensions of a cubic cell existent in each point of the space and that is repeated in a periodic way, like it was referred before. The material heterogeneity is due to the fact of for each point in the space, the behaviour of the cell condition the equivalent elastic properties. For detailed description of this method see [109].

2.4.3.2. Mathematical formulation

The law of bone remodelling is derived considering that bone adapts to achieve the stiffest structure with the total bone mass controlled by some biological parameters. Thus, the bone density distribution is obtained solving an optimization problem that can be formulated, using a multiple load formulation, as,

$$min_a \left[\sum_{P=1}^{NC} \alpha^P \left(\int_{\Gamma_f} f_i^P u_i^P d\Gamma \right) + k \int_{\Omega_b} (\mu(a))^m \, d\Omega \right] \tag{2.2}$$

subjected to

(2.3)

$0 \leq a_i \leq 1, \ i = 1,2,3$

Where the first term of the equation (4.2) is the weighted sum of work done by the external load case ***f*** for all load cases *P.* In this equation ***u*** is the displacement field obtained by the solution of the equilibrium equation for an elastic body (with domain Ω_b and boundary Γ) subject of a set of loads ***f*** on Γ_t. The second term controls the total bone mass where the parameter k and m are biologic driven parameters and $\boldsymbol{\mu}$ is the bone relative density computed by equation (4.1). It should be noted that NC means the number of load cases, while α^P symbolizes the respective load weight factors, leading to the equality $\sum_P^{NC} \alpha^P = 1$.

Regarding to the cost parameter κ, it is important to say that it is constant, with no changes, during all the bone remodeling process, because it does not vary with the location, and that it has an important role in the resulting bone mass. Given that the maintenance of bone homeostasis exhibits a higher cost

to the organism, when k has higher values, the resulting bone mass of the optimal structure is lower. It is hard to establish an exact value for this parameter for a specific individual, because the bone remodeling is a complex and intricate process that varies from person to person, even it is possible to observe the same loading situations. This way, there are many biological factors that interfere with k, the cost parameter, like disease, age, hormonal characteristics, and so on. In the right side of the objective function there is other parameter, m, that symbolizes a corrective factor for the preservation of the intermediate densities.

The solution of the problem stated above is obtained using an augmented Lagrangian formulation. The optimal condition of the problem given by,

$$\sum_{P=1}^{NC}\left(\alpha^{P}\frac{\partial E_{ijkl}^{H}}{\partial a}e_{kl}(u^{P})e_{ij}(v^{P})\right)-k\frac{\partial \mu^{m}}{\partial a}=0 \tag{2.4}$$

corresponds to the bone remodelling law, in the sense that whenever it holds the remodelling equilibrium is achieved. In the equation (4.4) E_{ijkl}^{H} defines the homogenised material properties tensor, e_{ij} the strain field and u^{P} and v^{P} are the displacement and the virtual displacement field, respectively. The major steps of the numerical process used to solve the above equation are presented in the next section. For a more detailed description of the model see [69-74].

2.4.3.3. Computational implementation

To solve the equations from the last section, a numerical procedure is adopted and below it is possible to see the actions that complete this procedure.

1. It is verified the calculation of the homogenised elastic properties for an initial solution, represented by a_0. However, this operation demonstrates a high computational cost and in order to minimize it, a polynomial interpolation is made for each iteration, with the purpose of obtain the mentioned properties. This interpolation is realized for values of a_i between 0 and 1, when *i* takes the values of 1, 2 and 3 [114].
2. Take into account the loading conditions and thanks to the ABAQUS®, the virtual displacement field - v^{P}, and the displacement field - u^{P}, are calculated by FEM.
3. The equation (2.4), present in the last section, is constituted by the stationary/optimal condition, which is verified, due to the FE approximation. The stationary condition can present two situations, described below:
    a. If the stationary condition takes the zero value, the solution of the problem was obtained and the model is in an equilibrium state. The solution of the problem is equivalent to the optimal distribution of bone density and the equilibrium state means that it is verified the equilibrium between bone formation and bone

resorption. In anatomic terms, this happens when the stiffest material of bone for a given loading conditions is observed [112, 114].

b. If the stationary condition does not take the zero value, in other words, is not respected, it takes place a sequence of situations: the computation of the improved values of the Lagrange multipliers and the design variables happens, which leads to the updating of the contact conditions, restarting all the process, like it is a loop situation. This way, is easily understandable that the process only finish when the stationary condition is satisfied (or the equation (2.4) is verified) [28, 114].

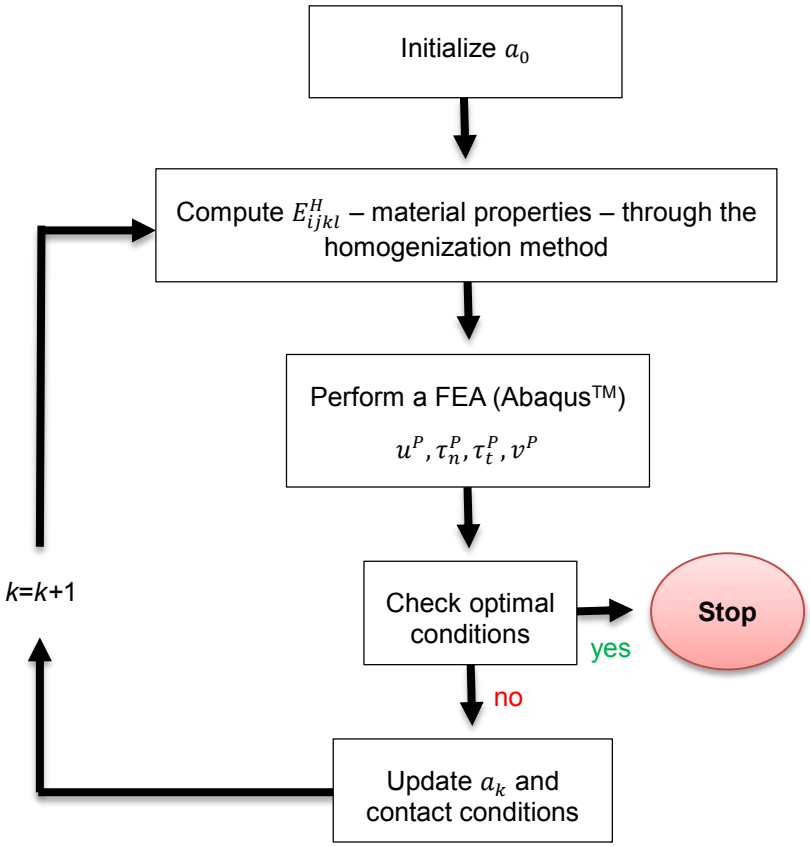

Figure 2.10 - Flowchart of the bone remodeling algorithm (adapted from [114])

Each node of the structure circumscribes a region of porous material that presents the same properties, which is equivalent to the same microstructure. This characteristic is verified due to the fact that the relative density be constant on each node of the structure. Like it was mentioned before, the parameters that describe the distribution of material and consequently are related to the density are $\boldsymbol{a} = (a_1, a_2, a_3)^T$. They are called design variables and characterize each node in the space. The FEM allows the discretization of the problem, which is important because it makes possible to found, for each node in the structure, the optimal condition. This way, each node has its own optimal condition, independently of the others [23]. A 1st order Lagrangian method [116] is used to found the solution of the problem in

an iterative way and below it is possible to find the mathematical expressions that update the cell parameters at the k^{th} iteration, for the cases where *i* takes the value 1, 2 and 3.

$$(a_i)_{k+i} = \begin{cases} max[(1-\zeta)(a_i^e)_k, 0] \; if \; (a_i^e)_k + d(D_i^e)_k \leq max[(1-\zeta)(a_i^e)_k, 0] \\ (a_i^e)_k + d(D_i^e)_k \; if \; max[(1-\zeta)(a_i^e)_k, 0] \leq (a_i^e)_k + d(D_i^e)_k \leq \; min[(1+\zeta)(a_i^e)_k, 1] \\ min[(1+\zeta)(a_i^e)_k, 1] \; if \; min[(1+\zeta)(a_i^e)_k + d(D_i^e)_k \end{cases} \quad (2.5)$$

In the above equation (6) it is important to describe some of its elements, to easily understand their meaning: e varies over all the finite nodes, D_i^e symbolizes the component of the downward direction vector relatively to the parameters of the microstructure - a_i^e, that is obtained thanks to the negative of the Lagrangian gradient, also relatively to a_i^e, like it is possible to observe below:

$$D_i^e = -\sum_{P=1}^{NC} \left(\alpha^P \frac{\partial E_{ijkl}^H}{\partial a_i^e} e_{kl}(u^P) e_{ij}(v^P) \right) + k \frac{\partial \mu^m}{\partial a_i^e} = 0 \quad (2.6)$$

To achieve a smoother iterative process, without drastic changes between iterations, it is defined the condition $\zeta > 0$ which establishes both active lower and upper bound constraints to obligate small changes in density. Other parameter, a real number, is the length of the step, symbolized by *d*, which is selected by the user at the beginning of the process and it is constant. Finally, there are considered steps proportional to the negative of the gradient with the purpose of find a local minimum of the function, in other words, it is used the method of steepest descent. For a more detailed description of the model see [69-74].

3. Computational modeling

This section essentially presents the way how the FEA was processed, using the ABAQUS®, besides other considerations, such as the geometric models used and some characteristics related to the use of the remodeling model. It is not presented a subsection about the geometrical modeling, including the assembly of the geometric parts, in SolidWorks®, because it was done by Daniela Rodrigues, in her Master Thesis [30]. However, it should be referred that the 3-D solid models of the intact AJC include cartilages, interosseous membrane and, of course, the four bones mentioned before – tibia, fibula, talus and calcaneus, and the two prostheses under study are the Agility™ and S.T.A.R.™. Then, options selected and taking into account during the FEA will be mentioned, besides the specifications of the bone remodeling model, which is attached to the FEM, to obtain the mentioned analyses.

3.1. FE modeling

Like it was mentioned before, it was verified the importation, from the SolidWorks® to ABAQUS®, of the three models that were developed by Daniela Rodrigues [30] and are under study in this work. After this importation, there are introduced ligaments which characterize mostly the AJC and that were mentioned before:

- LCL (ATaFi, PTaFi and CaFi), MCL (DATiTa, DPTiTa and TiCa) and two ligaments of the SLC (ATiFi and PTiFi), according to some previous studies [54, 117, 118].

It was an important action due to the fact of some of these ligaments, namely TiCa and CaFi, play a central role in the guide of passive motion. There are not included every ligaments because some of them do not guide the motion, limiting it [127].

The main purpose of the ligaments insertion is to maintain the same area for each ligament anchoring, this is, for all the models under study, it was taken care the respect of the same area for the insertion, on the bone surface, of each ligament. These areas respected anatomical data and images, from a specific study. The referred anchoring was performed through the association of a reference point (RP) to each area corresponding to an anchoring surface. The approach used in this association was the coupling and the definition of each ligament was the connection between two corresponding RPs, that have logic in the anatomical point of view. The coupling is verified between the anchoring surface and its corresponding RP, which causes the association between each ligament and the anchoring surfaces. Thus, the avoidance of artefacts from the stress concentration and the representation of the physiological state are possible due to the mentioned association, which causes the uniform distribution of the forces in the surfaces [38].

Situations of laxity or pre-tension were not taken into account in this insertion and the modelation of each ligament was made as a tension-only truss element. To avoid the occurrence of compressive

stress, due to the fact of the ligaments just support the tensile force, it was taken into account an option, in the software, that modify the elastic characteristic of the material, not allowing the compression.

3.2. Material properties

Bone is a material with some characteristics that are hard to represent in computational models, namely, FE models. These characteristics are the anisotropy, the heterogeneity and the viscoelasticity. Bone is called an anisotropic material due to its dependence of the direction and its heterogeneity is related with its density, mechanical resistance and density [93, 119]. Bone and other tissues involved in this study were represented differently:

- **Bone:** Isotropic; heterogeneous, due to the distinction between cortical and trabecular bones, and linearly elastic.
- **Cartilages and interosseous membrane:** Isotropic; homogeneous and linearly elastic.

Table 3.1 - Material properties of the natural constituents of the models (for Abaqus®, not for the remodeling model).

	Cortical bone	Trabecular bone	Cartilage	Interosseous membrane	Bone graft
Young's modulus	19 GPa	500 MPa	1 MPa	99.5 MPa	200 MPa
Poisson's coefficient	0.3	0.3	0.4	0.49	0.3

It is important to note that the information presented in the table 3.1 refers to the values take into account for the FEM in Abaqus®, not for the remodeling model, where the bone just has one value for the Young's modulus and Poisson's coefficient, not being divided in cortical and trabecular bones.

The real thickness of the cortical layer was not respected which is important to take into account. The cortical layer consisted only in the external surface of each bone (its nodes and elements), which presents a Young's modulus of 19 GPa [120]. The remaining elements and constituent nodes, localized more internally, presents a Young's modulus of 500 MPa [122]. Since the thickness of the cortical layer varies with the length of the bone (it is greater in the diaphysis that in the extremities), this assumption is a negative aspect of the present work.

The bone was compared to a cellular material in its modelation, and it is assigned to it a microstructure characterized by the orthotropy. In this case, the relative density comes from the solution of the optimization problem (coming from the material optimization problem). This comparison was made to perform the analysis of the bone remodeling. Thanks to the homogenization method [109], it was possible to obtain the elastic equivalent properties. The layer of the cortical bone presents a Young's modulus of 19 GPa as it was mentioned. The cortical bone is very dense and the maximum value of the relative density that is possible to exist, $\mu = 1$, for this situation, corresponds to its layer. This way, the other values of the relative density, considered intermediate values, are equivalent to the intermediate values of Young's modulus and, in this situation, the elastic properties are functions of relative density. Then, for the two bones under bone remodeling analysis, the tibia and talus, there are established different values of density, consonant the layer of bone that is considered. For all the nodes that do not

correspond to the external surface, corresponding to the cortical bone, it was considered as initial condition a value of relative density – 0.3 - which allows to vary the values from 0.05 to 0.99. For the remaining nodes, the nodes that composed the external surface of the bones, it was considered as initial condition a relative density of 0.9 which allows to vary the values between 0.75 and 0.99

The material properties of the bone graft and interosseous membrane are not mentioned in the literature, such as books, scientific articles. This way, the bone graft is compared to the trabecular bone, although it as treated as it was weaker than the mentioned bone, with a Young's modulus of 200 MPa. In relation to the interosseous membrane, it is compared to the DPTiTa, which is the ligament with smaller stiffness, like is was mentioned, so its Young's modulus was 99.5 MPa and Poisson's coefficient was 0.49. Finally, the cartilage presented a Poisson's coefficient of 0.4 and a Young's modulus of 1 MPa [123]. Below, it is possible to see the material properties of the constituents of the models that do not represent natural parts but artificial ones.

Table 3.2 - Material properties of the artificial constituents of the models.

	Agility™				**S.T.A.R.™**		
	Talar part	**Tibial part**	**Polyethylene part**	**Plate and screws**	**Talar part**	**Tibial part**	**Polyethylene part**
Young's modulus	193 GPa	110 GPa	557 MPa	110 GPa	210 GPa	210 GPa	557 MPa
Poisson's coefficient	0.29	0.33	0.46	0.33	0.3	0.3	0.46

3.3. Interaction among parts

Below it is possible to observe a synthetic list that characterizes the interactions existent between the parts of the models present in this work. The list is organized by parts.

- **Between cartilages** → This type of tissue is characterized by its lubrication, existents in their surfaces which present an articular nature. This way, the interaction between cartilages was considered frictionless [58], with a value of coefficient of friction of 0.01 [124]. It was selected a surface-to-surface contact between cartilages.
- **Between cartilage and bone** → The surface interactions between the cartilage and bone were rigidly bonded – tie.
- **Between interosseous membrane and bones** → the bones that are mentioned in this topic are the tibia and fibula. The surface interactions between them were rigidly bonded – tie.
- **Between prostheses and bones** → The surface interactions between them were rigidly bonded – tie. This was possible considering that the components of prostheses were correctly fixed to each other. The mentioned interactions occur between the bones and the talar and tibial components of prostheses.
- **Between prosthetic components** → The interactions between them were established to be surface-to-surface contact. However, due to the nature of the materials that constitute the components of the prostheses, the coefficient of friction was increased, when compared to the value used for the interactions between cartilages: 0.04 [54]. This coefficient was established

for the contact between the polyethylene and talar components, in both types of prostheses, and between the polyethylene and tibial components, in the case of the S.T.A.R.™ prosthesis, as it was easily understandable if their constitution is remembered.

To simulate perfectly the real situation that happens in the physiologic state, it was necessary that the parts of the studied models was not strongly fixed to each other. This way, it was selected the option of small-sliding, when the contact modeling was performed. The mentioned option allows a small movement between the contacting surfaces. To overcome a possible situation of overclosure, due to the high proximity between the contacting surfaces, other option was selected: adjust only to remove overclosure.

Other option that was selected and taken into account to achieve the pretended behaviour in terms of friction was the automatic stabilization. This option attributed to a contact control and allowed the use of the specified values of the coefficients of friction.

Finally, in one of the previous sections was mentioned the necessity of an introduction of some components, when the Agility™ prosthesis is used, such as two screws, a plate and, of course, bone graft, to enable the realization of the arthrodesis during the TAA. The surface interaction that predominated in this situation was the tie that rigidly bounded the components. This was applied between the screws and bone, the plate and bone, the bone graft and tibia/fibula, and the screws and plate.

3.4. Loading and boundary conditions

The loading that were applied in the FEA were taken from several two-dimension studies. This way, the third component of the concentrated force was conveniently scaled and it was taken from the works of Seireg and Arvikar [64], previous mentioned. For the moment, the other components were not found and just one was applied. Below, it is possible to see specifications about the loading and boundary conditions.

- **Boundary conditions:** thanks to the “encastre” boundary condition, the calcaneus was fixed in three surfaces, according to the studies of Giddings *et al.*
- **Loading conditions:** The concentrated forces (just contact forces) and the moment (according to Seireg and Arvikar), applied in the ankle joint:
    - **Concentrated force:**
        - **Axial force:** 600 N (neutral position, 0º), 1600 N (dorsiflexion, -10º), 400 N (plantarflexion, +15º);
        - **Interior-exterior force:** -150 N (neutral position, 0º), 185 N (dorsiflexion, -10º), -100 N (plantarflexion, +15º);
        - **Anterior-posterior force:** -280 N (neutral position, 0º), -185 N (dorsiflexion, -10º), -245 N (plantarflexion, +15º);
    - **Moment:**
        - **Interior-exterior torque:** 2.85 N (neutral position, 0º), 6.2 N (dorsiflexion, -10º), -0.1 N (plantarflexion, +15º).

To achieve the forces that originate the above contact forces, the FEM was used, starting with the constrained separation of the proximal extremities of the tibia and fibula. The talus and calcaneus, the remaining bones, were despised by the calculations. Reversed forces proportionally scaled were applied on the tibia, and then it was defined a new coordinate (to reproduce the study of Seireg and Arvikar [64]). After that, there was the application of the forces in a RP coincident with the center of the new coordinate system mentioned, and the reaction forces resulted from the constrained distal extremities of the tibia and fibula were associated to loading conditions. To rapidly access the reaction forces, a RP was associated to the mentioned extremities.

Relatively to the bone remodeling analysis, it is important to mention that the three load cases were considered in the same simulation, this is, the computer simulation study, at a time, the three positions, considering for each of them 1/3 of weight. Of course the load cases just respect discrete times of the first phase of the gait, whereby this cases are considered just representative (of the broad range of loads that are verified during the referred phase). This work contemplates an activity, walking, which does not characterize all the complex activities of every physiological and workday moves, despite being the most frequent activity. This way, the studied three cases of load are considered capable of represent the daily loading report of the two bones under bone remodeling analysis, the tibia and talus, whereby they promote the viability and valuably of the results obtained from the bone remodeling analysis. It is also impossible to take into account the entire spectrum of loading data related to the first phase of the gait because it wastes very computation resources. The muscular forces were not included in the analyses due to the lack of information. Finally, when a force or an “encastre” boundary condition are applied in the models, the physiological condition is represented and the stress concentration artefacts are avoid due to the use of RP, which promotes the uniform distribution of forces in the selected surfaces. The RP are related to the coupling approach which is an important way to represent and simulate the normal state (or physiological condition): the forces are applied in a given area, not point. Below, it is possible to see the forces applied to the fibula (firstly) and to the tibia (lastly), using a global coordinate system of the software.

Fibula:

- **Concentrated force:**
    - **Axial force:** -741.908 N (neutral position, 0º), 385.137 N (dorsiflexion, -10º), -544.748 N (plantarflexion, +15º);
    - **Interior-exterior force:** -167.375 N (neutral position, 0º), 121.068 N (dorsiflexion, -10º), -128.450 N (plantarflexion, +15º);
    - **Anterior-posterior force:** -173.072 N (neutral position, 0º), 147.731 N (dorsiflexion, -10º), -129.061 N (plantarflexion, +15º);
- **Moment:**
    - **Axial torque:** -2125.42 N (neutral position, 0º), -1265.88 N (dorsiflexion, -10º), -1856.35 N (plantarflexion, +15º).
    - **Anterior-posterior torque:** 6515.09 N (neutral position, 0º), 12306.7 N (dorsiflexion, -10º), 6525.27 N (plantarflexion, +15º).

- **Interior-exterior torque:** 11171 N (neutral position, 0º), 9463.67 N (dorsiflexion, -10º), 10137.2 N (plantarflexion, +15º).

Tibia:

- **Concentrated force:**
  - **Axial force:** 1343.27 N (neutral position, 0º), 1189.77 N (dorsiflexion, -10º), 943.960 N (plantarflexion, +15º);
  - **Interior-exterior force:** -144.116 N (neutral position, 0º), -182.079 N (dorsiflexion, -10º), -130.809 N (plantarflexion, +15º);
  - **Anterior-posterior force:** 220.303 N (neutral position, 0º), 232.260 N (dorsiflexion, -10º), 187.705 N (plantarflexion, +15º);
- **Moment:**
  - **Axial torque:** -2172.71 N (neutral position, 0º), -1531.41 N (dorsiflexion, -10º), -1902.34 N (plantarflexion, +15º).
  - **Anterior-posterior torque:** 10103.8 N (neutral position, 0º), 27603.6 N (dorsiflexion, -10º), 11022.9 N (plantarflexion, +15º).
  - **Interior-exterior torque:** 31151.1 N (neutral position, 0º), 15860.7 N (dorsiflexion, -10º), 26802.6 N (plantarflexion, +15º).

3.5. Mesh generation

The type of elements used in all of the parts that constitute the models of the present work was 4-noded tetrahedral elements. Although they were not the perfect choice for the geometry modeling, which would be the hexahedral elements, they were chosen due to the inability of the ABAQUS® software to easily and automatically perform meshes with the hexahedral elements. The hexahedral elements are considered the adequate ones, for the structures more elaborated in geometric terms, due to their capability of generate a solution with increased precision and with lower computational and time costs [125].

Other parameter that was taken into account, when the meshes were generated, was the mesh refinement. This refinement can be adjusted through the introduction of the element size [126, 127]. The good conjugation of the element type with the right choice of the element size can improve the precision of the solution obtained through the FEA, and reduce or promote an adequate computational cost; both of these parameters were selected take this into account.

Finally, regarding to the axis of rotation, mentioned in the previous sections [56], where its evolution was detailed, it was not possible to consider it as a changing one. This way, a fixed axis was considered.

3.6. The use of the bone remodeling model

Like it was said before, to concretize the bone remodeling analysis, a specific software was used: the model of bone remodeling developed in IDMEC/IST, in doctoral thesis scope. The model used in the present work is a fusion between the model developed by Fernandes *et al.* and the equilibrium

equation established for the contact problem, studied by Folgado *et al.* This model is competent in its roles and is user-friendly, facilitating its understanding and utilization. Below, it is possible to see the interface of this model, and in an approximated view, some options that were taken and their further explanation.

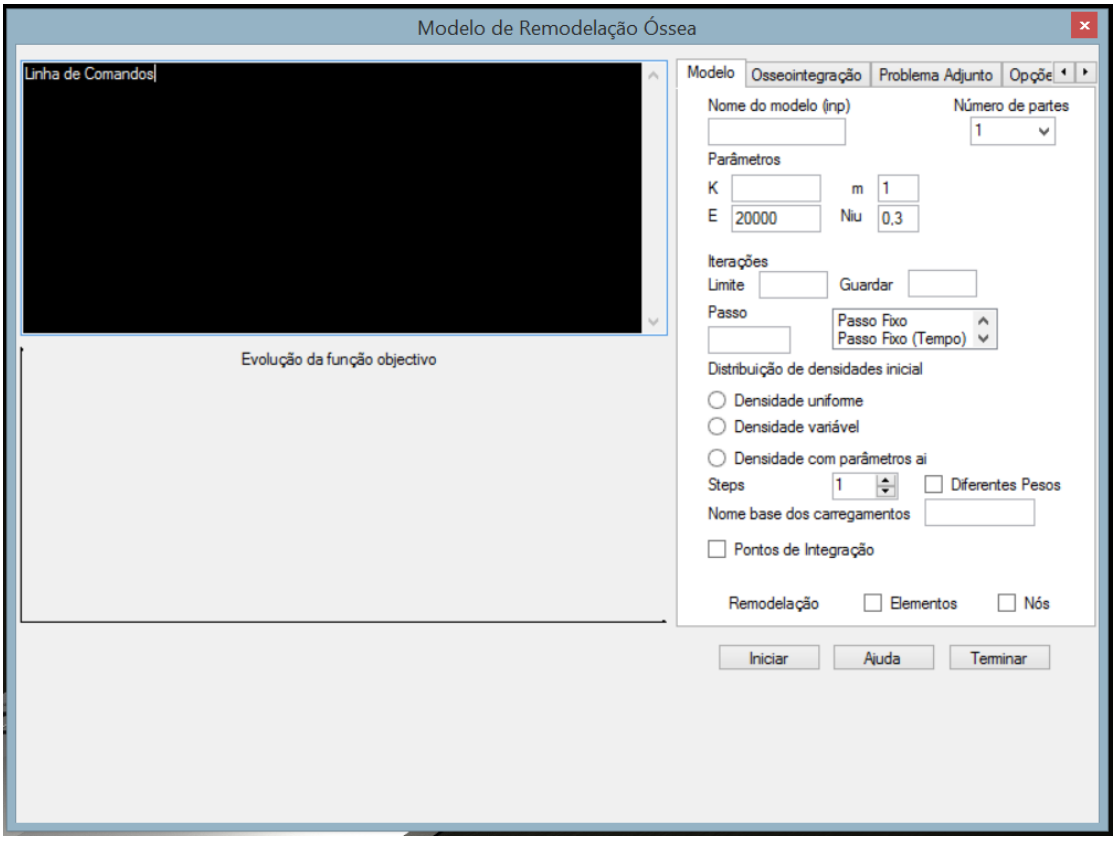

Figure 3.1 - Interface of the bone remodeling model.

Like it was possible to see in the interface of the bone remodeling model, it presents several menus, such as “Model”, “Osteointegration”, “Deputy problem”, “Advanced options” and “Extras”. However, the alterations made for this work, in the model, just took place in two of them, the “Model” and the “Advanced options”. Below, it is possible to see approximated views of these two menus, with examples of some options marked, followed by a brief explanation of them.

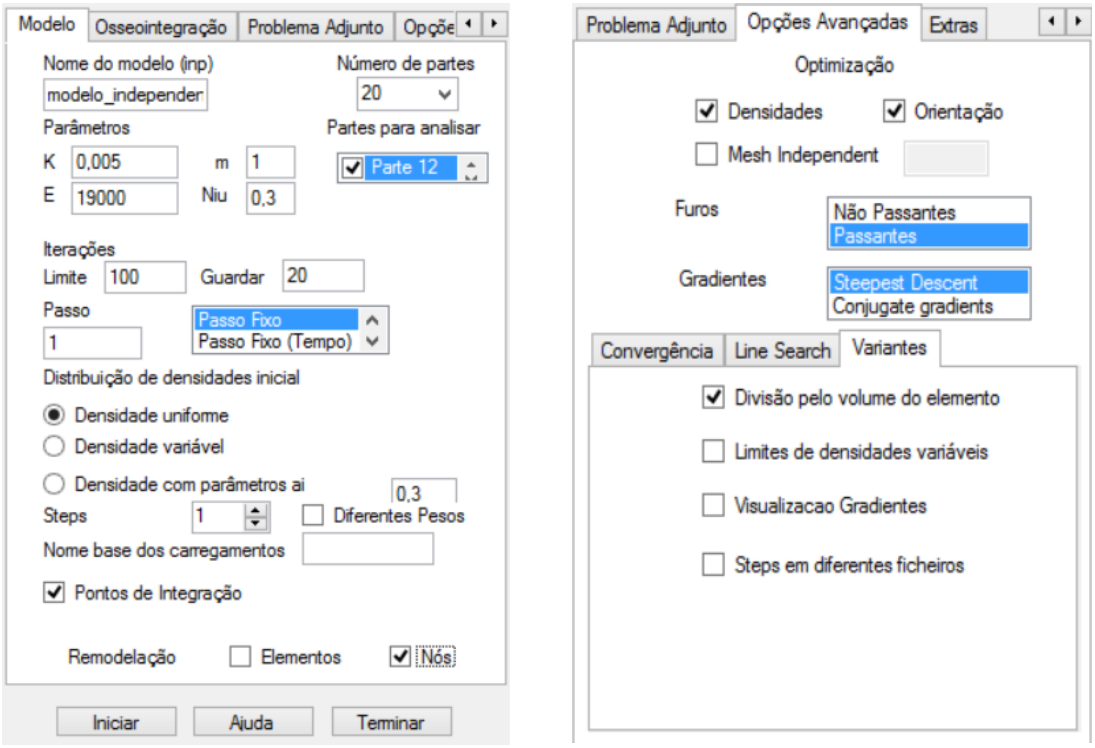

Figure 3.2 – Menus of interest of bone remodeling model, with the important options marked.

In the menu of the left side, observed in the last figure, are marked several options. Firstly, it was introduced the name of the input file (*.inp*), that is mesh-independent and it was obtained from a Matlab® code, developed in IDMEC/IST, which purpose was to transform the dependent meshes of the FEA, described in the input file, in independent ones. This way, the model has a greater performance. Then, the number of parts that constitute the model under study was selected as well as the parts of interest, to be analysed. Regarding the parameters, they are four: the Young's modulus, *E*, the Poisson coefficient, *Niu,* the biological cost of the organism in maintaining bone homeostasis, *k*, and a corrective factor for the preservation of the intermediate densities, *m*. The first two mentioned parameters, *E* and *Niu*, were established to be the same for every simulations performed and assumed, respectively, the values: 19000 GPa and 0.3. Regarding the values of *k* and *m*, they were assumed to simulate six combinations of values, each one representing a different analysis: *k*=0,005 N/mm^2 and *m*=1*, k*=0,007 N/mm^2 and *m*=1*, k*=0,009 N/mm^2 and *m*=1*, k*=0,005 N/mm^2 and *m*=2*, k*=0,007 N/mm^2 and *m*=2*,* and *k*=0,009 N/mm^2 and *m*=2. The number of iterations was also selected: 30 iterations for each analysis performed for the intact model of the AJC and 100 iterations for each analysis performed for the combined models, TAA+prosthesis. For the intact model, the results were saved every ten iterations, and for the combined models, the results were saved every twenty iterations. Relatively to the step, it was selected to be fixed and assumed a value of 1, for every simulations, except the ones where the value of step were modified and studied. The densities initial distribution were selected to be uniform and starting with a value of 0.3, for about half of the simulations. For the other half, it was selected an option that recovers the density values from two files: *desin.inp* and *desin_integracao.inp*. This recover is possible if these files are localized at the same folder of the bone remodeling model. The recovered density values were obtained from the transferring of the final densities from the intact model to the

combined one. This transference was performed thanks to a Matlab® algorithm that is described in the Annexes. The remodeling was assumed to be performed in the nodes and taken into account the integration points. This last option is selected when the user pretends the calculation of the stresses and strains in the integration points, namely in the element centroid.

In the menu of the right, for the optimization section, both densities analysis and orientation analysis were selected to be performed. The cells were assumed to be "*passing*", which means that it was assumed, for each one, a hole/space that is in the middle of a standard cell (the open cell configuration). To calculate the gradients, it was selected the steepest descent method, which is the most simple, although the less effective. This method was selected because it is believed that it satisfies the bone remodeling analyses of the present work. In both sections of convergence and line search, the values chosen were the ones that are proposed by default of the model. Finally, for the variants section, the division by the element volume was selected.

Every decisions that were taken for the bone remodeling model were based on the previous studies, always taking into account the nature of the models of the present work. After the bone remodeling analysis, the obtained results were analysed through the commercial software Excel 2013 and the images were obtained thanks to the *visualization* section of the Abaqus®.

4. Results and discussion

4.1. Model of intact bone (AJC)

The remodeling process was applied just in two bones of four mentioned: the tibia and talus. To start the remodeling simulation, there was introduced two special parameters, *k* and *m*. In a previous section, these two parameters were explained but briefly it is possible to say that *k* will influence the bone mass that results from the remodeling simulation and is value symbolizes the metabolic cost of maintaining bone. The other parameter, *m*, is important like *k* but its role focuses in the preservation of the intermediate densities, acting as a corrective factor. To validate and give some meaning to the bone remodeling results, it is central to obtain the values of *k* and *m* and, to achieve them, there were made many computer simulations that processes the bone remodeling, always using the intact model (with different initial densities values for the cortical and trabecular bone), which do not have prosthesis included and represents the normal condition of the AJC. In these simulations were introduced, as input conditions, different values of the two parameters and they were chosen by their capability of simulate the physiological state of the two bones analyzed, this is, by their capability of represent the real (or at least, the most close) distribution of bone density. This way, there were chosen for every models under study in this work six combinations of values: k=0,005 N/mm^2 and m=1, k=0,005 N/mm^2 and m=2, k=0,007 N/mm^2 and m=1, k=0,007 N/mm^2 and m=2, k=0,009 N/mm^2 and m=1, and, finally, k=0,009 N/mm^2 and m=2. The best values for the parameters *k* and *m* were selected through a qualitative analysis, due to the comparison of the bone density distributions obtained thanks to the bone remodeling computer simulations and the CT scan images. However, there are other parameters that should be introduced in the remodeling model, like it was said in the previous sections and one of these input values is the value of the step, which was evaluated for the optimization problem. Below, it will be possible to see results obtained through the use of different values of step (1, 5 and 10). Due to the results obtained, the value of step is assumed to be 1 for every simulations. Relatively to the number of iterations, for the intact model which is very elaborated and complex, the value of iterations were established to be 30 and for the models which included the prostheses (Agility™ and S.T.A.R.™) this value was 100. For both situations, the values chosen did not compromise neither the obtained results for each simulation nor the computational time, conjugating these two aspects appropriately.

Relatively to the images (disposed in figures 4.1 and 4.2) that show the bone density distribution, which result from the computer simulations performed for the bone remodeling process, it is possible to say that, in general, they present morphological characteristics in common with the density distributions known for the two bones under study, the tibia and talus. The most notorious feature observed is the difference between the outer zone and the inner one of the cross section (transversal slice) of the bones under study: the outer zone presents high values of density, reflected by the colour scale as the brighter/lighter region (near to the white), and corresponding to the cortical bone; in opposition, the inner region is characterized by lower values of relative density which are related to the trabecular bone and are represented in the images obtained by the most darker colours (near to the black).

Regarding to the tibia, it is important to established that the present results just show part of this bone (in fact, a big part), not all of it. This way, one of its extremities, the proximal one, is not visualized here but it can be said that the cortical bone behaves the same way in both extremities: in the epiphyses, this layer is thinner, contrarily to what is observed in the diaphysis, where it is thicker. This observation is strongly supported by the image of the frontal plane view. In turn, the image of the view of the sagittal plane shows, relatively to the tibia, the cortical bone thinner in the posterior side than in the anterior side, which does not agree with the CT scan images, where both sides are more uniform and similar. Balancing these two aspects, it is possible to affirm that the results of the tibia match, in general, the CT scan images.

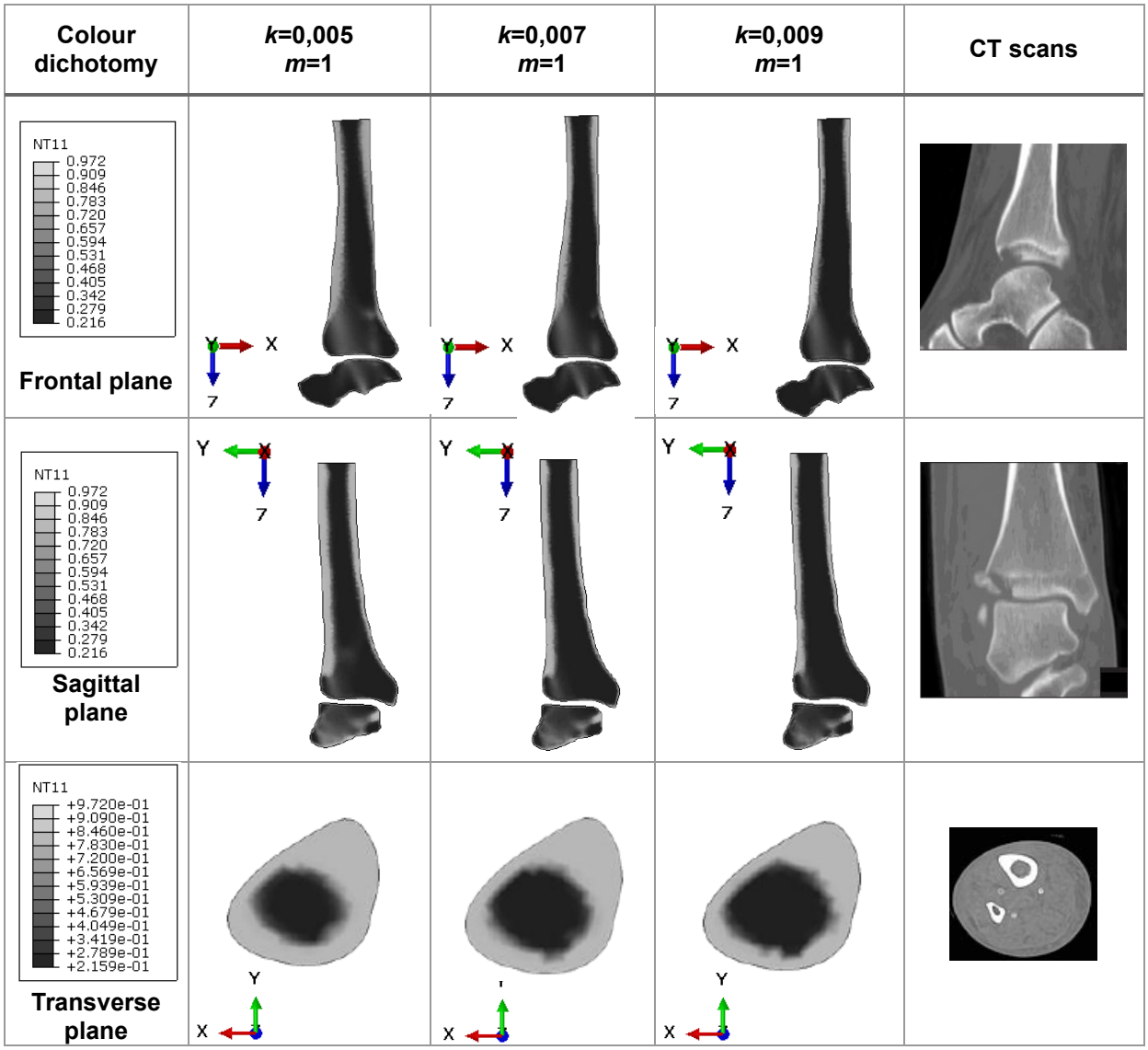

Figure 4.1 - Comparison of the bone density distributions resulting from the bone remodeling computer simulations (after 30 iterations) and the CT scan images. (for all values of k and m=1).

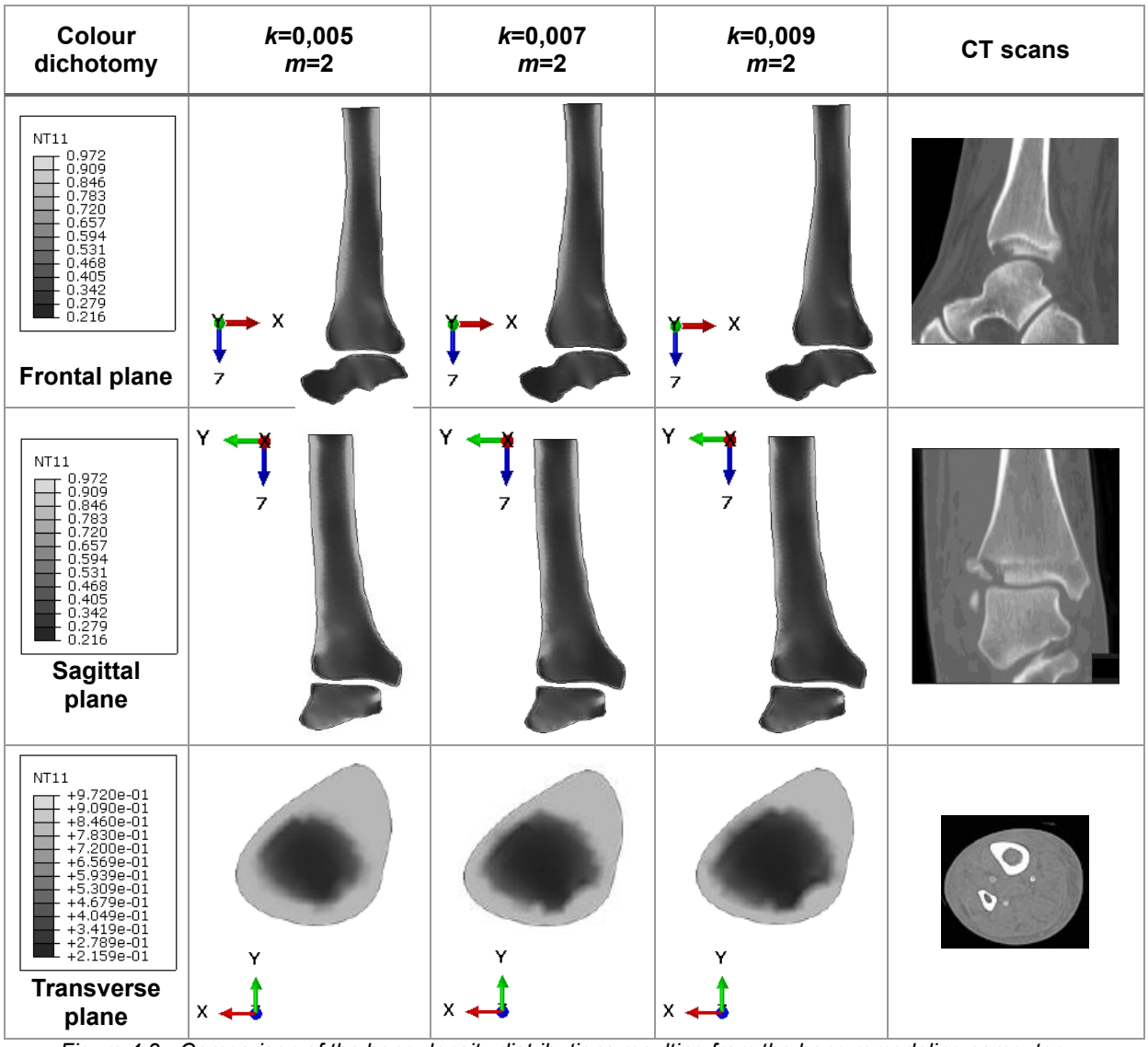

Figure 4.2 - Comparison of the bone density distributions resulting from the bone remodeling computer simulations (after 30 iterations) and the CT scan images. (for all values of k and m=2).

The navicular bone is not present in the studied model, and as it contacts the talus in its anterior region, the effect of the loads stemming from this contact surface (between the navicular and talus) is not verified in the present results. So, regarding the talus and take this into account, the anterior region presenting very low values of relative density, observed in the figure of the view of the sagittal plane, is easily understandable and have their logic. In the same plane, the sagittal, it is possible to observe a bright region in the distal and middle portions of the talus, which is due to the transmission of forces to the calcaneus that bordering with talus at the mentioned sides (these affirmation is corroborated by the obtained results and the CT scan images). These observations allow to obtain a general conclusion, related to the bone remodeling: bone formation does not happen when there are not verified applied loads. In addition, there are small areas with very low relative densities, observed in the view of the frontal plane. These areas are dark, near the black (due to the very low values, as it was mentioned) and they cannot be observed in the CT scan images. They are due to the fact of the representation of the binding sites was not very trusted, which influences the bone remodeling process: their real area should be larger than the one that was represented. Contrarily to the mentioned situation, in the medial

portion of the talus, a concentrated binding region it is possible to be observed, through the view of the frontal plane, due to the connection of a ligament into the referred bone. This region presents a bright colour due to the very high values of relative densities. Synthetically, it is possible to affirm that the model used in the present work shows a solution with high concordance with the real aspect/morphology of the tibia. This way, the solution obtained through the model simulates the behaviour of the real tibia. However, regarding the talus, the similarity between the obtained solution and the morphology of the real bone is lower than the aforementioned.

Like it was mentioned, the value of the parameter *m* influences in a strong way the distributions of the bone densities obtained from the computer simulations that were performed to study the bone remodeling. Below, it is possible to see a relation between the value of the parameter *m* and what is observed in the solutions of the computer simulations performed.

- ↑ *m* → homogeneous distribution → nodes with higher densities are despised and all of them converged to an intermediate value of relative density:
    - **Increase of the average global density**

The mentioned observations and their consequences are supported by the pictures present in the figures 4.1 and 4.2 that show, for the lower value of *m*, *m*=1, higher average density and a well-established (well-defined) layer for the cortical bone, when compared with the results obtained from the simulations with *m*=2. On the other hands, the trabecular bone presents lower average density, when it is used *m*=1 than when it is used *m*=2. Relatively to the value of the parameter *k*, it also influences the distributions of the bone densities obtained from the computer simulations that were performed to study the bone remodeling. Below, it is possible to see a relation between the value of the parameter *k* and what is observed in the solutions of the computer simulations performed.

- ↑ *k* → lower average global density
    - **The biological cost for the organism to maintain bone homeostasis is higher: it is more costly for the organism to allow processes, such as bone formation or resorption.**

Like it was said, it is important to select the best values for the parameters *m* and *k*. The best values are considered the ones that promote the perfect simulation of the real bone relative densities distribution in both studied bones, the tibia and talus. The real bone relative densities distribution of the two bones is considered the one that occurs at the physiological state. Then, it will be presented some characteristics which allow the choice of the best values.

Relatively to the value of the parameter *m*, some considerations were done and, synthetically, the simulations for *m*=2 present more identical results to the CT scan images, when compared to the results obtained from the simulations for *m*=1. Despite not despise too much the nodes which present extreme densities, in the simulations for *m*=2 it is verified a convergence of the nodes to an intermediate value of density, which leads to a homogeneous distribution of the bone density.

Relatively to the value of the parameter *k*, it is important to achieve the best reproduction of what happens in real bone, namely, a concordance between the thickness of the cortical layer in the diaphysis and in the epiphysis/metaphysis (the last one is the region between epiphysis and diaphysis). The first value (from those presented) tested for the parameter *k* was k=0,005 N/mm^2, which presents, in the diaphysis, a cortical layer with a thickness matching with the real situation (presented in CT scan images). However, regarding the thickness of the same layer in epiphysis/metaphysis, there is no matching: the real case presents a much more thinner cortical layer, than the one in the obtained results. The second value tested for the parameter *k* was k=0,007 N/mm^2 and it was considered the most suitable value as it will be explained after. The last value of *k* was k=0,009 N/mm^2 and the results obtained from the simulations performed with this value showed a thinner cortical layer due to the marked loss of relative densities in its external side. Finally, it will be explained why the k=0,007 N/mm^2 is the choice that better fits in the real situation:

- k=0,007 N/mm^2 is the one that promotes better results in that they are more identical to the real distribution of densities of the real tibia;
- Looking to the results with other values of *k* (k=0,005 N/mm^2 and k=0,009 N/mm^2) it is easily understandable that a value localized between them is the best choice to obtain better results.

However, computational simulations are not the real situations and present some disadvantages/limitations. This also happens with the simulations using k=0,007 N/mm^2. Below, it is possible to see some of these limitations.

- In the view of the sagittal plane: the posterior and anterior portions should present an uniformity. However, in the tibia, it is verified a thinner cortical layer in the posterior portion.
- Just one of the extremities of the tibia presents a thinner cortical layer, not both.

It is also important to mention that the densities distribution of the talus was not influenced by the changing of the value of the parameter *k*.

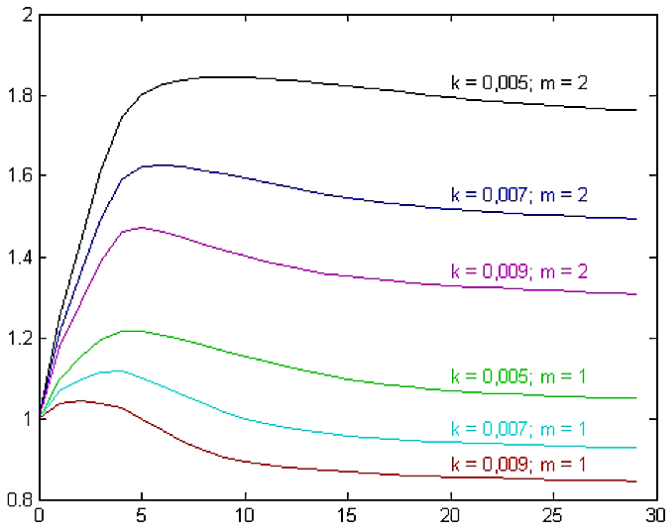

Figure 4.3 - Bone mass during the iterative process of bone remodeling (30 iterations), dimensionless by its initial mass, for different values of parameters k and m.

Regarding to the figures 4.1 and 4.2 that distinguished the results (performed for the three values of *k*) relatively to the value of the parameter *m*, it is possible to observe that this one promotes the existence of differences between these bone density distributions. For *m*=2, the results obtained show a negligence of the nodes characterized by the extreme densities, like it was said before. This way, the distributions obtained are more homogeneous, due to the fact that all the nodes of the two remodelled parts converge to an intermediate value of density. This situation leads to an increase of the average global density, proven by the figure 4.3. For the simulations performed with *m*=1, and, in particular, for the cortical layer, it is possible to observe that it has a high definition and average density. However, when the trabecular bone is particularly observed, the average density is lower. Looking again to the figures 4.1 and 4.2, and paying more attention to the parameter *k*, the lower average global density is observed when the *k*-value is higher, which is concordant to the association of the parameter *k* with the biological cost: ↑ *k*-value → more outgoing to allow bone formation.

In conclusion, it can be said that the right choice for the values of both mentioned parameters is: *k*=0,007 N/mm^2 and *m*=2.

4.2. Analyses of the tibia: transversal slices

Then, the tibia was divided into 8 portions, with the purpose of analyse it in several transverse slices. These 8 portions leaded to 7 sections, which were analysed for many situations, characterized by different conditions: for distinct parameters, several models (both prostheses and intact bone), different initial densities, and different numbers of iterations. Below, it is possible

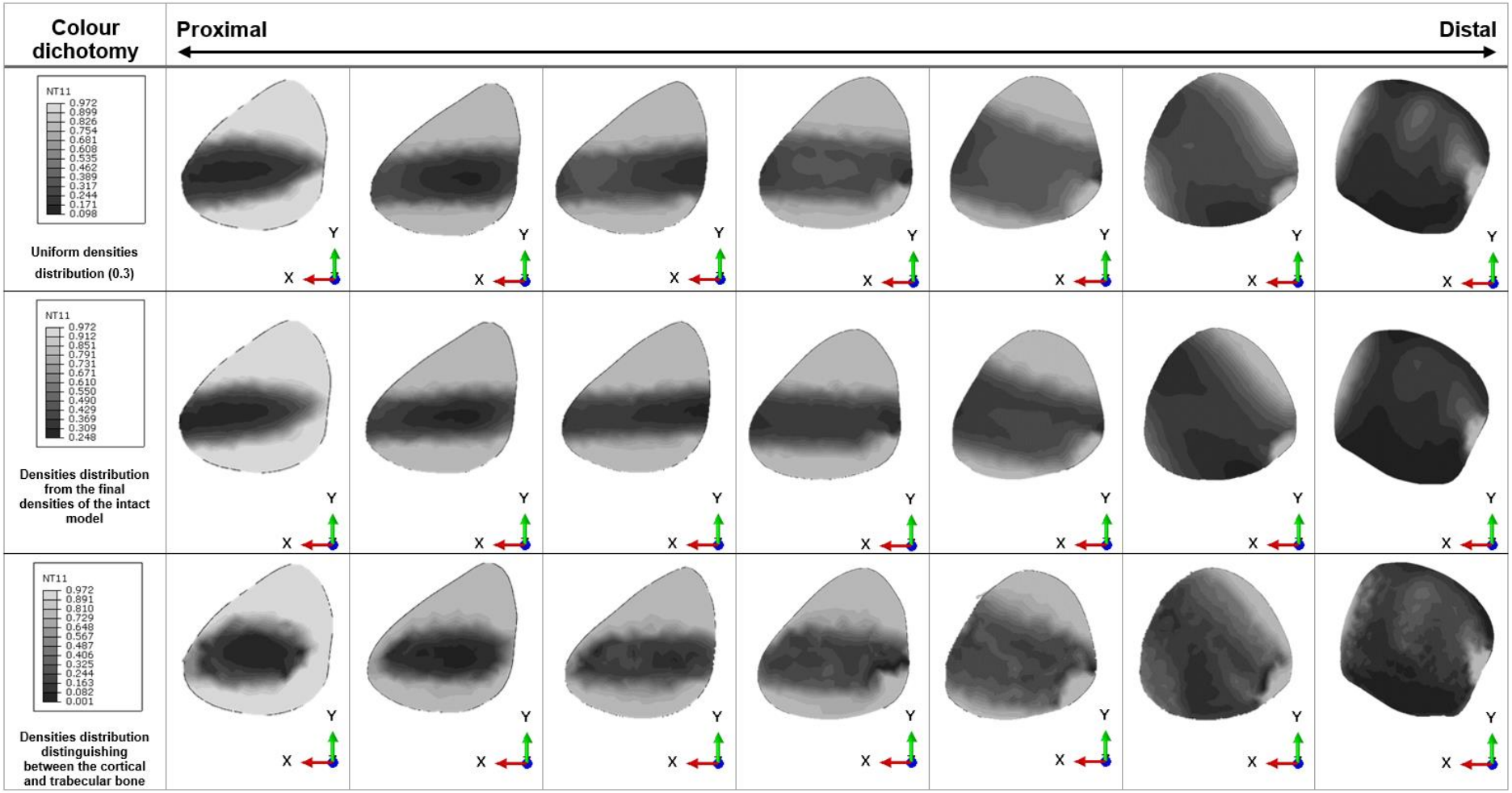

Figure 4.4 - Comparison between three sets of tibial slices, from the same model (TAA+S.T.A.R.^{TM}), but under different initial conditions, relatively to initial densities distribution: uniform densities distribution (0.3), densities distribution obtained from the final densities of the intact model and densities distribution distinguishing between the cortical and trabecular bone.

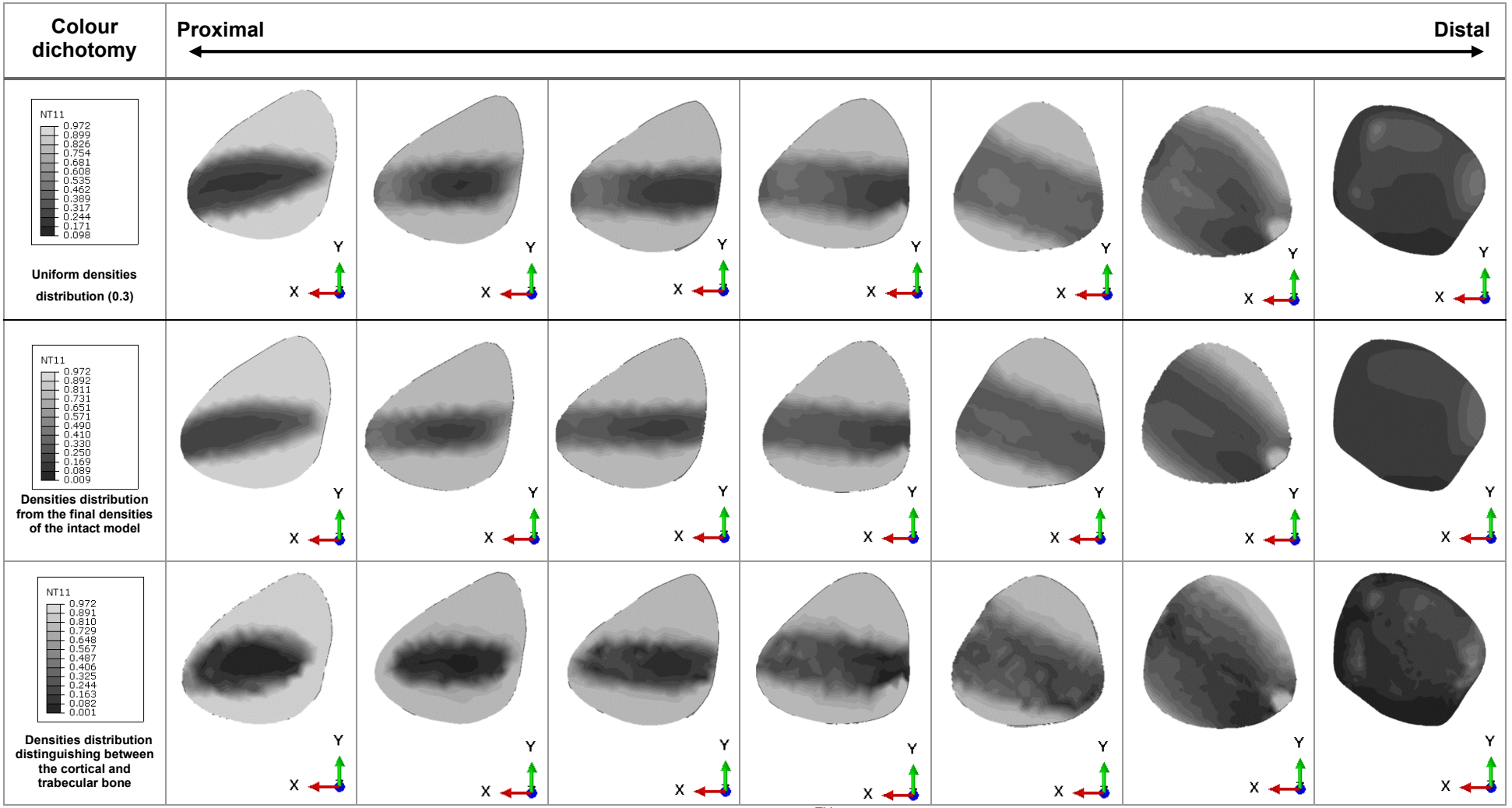

Figure 4.5 - Comparison between three sets of tibial slices, from the same model (TAA+Agility™), but under different initial conditions, relatively to initial densities distribution: uniform densities distribution (0.3), densities distribution obtained from the final densities of the intact model and densities distribution distinguishing between the cortical and trabecular bone.

In the figure 4.3, it is possible to see transversal slices of the tibias from the same model, the TAA+S.T.A.R.™, but with different initial conditions. The parameters *k* and *m* that were chosen for exemplify the differences between the mentioned tibias were, respectively, 0,007 N/mm^2 and 2, that demonstrated, in the previous results, to be the most adequate. The first line of the figure presents slices from the model subjected to uniform initial densities (all nodes with 0.3). This way, the remodeling model did not distinguished between the cortical and trabecular layer, assuming that both had an initial density of 0.3. The second and third lines of the figure show slices from the model subjected to a non-uniform distribution of initial densities. In the second case, the initial densities distribution was obtained from the final densities achieved in the remodeling of the intact model (in the case of the remodeling with uniform initial densities – 0.3), thanks to a Matlab® algorithm developed in this work (presented in the Annexes). In third case, the initial densities distribution was made taking into account a distinction between the cortical and the trabecular layers. To the superficial nodes of the cortical layer (just the nodes constituent of the external surface) was attributed a high density value, 0.9, while to the remaining bone were attributed lower values, between 0 and the maximum value, simulating the trabecular bone, which is characterized by these intermediate densities. Comparing the first two cases, it is possible to observe a similar behaviour, which maybe is due to the provenience of the initial densities values of the second case. However, in the case that the initial densities values come from the final densities values of the remodeling of the intact bone (with an uniform distribution of densities), the slices present a slightly higher bone loss. This is justified with the existence of several lower (when compared with 0.3) values in its initial distribution, which lead to lower final densities. If the three cases are observed, it is possible to verify better results in the last line, where the distinction between the cortical and trabecular layers were made. In these 7 slices, the bone lost is lower, which is better for the overall bone structure. In the more proximal slice it is possible to observe the existence of almost the cortical layer. The region where lower values are still further presents higher densities values when compared to the two previous cases, presented in this figure. However, the real cortical layer presents different thickness values along the tibia and in this case it is considered always with the same thickness (just the external surface). In conclusion, the densities values in some regions may not correspond to the reality, due to the mentioned difference of thickness along the real tibia and the fact that just the nodes of the external surface were chosen to constitute the cortical layer in the model (they can be few for the required thickness). This way, it is easily understandable that the case where the initial condition is the uniform densities distribution may contribute for less errors than in the other where the cortical layer is distinguished from the trabecular one.

In the figure 4.4, the results that are presented correspond to the same three cases of the figure 4.3, under the same parameters and conditions, but for the TAA+Agility™ model. The conclusions that can be obtain are similar to the obtained for the TAA+S.T.A.R.™, described in the last paragraph, with the difference that for the present model, some regions appear to be slightly lighter, may be due to their geometry, like it was explained before.

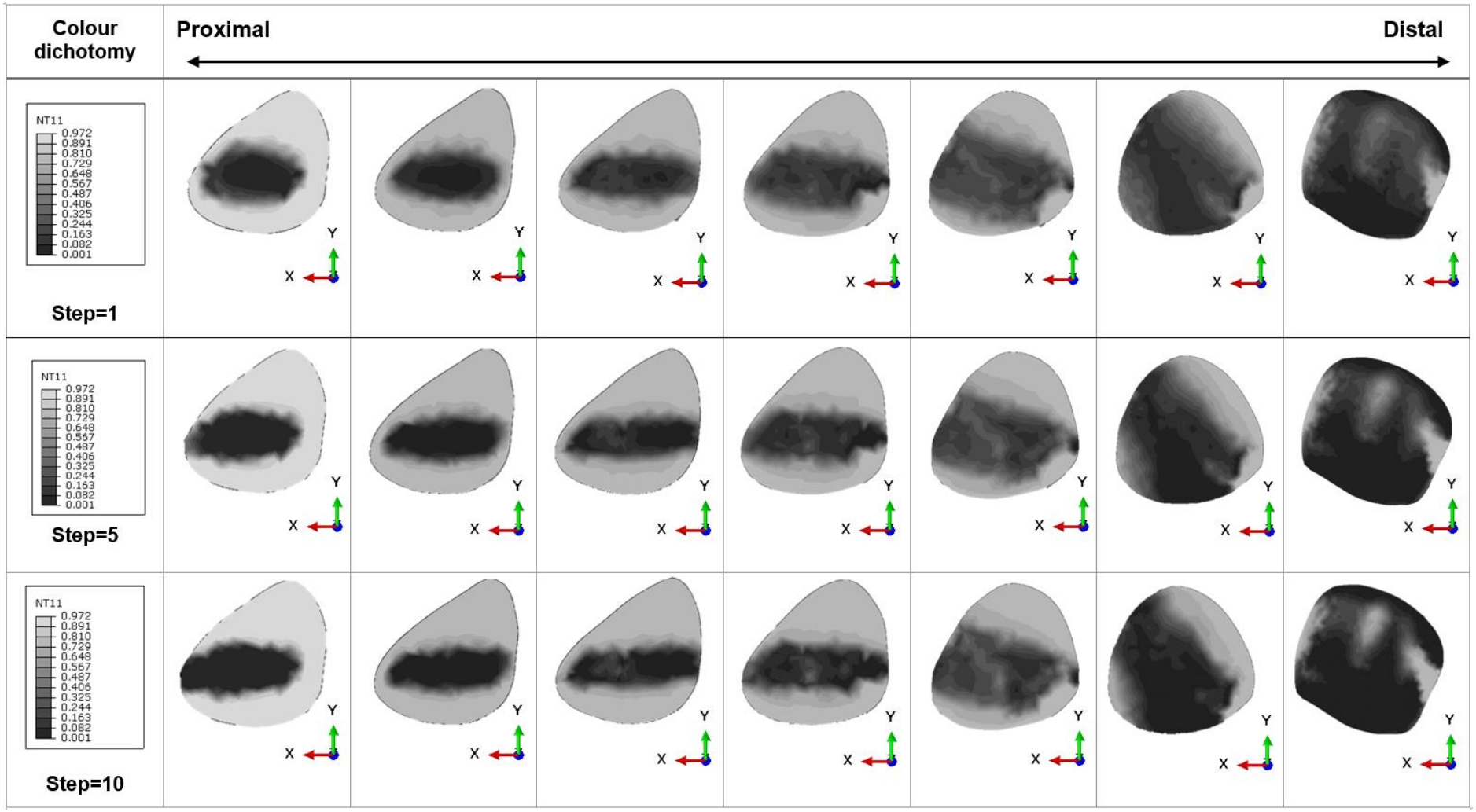

Figure 4.6 - Comparison between three sets of tibial slices, from the same model (TAA+S.T.A.R.™), but under different initial conditions, relatively to the fixed step: step=1, step=5 and step=10.

In the figure 4.5, it is possible to observe the disposition of three sets of 7 slices, corresponding to the tibia of the TAA+S.T.A.R.^{TM} model. These results were all obtained with the parameters of k=0,005 N/mm^2 and m=1, for three different values of fixed step, 1, 5 and 10, with the purpose of understand which is the most adequate value for the performing of the simulations. Each of the mentioned three types of results were performed during just 60 iterations, because it is a sufficient number to understand their behaviour, regarding the change of the step. Relatively to what is observed, it is understandable that the better results come from the simulations performed with a fixed step of 1, although the differences between them are not very notorious. Despite the higher computational time, it is preferable a lower value of fixed step, because a higher step means a higher distance covered in the direction D (See *Mathematical formulation*), which can lead to a contempt of information. In this work, the step was maintained fixed in all the iterative processes, although it is usually used, by the Lagrange direct method, the line search method that calculates, for each iteration, the optimal step. Since the purpose of the model is to achieve the minimal solution, a higher step can lead to the contempt of the “right” minimum, stopping the process in the relative minimum values. Balancing the higher computational cost of the small steps, when compared with the bigger values, and the risk of discarding the minimum solution, it is preferable to use small values.

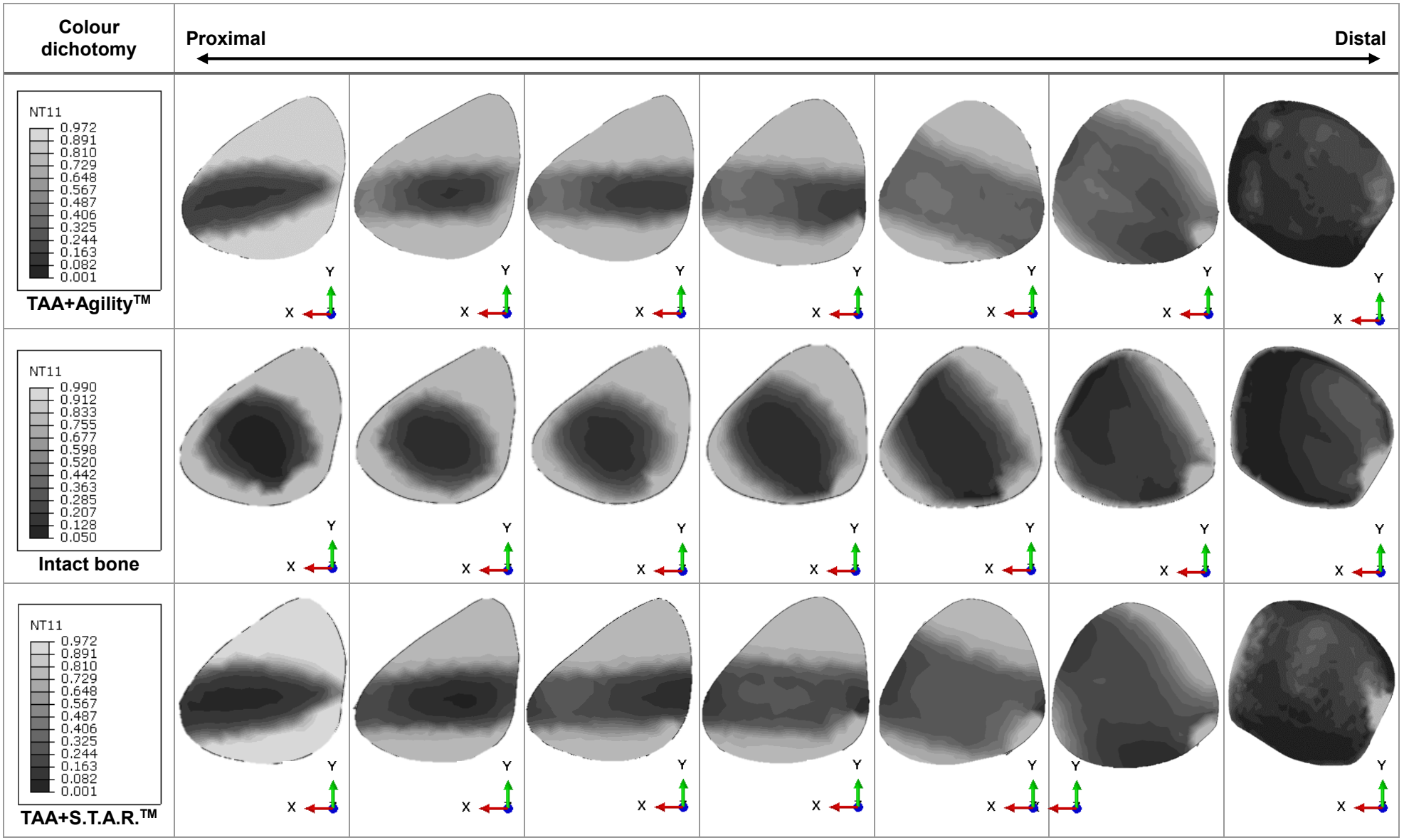

Figure 4.7 – Comparison between three sets of tibial slices, from different models: the TAA+Agility™, intact model and TAA+S.T.A.R.™.

In the above figure, it is possible to see the disposition of both set of 7 slices, corresponding to the tibias of three different models: the TAA+Agility™, intact model and TAA+S.T.A.R.™. The remodeling of these models was made taken into account the final density values obtained from the intact model. Like it was said before, the initial density values that were introduced in the bone remodeling model, to initiate the remodeling process of the results above, were obtained through the Matlab® algorithm, described in the Annexes. The parameters *k* and *m* that were chosen for exemplify the differences between the mentioned tibias were, respectively, 0,007 N/mm^2 and 2, that demonstrated, in the previous results, to be the most adequate. This way, it is possible to observe in the referred slices that bone remodeling process, after the performance of 100 iterations, show a similar behaviour/pattern, demonstrate just smooth differences. Despite of the darkest colour of the dichotomous scale for the Agility™ symbolize lower density values, this tibia shows a better behaviour than the tibia of the model with S.T.A.R.™ prosthesis, which is verified through the presentation of lighter colours in the first case. However, and that it was expectable, for both cases as the slices down in the length of the tibia (from the proximal extremity to the distal extremity), it is possible to prove the approximation of the prosthesis local, through the loss of bone verified. In the first slice observed, for both cases, it is possible to verify a bone loss in the cortical layer, internally in the tibia, while the remaining layer is intact. As the slices descend along the tibia, it is verified a bone loss in the opposite side of the lost region, observed in the first slice. From the third most distal slice, it is possible to see almost a completely lost of the bone of the cortical layer. In fact, it is revealed by the results that the cortical layer is thicker in the diaphysis and becomes thinner toward the distal extremity, closer to the location of the prosthesis. However, since the model does not take into account biological conditions like the muscles associated to the ankle joint, some portions/areas of the tibia may be subjected to load underestimation. For the Agility™ prosthesis, the verified loosening, which is associated to an increased wear debris production [77] is due to the semiconstrained design of this prosthesis, which does not replicate normal ankle motion, as the ankle slides from side to side during dorsiflexion and plantarflexion and rotation motion. Moreover, a non-union of the attempted tibio-fibular arthrodesis, risks loss of fixation on the proximal side, thus compromising stability [17]. Like it was said, the S.T.A.R.™ has a convex talar component with a longitudinal ridge (congruent with the distal surface of the mobile meniscus). The dorsiflexion and plantarflexion are allowed at the menisco–talar interface, but no talar tilt, while rotation is allowed at the menisco–tibial interface. This way, when compared with some other prostheses designs, the S.T.A.R.™ presents a lower surface area for stress distribution, in the distal tibia, which may justify the slightly darker areas in comparison with Agility™, due to lightly superior quantities of bone loss.

Finally, when the densities distribution of the intact model is compared with both distributions of the models where the prostheses were introduced, the main observed difference is clear: the remaining of the cortical layer, along the tibia. In fact, this layer remains almost intact until the third distal slice, which clearly does not happen in the tibias from the models with prostheses.

4.3. Comparison between both TTA+prosthesis and radiographies

Colour dichotomy	Remodeled model	Ankle joint radiographies after TAA
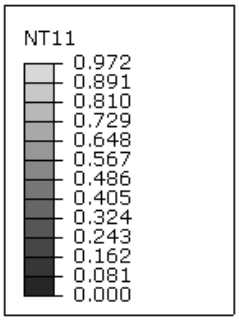 **TAA+S.T.A.R.™**	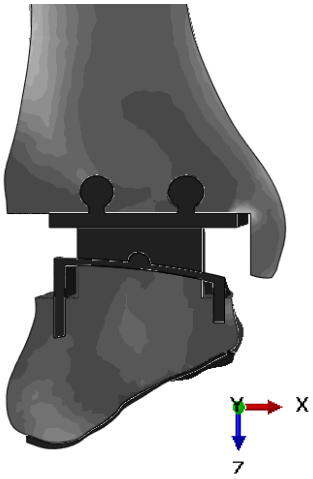	
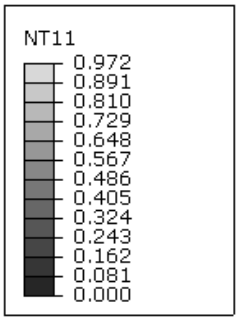 **TAA+Agility™**	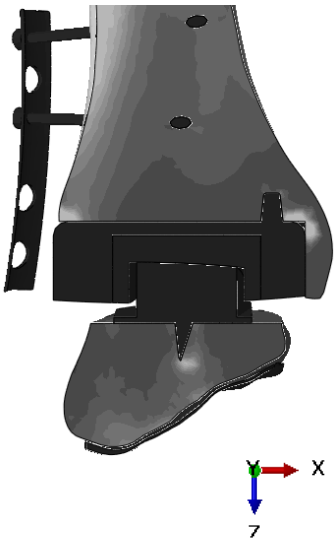	

Figure 4.8 - Comparison between the obtained results from the bone remodeling model and radiographies, for both prosthesis.

In the figure 4.8, it is possible to see, at the central column, the frontal views of both models, where the prostheses were included, after the occurrence of the bone remodeling. In the column of the right side, it is possible to observe two radiographies (of frontal view), obtained some time after the TAA. The upper radiography, of the ankle with S.T.A.R.™ was obtained from [128] and the other one, of the ankle with Agility™, was obtained from [129]. Although they both are from contrary ankles, this little comparison can be done. The region that was zoomed in every figures is specifically the ankle joint, including the

distal extremity of the tibia, talus and prosthesis. Relatively to both radiographies, it is possible to observe a bone lost specially in the distal extremity of the tibia, which is noticeably darker in the radiologic images, when compared, for example, with the talus (in the case of the S.T.A.R.™ prosthesis) and with the talus, navicular and the rest of midfoot bones (in the case of the Agility™ prosthesis). This lost is verified, for both cases, in the frontal views of the images obtained from the bone remodeling model, due to their darker colour. However, in both models, it is possible to observe the existence of lighter colours in the internal region of the distal tibia, which corresponds to the cortical layer. This cortical layer verified in the models is also observed in both radiologic images. A common etiology of the failure of these prostheses is the periprosthetic bone cyst formation, resulting from UHMWPE wear debris, leading to the bone erosion, subsidence or even component loosening. These cystic changes sometimes enlarge progressively over time and may remain relatively asymptomatic until catastrophic failure is imminent. When the presence of cysts is verified, annual radiological surveillance is required. This etiology is observed in the radiographies as circular or rounded areas, which are darker than the involving region, and, due to their colour, translate bone lost. They are hollow spaces filled with liquid and can also appear in soft tissues. Structures, like the described, are observed in the radiographic images, although they do not appear in the images from the bone remodeling, which may be explained by the fact that the bone remodeling model does not take into account some biological factors.

4.4. Convergence study

The processes achieved the expected convergence, which is possible to prove through the observation of the next figures. This convergence is the term used for describe the stabilization in the bone volume, according to the number of iterations considered. When the convergence is achieved, the solution of the model achieved an equilibrium state, where bone formation and bone resorption successively happen. To achieve the mentioned solution, it was necessary about two weeks for the performing of one hundred iterations for all the combined models, TAA+prosthesis. However, it is possible to observe in the below data that the value one hundred iterations are not mandatory, because after a lower value, about thirty/forty, the bone remodeling computer simulations do not develop in a different way, being constant, through the iterative process.

In the figures 4.9 to 4.20, there are presented three types of information, all in function of the iterative process, obtained from the simulation of TAA+Agility™. The first one represents the evolution of the compliance, which translates the work of the applied forces, during the iterative process. The second graphic demonstrates the progress of the volume, in function of the iterations number. Finally, the last graphic presented, represents the evolution of the objective function, during the iterative process, over the time. The objective function translates both compliance and volume, being a combination of these two information. In each graphic, all values of k are compared, for each value of m and model.

4.4.1. Initial condition: uniform densities distribution

4.4.1.1. With *m*=1

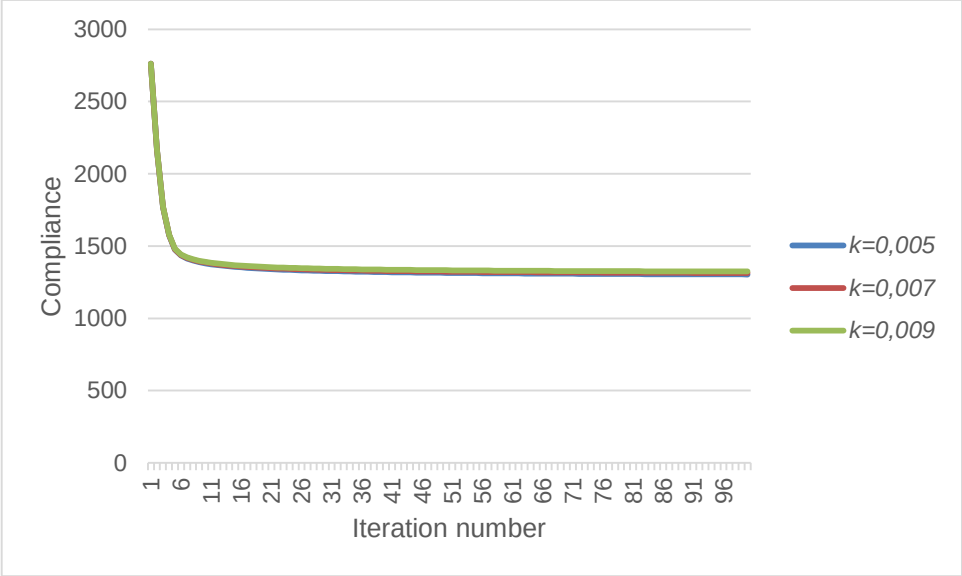

Figure 4.9 – Evolution of the compliance of the bone mass, for all values of k and m=1 (TAA+Agility™ prosthesis).

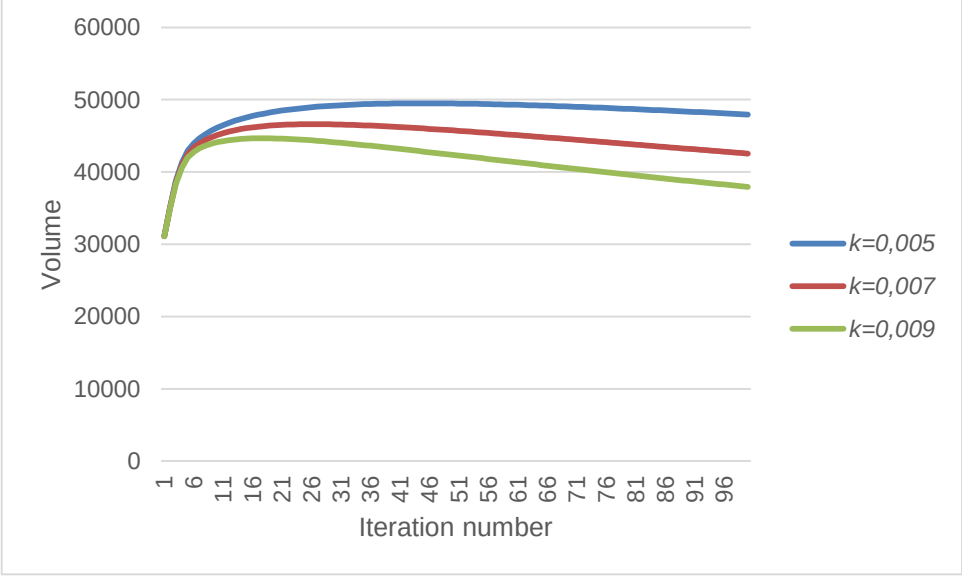

Figure 4.10 - Evolution of the volume of the bone mass, for all values of k and m=1 (TAA+Agility™ prosthesis).

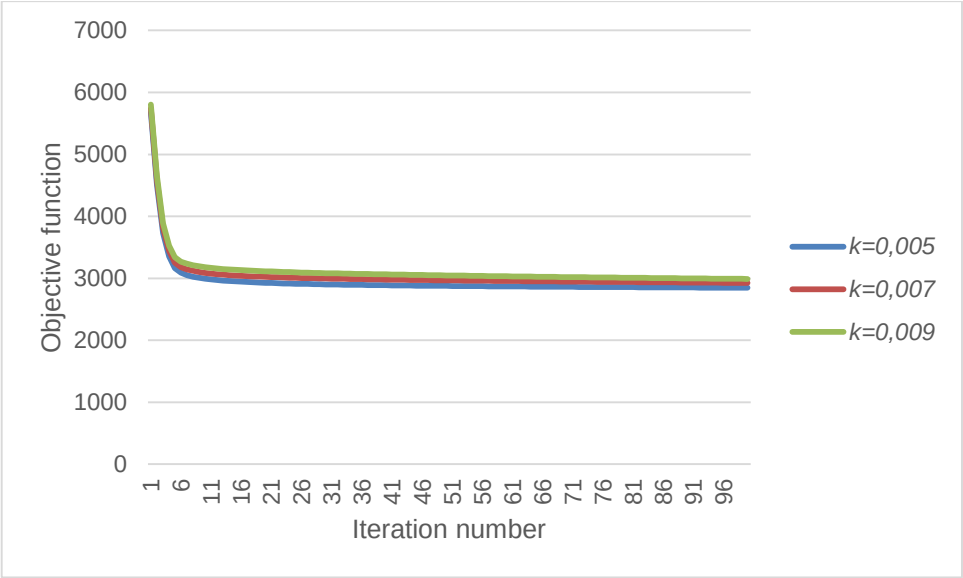

Figure 4.11 - Evolution of the objective function related with the bone mass, for all values of k and m=1 (TAA+Agility™ prosthesis).

4.4.1.2. With *m*=2

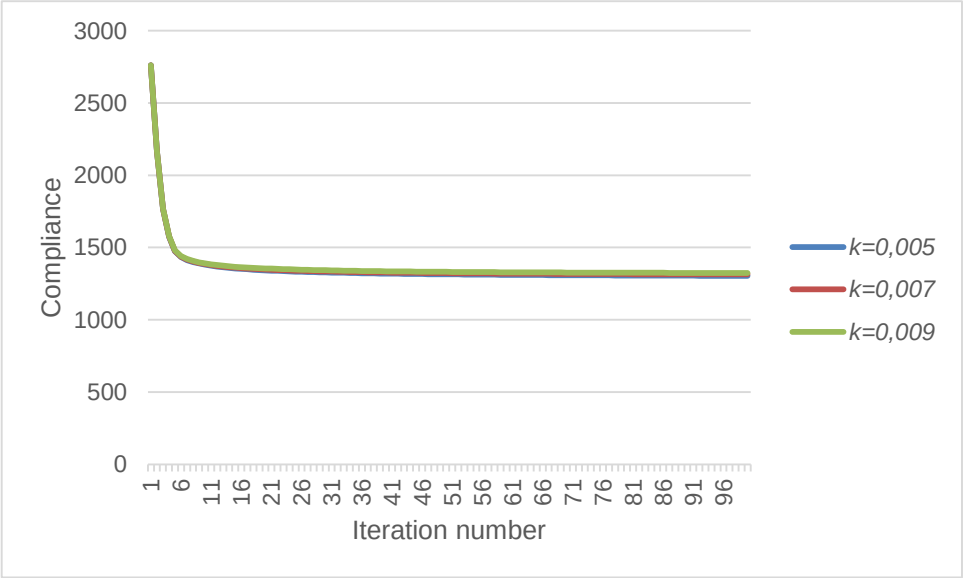

Figure 4.12 - Evolution of the compliance of the bone mass, for all values of k and m=2 (TAA+Agility™ prosthesis).

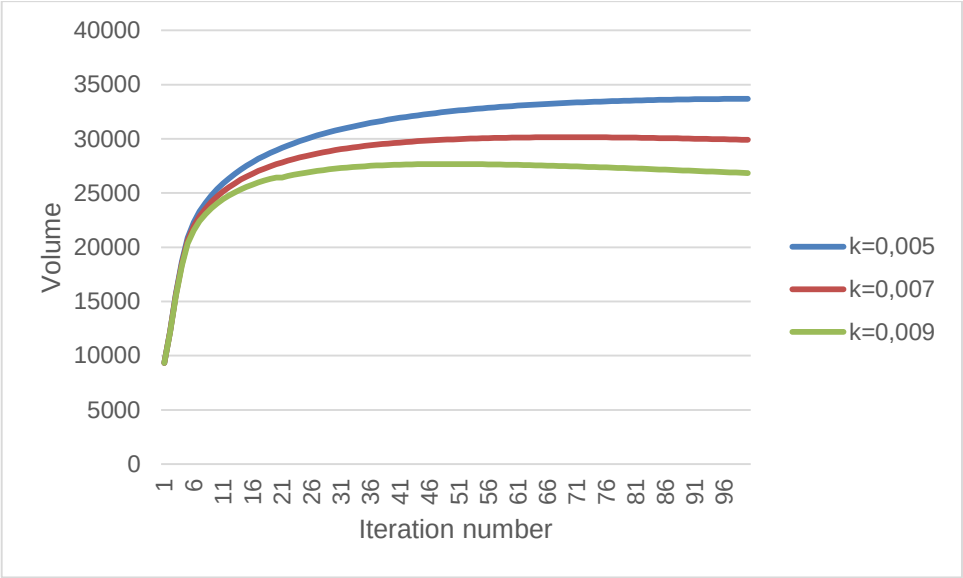

Figure 4.13 - Evolution of the volume of the bone mass, for all values of k and m=2 (TAA+AgilityTM prosthesis).

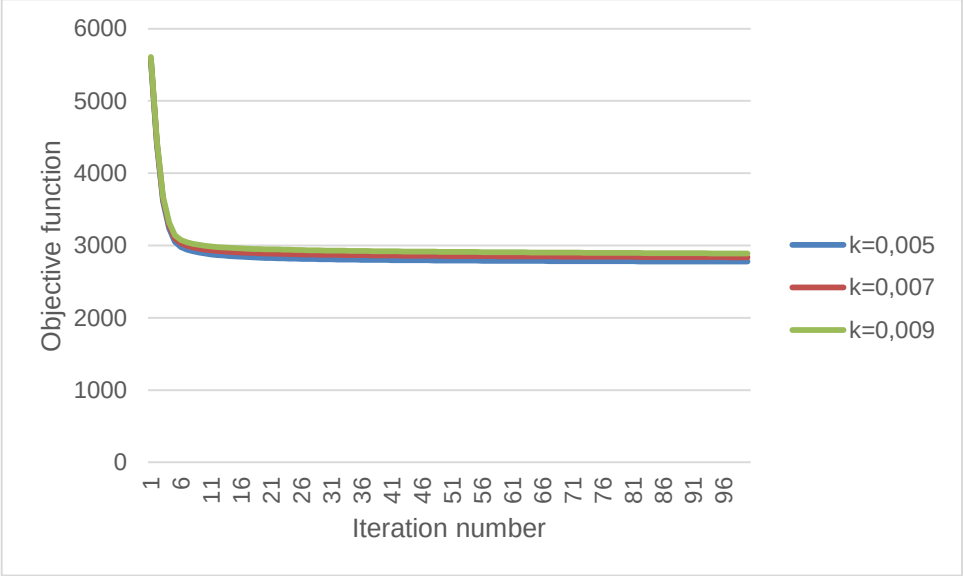

Figure 4.14 - Evolution of the objective function related with the bone mass, for all values of k and m=2 (TAA+Agility^{TM} prosthesis).

In the aforementioned graphics, for both values of *m*, it is possible to observe the decrease of the bone mass as the value of *k* increases. In figure 4.13, it is verified that the increase of the parameter *m* corresponds to an increase of the intermediate density regions, with the attenuation of some regions of minimum or maximum density. A higher value of *m* becomes less sharp the transition between the regions of higher and lower density, attenuating the formation of minimum density regions. In other words, the dichotomy of densities, 0 to 1, is decreased with a higher value of *m*, although not being destroyed. As it is possible to observe in the figures 4.10 and 4.13, the influence of the *m*-value on the bone mass volume is a bit uneven.

If different values of *m* (*m*=1 and *m*=2) are compared, for equal values of *k*, it is possible to observe that the behaviour of the evolution of the bone mass volume, during the iterative process, is very similar.

However, for *m*=1, at the beginning, the volume is about 30.000, stabilizing near the 50.000, and, for *m*=2, these values are inferior: the initial volume is about 10.000 and the stabilization occurs near the 35.000, at the hundredth iteration. The largest value of bone mass volume is observed for *k*=0,005 and *m*=1. The compliance resents itself from the volume differences but the changes observed are not substantial.

Finally, to achieve the optimal solution, the minimisation of compliance should happens. This minimisation allows the maximization of the overall structural stiffness and it is verified for all the values of *k* and *m*, in the above figures.

4.4.2. Initial condition: densities from the analysis of the intact bone (values obtained with Matlab® algorithm)

4.4.2.1. With *m*=1

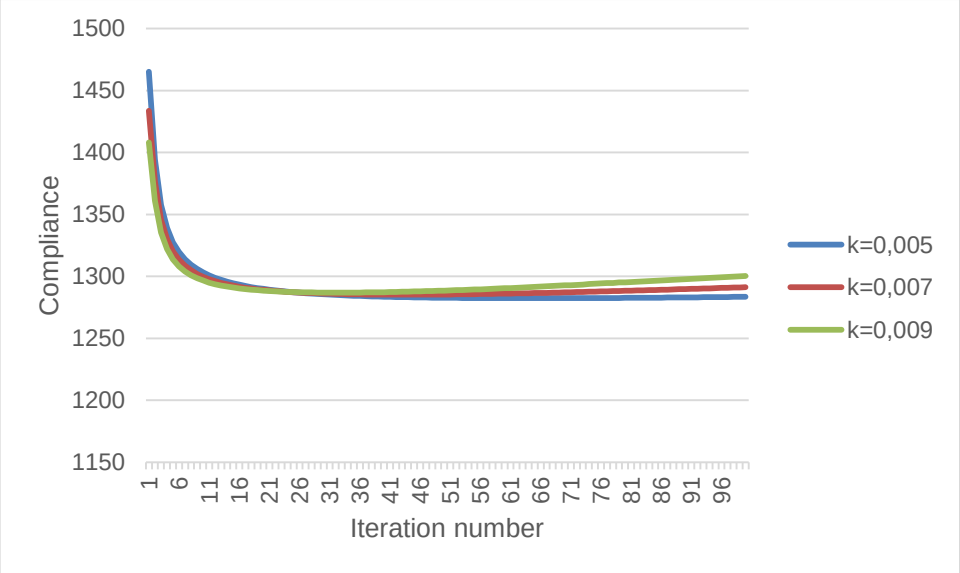

Figure 4.15 - Evolution of the compliance of the bone mass, for all values of k and m=1 (TAA+Agility™). Initial densities obtained from the analysis of the intact bone.

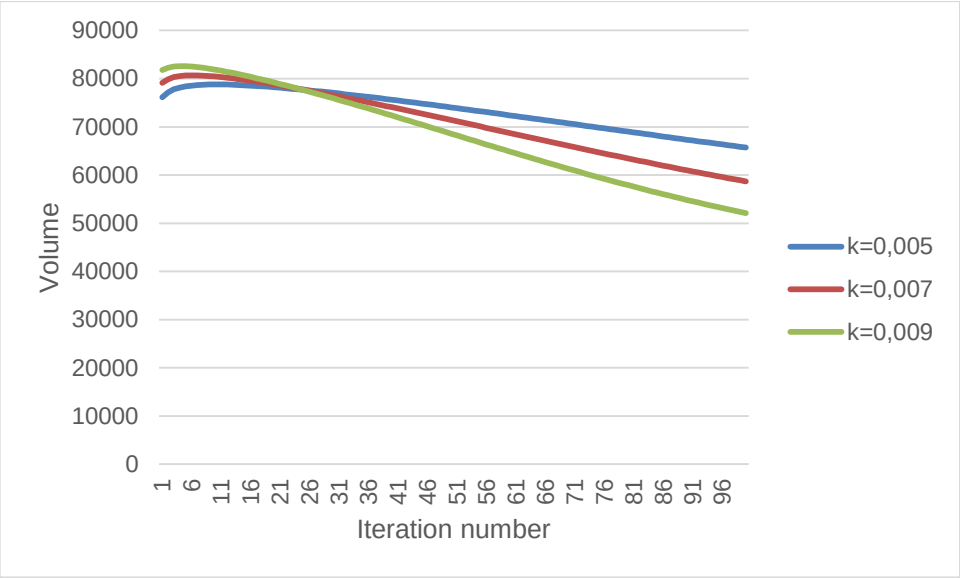

Figure 4.16 - Evolution of the volume of the bone mass, for all values of k and m=1 (TAA+Agility™). Initial densities obtained from the analysis of the intact bone.

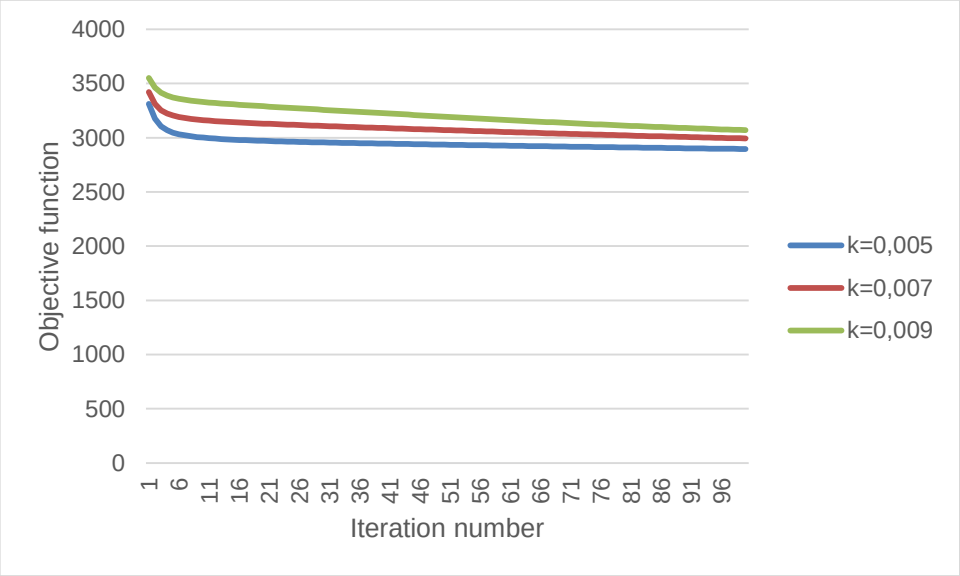

Figure 4.17 - Evolution of the objective function related with the bone mass, for all values of k and m=1 (TAA+Agility™). Initial densities obtained from the analysis of the intact bone.

4.4.2.2. With *m*=2

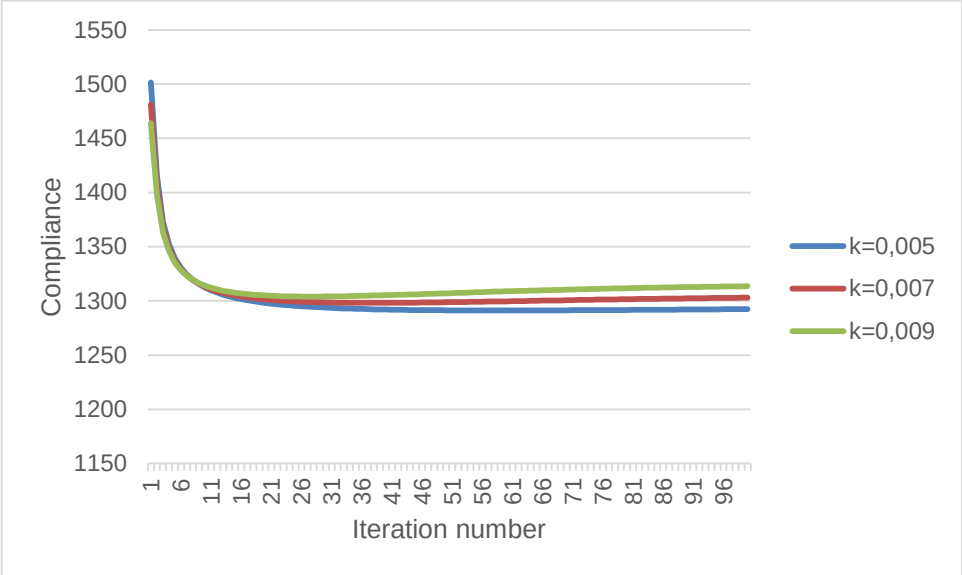

Figure 4.18 - Evolution of the compliance of the bone mass, for all values of k and m=2 (TAA+Agility™). Initial densities obtained from the analysis of the intact bone.

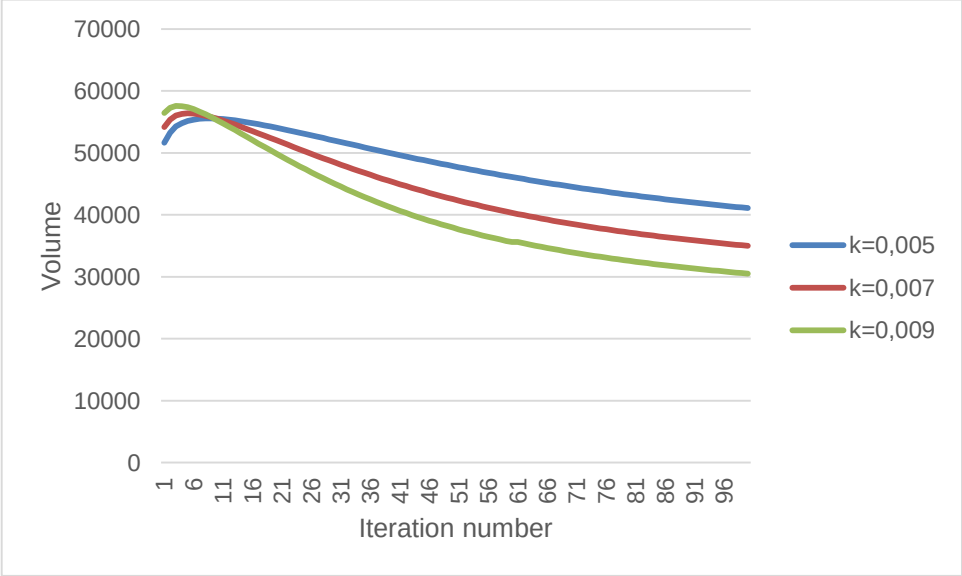

Figure 4.19 - Evolution of the volume of the bone mass, for all values of k and m=2 (TAA+Agility™). Initial densities obtained from the analysis of the intact bone.

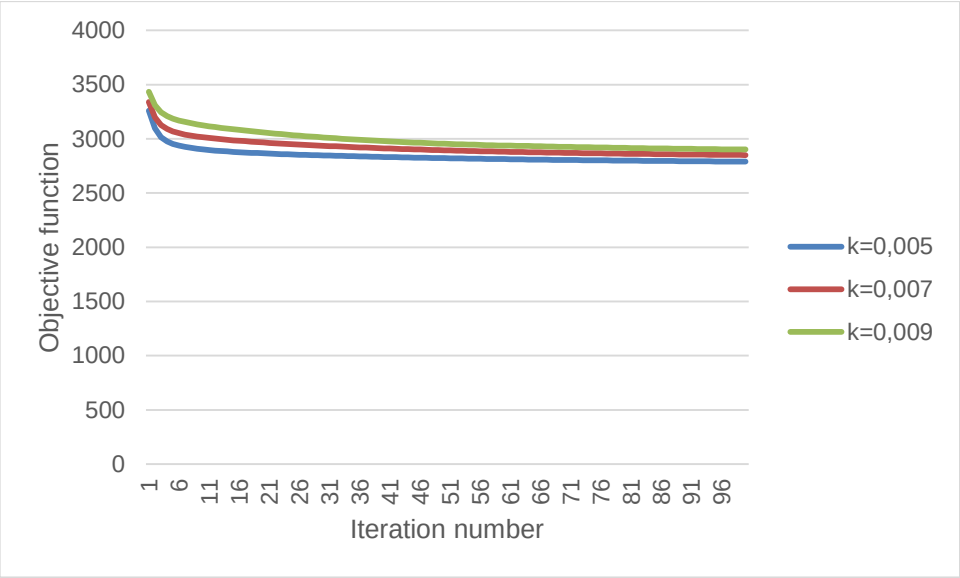

Figure 4.20 - Evolution of the objective function related with the bone mass, for all values of k and m=2 (TAA+Agility™). Initial densities obtained from the analysis of the intact bone.

Regarding the information about the *k* values and the minimization of the compliance, they are also verified in the present bone remodeling analysis, like it happened for the bone remodeling analysis in the previous subsection. This way, the main difference verified in the present case, when compared to the previous situations, where the initial conditions are different, is the behaviour of the evolution of the bone mass volume. In this case, the bone mass volume, contrarily of that it has been observed, reduces through the iterative process (through the time). This maybe can be explained due to the initial condition be the densities obtained from the solution of the bone remodeling analysis of the intact bone. This could be done thanks to a Matlab® algorithm, like it was explained before and is explained in the Annex A. It is also verified a difference between the bone mass volume values of the results obtained from the analysis with *m*=1 and *m*=2. For the first case, the bone mass volume is between 80.000 (at the beginning of the analysis) and 50.000 (ate the hundredth iteration). For the case with *m*=2, the bone mass volume is between 60.000 and 30.000. As it is possible to verify, there is a huge difference among them. The bone remodeling analysis, with *m*=1, originates solutions with more cortical bone than trabecular one, while the analysis with *m*=2 provide opposite solutions, with more trabecular bone than cortical one. This way, it is easy to understand the difference between values, since the cortical bone occupies more volume than the trabecular bone, due to the porosity of the latter.

5. Conclusions and future directions

5.1. Conclusions

The bone remodeling of the AJC was analysed, in this work, before and after the simulation of a TAA using two different prostheses, the Agility™ and S.T.A.R.™. The mentioned analysis was possible due to the use of the commercial software ABAQUS®, which was the tool that provide the FEM. However, to concretize the bone remodeling analysis, other software was used: the model of bone remodeling developed in IDMEC/IST, in doctoral thesis scope. In this work, the geometric modeling was not performed: the 3-D geometric models used (the intact AJC, and the Agility™ and S.T.A.R.™ prostheses) were recovered from the work developed by Daniela Rodrigues, in her Master Thesis [30]. Relatively to the 3-D intact AJC (which is constituted by the tibia, talus, fibula and calcaneus), she obtained it from a project, the VAKHUM project, and regarding to the models of both prostheses used, the Agility™ and S.T.A.R.™, she modelled them through the commercial software SolidWorks® (following the indications of DePuy Orthopaedics, Inc. and Small Bone Innovations, Inc. companies). However, to correctly simulate the TAA, she introduced, through the SolidWorks®, both prostheses in the intact AJC, doing the appropriate cuts, originating two different combined models: the TAA+ Agility™ and the TAA+ S.T.A.R.™. This way, the first stage of this work was the FEA, performed by ABAQUS®, in which were considered all the material properties, boundary conditions, loading conditions and interactions between parts, with the purpose of generate the appropriated mesh, with the adequate type and size of element. After that, the bone remodeling analysis was made, using different initial conditions (different values of the parameters *k* and *m*, uniform initial density, initial density obtained from the solution of the bone remodeling analysis in the intact bone, among others). This bone remodeling analysis was made just in two bones, the tibia and talus, before and after the realization of the TAA.

Relatively to the obtained results from the bone remodeling analysis (made for two specific bones, like it was mentioned before, the tibia and talus), it was verified a convergence to a solution that proved to be somewhat identical to the morphology of the talus and very identical to the morphology of the tibia, which allowed a good reproduction of the behaviour of the physiologic state of the bone, the real bone. In order to validate the bone remodeling models used for the simulation of the real tibia and talus, it was evaluated the bone remodeling process before the insertion of the prosthesis. This validation is very important to the correct analyse of the effects and consequences of the ankle prostheses on the four mentioned bones, that constitute the AJC. This way, one of the analyses made is the study of the clinical importance of the insertion of an ankle prosthesis into the AJC, on the bone remodeling process, considering as initial condition the final bone density distribution/values of the intact model of the AJC, after the colocation of the prosthesis. Due to that, it is possible to analyse/investigate the modifications arising from the insertion of the prosthesis.

According to what was mentioned in the last paragraph, one of the analyses performed is, in fact, the study of the modifications observed in the tibia and talus, during the bone remodeling process, after the occurrence of a TAA, using the widely mentioned prostheses, take into account the final density distributions of the two referred bones, in the intact model, as the initial density distribution (initial

condition) of them in the two combined models (the TAA+Agility™ and TAA+S.T.A.R.™). Below, it is possible to see the results obtained from the mentioned analysis:

- In the TAA+Agility™ model → decreasing in density in the medial area of the talus (under the talar component) → possibly derived from the stress shielding effect.
- In the TAA+S.T.A.R.™ model → decreasing of bone mass in distal tibia (its lateral area) and increasing in density above the two raised "cylinders" → possibly the explanation of stress shielding in nearest region of the two cylinders, due to existence of forces transmitted from them.
- In the TAA+S.T.A.R.™ model → Bone mass loss → lateral area under the talar component → possibly derived from the stress shielding effect.

The bone remodeling analysis also allows the influence study of the values of the parameters *k* and *m*. These influences studies are possible due to the evaluation of the behaviour of the compliance, volume and objective function, during the iterative process. Synthetically, it is possible to observe the decrease of the bone mass as the value of *k* increases, and for when the *m*-value increases, the intermediate density regions increases too. The compliance resents itself from the volume differences but the changes observed are not substantial and the optimal solution is achieved because the minimisation of compliance is verified, which allows the maximization of the overall structural stiffness and it is observed for all the values of *k* and *m*. Regarding to the bone mass volume, it increases when the initial condition is a uniform value of density, and decreases when the initial condition is composed by the density values obtained from the final bone density distribution/values of the intact model of the AJC. Finally, when the *m* is lower, the values of the bone mass volume are greater due to the fact of the solution contained more cortical bone than the trabecular one, which is very porous.

The bone remodeling model used is a good choice, according to the parameters selected before. Despite of not being, until recently, used in the AJC, it has been applied in investigations of other body joints: the shoulder, the spine, and more commonly, the hip.

It is possible to say that the obtained results demonstrate logic and agreement with the only study found in this area, although it considers the tibia and talus separately, contrarily of what is done in this work.

5.2. Problems and future directions

Below, a list of future guidelines, which are possible to be followed is presented. Some of them are suggested taking into account some limitations of the present work.

- Analysis of other total ankle prostheses, for instance the new designs existent on the market.
- Changing of the contact of the bone-prosthesis interface (with friction or frictionless) and study of the effect of this in the obtained results. Then, compare both results and discover which situation reveals more reliability.
- Promotion of the interest of some investigators in bone remodeling analysis of the AJC in humans. This way, it will allow the comparison between the bone remodeling results obtained

from the studied model and the real bone density of the humans. Thus, the validation of the bone density distributions obtained for the intact bones (the tibia and talus), through the bone remodeling model, is possible.

- The inclusion of force patterns derived from multibody simulations should be performed into the FE models with the purpose of examine the influence of the muscular forces in the bone remodeling analysis.
- The inclusion of a greater number of bones (from different subjects) to analyse the dependency of the bone remodeling results on bone geometry.
- The inclusion of the navicular bone in the models is important to better analyse the bone density distribution after a TAA due to the simulation of the contact forces originated at the anterior side of the talus.
- Establish different ways of modeling the ligaments (specially, for the area of the attachment sites for the ligaments into talus) to analyse their direct impact on the bone remodeling.
- Try to overcome the limitations that lead to the poor similarity between the solution obtained from the convergence model to the talus and the real morphology of this bone.
- Apply load conditions that reproduce with more reliability the real and complex situation, which should consider the entire, or at least a large part of the range of loads that characterize the stance phase of gait. This way, more real bone remodeling results will be achieved.
- To achieve more real bone remodeling results, different loading conditions should be considered for the three models under study, because in the real situation each model is characterized by a different set of loading conditions.

6. References

[1] van den Heuvel, A., Van Bouwel, S., and Dereymaeker, G., *Total ankle replacement. Design evolution and results.* Acta Orthop Belg, 2010. **76**(2): p. 150-61.

[2] *American Academy of Orthopaedic Surgeons* [cited 2014 June 8th]; Available from: http://orthoinfo.aaos.org/topic.cfm?topic=A00214.

[3] *PubMed Health Home*. [cited 2014 June 8th]; Available from: http://www.ncbi.nlm.nih.gov/pubmedhealth/PMH0002223.

[4] *WebMD®*. [cited 2014 June 8th]; Available from: http://www.webmd.com/osteoarthritis/guide/arthritis-basics.

[5] Ray, R.G., Christensen, J.C., and Gusman, D.N., *Critical evaluation of anterior drawer measurement methods in the ankle.* Clin Orthop Relat Res, 1997(334): p. 215-24.

[6] Fujii, T., Luo, Z.P., Kitaoka, H.B., and An, K.N., *The manual stress test may not be sufficient to differentiate ankle ligament injuries.* Clin Biomech (Bristol, Avon), 2000. **15**(8): p. 619-23.

[7] *American Academy of Orthopaedic Surgeons*. [cited 2014 July 26th]; Available from: http://orthoinfo.aaos.org/topic.cfm?topic=A00208.

[8] Netter, Frank H.. Atlas de Anatomia Humana. 2ª ed.. Porto Alegre: Artmed, 2000.

[9] Espinosa, N. and Klammer, G., *Treatment of ankle osteoarthritis: arthrodesis versus total ankle replacement.* European Journal of Trauma and Emergency Surgery, 2010. **36**(6): p. 525-535.

[10] *American Orthopaedic Foot & Ankle Society®*. [cited 2014 August 27th]; Available from: http://www.aofas.org/medical-community/health-policy/Documents/TAR_0809.pdf.

[11] Bouguecha, A., Weigel, N., Behrens, B-A., *et al. Numerical simulation of strain-adaptive bone remodelling in the ankle joint*. BioMedical Engineering Online, 2011. **10**(58): 13 pages.

[12] Jordan, R.W., Chahal, G.S., and Chapman, A. *Is End-Stage Ankle Arthrosis Best Managed with Total Ankle Replacement or Arthrodesis? A Systematic Review.* Advances in Orthopedics – Hindawi Publishing Corporation, 2014. 9 pages.

[13] Relvas, C., Fonseca, J., Amado, P., Castro, P., Ramos, A., Completo, A., and Simões, J., *Desenvolvimento de uma prótese do tornozelo: desafio projectual*, in *4º Congresso Nacional de Biomecânica*. 2001: Coimbra.

[14] Leardini, A., *Geometry and mechanics of the human ankle complex and ankle prosthesis design.* Clin Biomech (Bristol, Avon), 2001. **16**(8): p. 706-9.

[15] Procter, P. and Paul, J.P., *Ankle joint biomechanics.* J Biomech, 1982. **15**(9): p. 627-34.

[16] Stauffer, R.N., Chao, E.Y., and Brewster, R.C., *Force and motion analysis of the normal, diseased, and prosthetic ankle joint.* Clin Orthop Relat Res, 1977(127): p. 189-96.

[17] Gill, L.H., *Challenges in total ankle arthroplasty.* Foot Ankle Int, 2004. **25**(4): p. 195-207.

[18] Hintermann, B. and Valderrabano, V., *Total ankle replacement.* Foot Ankle Clin, 2003. **8**(2): p. 375-405.

[19] Vickerstaff, J.A., Miles, A.W., and Cunningham, J.L., *A brief history of total ankle replacement and a review of the current status.* Med Eng Phys, 2007. **29**(10): p. 1056-64.

[20] Feldman, M.H. and Rockwood, J., *Total ankle arthroplasty: a review of 11 current ankle implants.* Clin Podiatr Med Surg, 2004. **21**(3): p. 393-406, vii.

[21] Prendergast, P.J., *Finite element models in tissue mechanics and orthopaedic implant design.* Clin Biomech (Bristol, Avon), 1997. **12**(6): p. 343-366.

[22] Gill, L.H., *Challenges in total ankle arthroplasty.* Foot Ankle Int, 2004. **25**(4): p. 195-207.

[23] Fernandes, P., *Optimização da Topologia de Estruturas Tridimensionais - Ph.D. Thesis*. 1998, Instituto Superior Técnico: Lisbon.

[24] Fernandes, P. and Rodrigues, H., *A material optimization model for bone remodeling around cementless hip stems*, in *ECCM'99*. 1999.

[25] Fernandes, P., Rodrigues, H., and Jacobs, C., *A Model of Bone Adaptation Using a Global Optimisation Criterion Based on the Trajectorial Theory of Wolff.* Comput Methods Biomech Biomed Engin, 1999. **2**(2): p. 125-138.

[26] Fernandes, P.R., Guedes, J.M., and Rodrigues, H., *Topology Optimization of 3D Linear Elastic Structures.* Computers & Structures, 1999. **73**: p. 583-594.

[27] Folgado, J., *Modelos Computacionais para Análise e Projecto de Próteses Ortopédicas - Ph.D. Thesis*. 2004, Instituto Superior Técnico: Lisbon.

[28] Folgado, J., Fernandes, P.R., and Rodrigues, H., *Topology Optimization of Three-Dimensional Structures under Contact Conditions.* IDMEC-IST: Lisbon.

[29] Wolff, J., *The law of bone remodeling (Das Gesetz der Transformation der Knochen, Hirschwald, 1892).* Translated by Maquet, P., and Furlong, R., Springer, Berlin, 1986.

[30] Rodrigues, D., *Biomechanics of the Total Ankle Arthroplasty: Stress Analysis and Bone Remodeling*. 2013, Instituto Superior Técnico: Lisbon.

[31] Marieb, E.N. and Hoehn, K., *Anatomia e fisiologia* 3rd ed. 2009, Porto Alegre: Artmed.

[32] Michael, J.M., Golshani, A., Gargac, S., and Goswami, T., *Biomechanics of the ankle joint and clinical outcomes of total ankle replacement.* J Mech Behav Biomed Mater, 2008. **1**(4): p. 276-94.

[33] Leardini, A., O'Connor, J.J., Catani, F., and Giannini, S., *A geometric model of the human ankle joint.* J Biomech, 1999. **32**(6): p. 585-91.

[34] Hintermann, B., *Chapter 4 - Anatomic and Biomechanical characteristics of the Ankle Joint and Total Ankle Arthroplasty*, in *Total Ankle Arthroplasty - Historical overview, current concepts and future perspectives*. 2005, SpringerWienNewYork.

[35] Gill, L.H., *Challenges in total ankle arthroplasty.* Foot Ankle Int, 2004. **25**(4): p. 195-207.

[36] Gray, H., *Anatomy of the Human Body*. 2000, New York: Bartleby.com.

[37] Barnett, C.H. and Napier, J.R., *The axis of rotation at the ankle joint in man; its influence upon the form of the talus and the mobility of the fibula.* J Anat, 1952. **86**(1): p. 1-9.

[38] Golano, P., Vega, J., de Leeuw, P.A., Malagelada, F., Manzanares, M.C., Gotzens, V., and van Dijk, C.N., *Anatomy of the ankle ligaments: a pictorial essay.* Knee Surg Sports Traumatol Arthrosc, 2010. **18**(5): p. 557-69.

[39] Kannus, P. and Renstrom, P., *Treatment of ankle sprains in young athletes.* J Bone Joint Surg [Am], 1991. **73**: p. 305-312.

[40] Mink, J.H., *Ligaments of the ankle.* In: Deutsch, A.L., Mink, J.H., Kerr, R., (Editors), MRI of the foot and ankle. New York, NY: Raven, 1992: p. 173-197.

[41] Bartonicek, J., *Anatomy of the tibiofibular syndesmosis and its clinical relevance.* Surg Radiol Anat, 2003. **25**(5-6): p. 379-86.

[42] Boss, A.P. and Hintermann, B., *Anatomical study of the medial ankle ligament complex.* Foot Ankle Int, 2002. **23**(6): p. 547-53.

[43] Milner, C.E. and Soames, R.W., *Anatomy of the collateral ligaments of the human ankle joint.* Foot Ankle Int, 1998. **19**(11): p. 757-60.

[44] Pankovich, A.M. and Shivaram, M.S., *Anatomical basis of variability in injuries of the medial malleolus and the deltoid ligament. I. Anatomical studies.* Acta Orthop Scand, 1979. **50**(2): p. 217-23.

[45] Sarrafian, S.K., *Anatomy of the foot and ankle - Descriptive, Topographic, Functional*. 2nd ed. 1993, Philadelphia: Lippincott.

[46] Hall, S.J., *Basic Biomechanics*. 6th ed. 2012: McGraw-Hill.

[47] Mann, R.A., *Biomechanics of the foot.* In: in Atlas of Orthotics, American Academy of Orthopaedic Surgeons. C. V. Mosby Company, St. Louis, Missouri, 1985: p. 112–125.

[48] Schumacher, S.A. *Achilles Foot Health Centre*. [cited 2014 August 22th]; Available from: http://www.footdoc.ca/www.FootDoc.ca/Website%20Definitions%20(Basic%20Terms).htm.

[49] Sammarco, G.J. and Hockenbury, R.T., *Chapter 9 - Biomechanics of the Foot and Ankle*, in *Basic Biomechanics of the Musculoskeletal System*. Lippincott Williams & Wilkins.

[50] Bromfield, W., *Chirurgical observation and cases.* Cadell, London: Ed by Bromfield, W., 1773. **2**.

[51] Fick, R., *Spezielle Gelenk- und Muskelmechanik.* In: Bardeleben, K., (Editor), Handbuch der Anatomic und Mechanik der Gelenke. Jena: Fischer,, 1911. **2**(3).

[52] Lazarus, S.P., *Zur Morphologie des Fufiskelettes.* Morphol Jahrb, 1986. **24**(1).

[54] Reggiani, B., Leardini, A., Corazza, F., and Taylor, M., *Finite element analysis of a total ankle replacement during the stance phase of gait.* Journal of Biomechanics, 2006. **39**(8): p. 1435-1443.

[53] Cunningham, D.J., *Text-book of Anatomy.* 8th ed. 1943: Oxford University Press.

[54] Hicks, J.H., *The mechanics of the foot. I. The joints.* J Anat, 1953. **87**(4): p. 345-57.

[55] Kapandji, J.A., *Physiologie articulaire*. 4th ed. Paris: Maloine, S.A. Vol. 2. 1974. 140.

[56] Inman, V.T., *The joints of the ankle*. 1st ed. 1976, Baltimore: Williams & Wilkins.

[57] Sammarco, J., *Biomechanics of the ankle. I. Surface velocity and instant center of rotation in the sagittal plane.* Am J Sports Med, 1977. **5**(6): p. 231-4.

[58] Lundberg, A., Svensson, O.K., Nemeth, G., and Selvik, G., *The axis of rotation of the ankle joint.* J Bone Joint Surg Br, 1989. **71**(1): p. 94-9.

[59] Morrissy, R.T., *Dynamics of the Foot and Gait*. 3rd ed. In: Lovell and Winter's Pediatric Orthopedics. Vol. 1. 1990, Philadelphia.: Lippincott.

[60] Whittle, M., *Gait analysis an introduction*. 4th ed. 2007: Oxford Boston: Butterworth Heinemann.

[61] Perry, J., *Gait Analysis: Normal and Pathological Function.* SLACK incorporated., 1992.

[62] Nordin, M. and Frankel, V.H., *Basic Biomechanics of the Musculoskeletal System*. 3rd ed. 2001: Lippincott Williams & Wilkins.

[63] Komistek, R.D., Stiehl, J.B., Dennis, D.A., Paxson, R.D., and Soutas-Little, R.W., *Mathematical model of the lower extremity joint reaction forces using Kane's method of dynamics.* J Biomech, 1998. **31**(2): p. 185-9.

[64] Seireg, A. and Arvikar, *The prediction of muscular lad sharing and joint forces in the lower extremities during walking.* J Biomech, 1975. **8**(2): p. 89-102.

[65] Andriacchi, T.P., Andersson, G.B., Fermier, R.W., Stern, D., and Galante, J.O., *A study of lower-limb mechanics during stair-climbing.* J Bone Joint Surg Am, 1980. **62**(5): p. 749-57.

[66] Bassey, E.J., Littlewood, J.J., and Taylor, S.J., *Relations between compressive axial forces in an instrumented massive femoral implant, ground reaction forces, and integrated electromyographs from vastus lateralis during various 'osteogenic' exercises.* J Biomech, 1997. **30**(3): p. 213-23.

[67] Dennis, D.A., Komistek, R.D., and Mahfouz, M.R., *In vivo fluoroscopic analysis of fixed-bearing total knee replacements.* Clin Orthop Relat Res, 2003(410): p. 114-30.

[68] Lambert, K.L., *The weight-bearing function of the fibula. A strain gauge study.* J Bone Joint Surg Am, 1971. **53**(3): p. 507-13.

[69] Takebe, K., Nakagawa, A., Minami, H., Kanazawa, H., and Hirohata, K., *Role of the fibula in weight-bearing.* Clin Orthop Relat Res, 1984(184): p. 289-92.

[70] Wang, Q., Whittle, M., Cunningham, J., and Kenwright, J., *Fibula and its ligaments in load transmission and ankle joint stability.* Clin Orthop Relat Res, 1996(330): p. 261-70.

[71] Hintermann, B., *Chapter 5 - History of Total Ankle Arthroplasty*, in *Total Ankle Arthroplasty - Historical overview, current concepts and future perspectives*. 2005, SpringerWienNewYork.

[72] Bolton-Maggs, B.G., Sudlow, R.A., and Freeman, M.A., *Total ankle arthroplasty. A long-term review of the London Hospital experience.* J Bone Joint Surg Br, 1985. **67**(5): p. 785-90.

[73] Kitaoka, H.B. and Patzer, G.L., *Clinical results of the Mayo total ankle arthroplasty.* J Bone Joint Surg Am, 1996. **78**(11): p. 1658-64.

[74] Kitaoka, H.B., Patzer, H.L., and Ilstrup, D.M., *Clinical results of total ankle arthroplasty.* J Bone Jt Surg, 1994. **76**: p. 974-9.

[75] Lord, G. and Marotte, J.H., *[Total ankle replacement (author's transl)].* Rev Chir Orthop Reparatrice Appar Mot, 1980. **66**(8): p. 527-30.

[76] Thomas, R.H. and Daniels, T.R., *Ankle arthritis.* J Bone Joint Surg Am, 2003. **85-A**(5): p. 923-36.

[77] Gougoulias, N.E., Khanna, A., and Maffulli, N., *History and evolution in total ankle arthroplasty.* Br Med Bull, 2009. **89**: p. 111-51.

[78] Kofoed, H., *Scandinavian Total Ankle Replacement (STAR).* Clin Orthop Relat Res, 2004(424): p. 73-9.

[79] Cowin, S.C., *Bone Stress Adaptation Models.* ASME Journal of Biomechanical Engineering, 1993. **115**: p. 528-533.

[80] Rodrigues, D., *Biomechanics of the Total Ankle Arthroplasty: Stress Analysis and Bone Remodeling*. IST, 2013.

[81] Cracchiolo, A. and Deorio, J.K., *Design features of current total ankle replacements: implants and instrumentation.* J Am Acad Orthop Surg, 2008. **16**(9): p. 530-40.

[82] Hintermann, B., *Total Ankle Arthroplasty - Historical overview, current concepts and future perspectives*. SpringerWienNewYork.

[83] Gould, J.S., Alvine, F.G., Mann, R.A., Sanders, R.W., and Walling, A.K., *Total ankle replacement: a surgical discussion. Part I. Replacement systems, indications, and contraindications.* Am J Orthop (Belle Mead NJ), 2000. **29**(8): p. 604-9.

[84] Conti, S. and Miller, M., *Agility™ Ankle Component Design: Preventing Subsidence, A Finite Element Study*. Allegheny General Hospital: Pittsburgh, PA.

[85] *"Agility Ankle Surgical Technique" – DePuy Orthopaedics, Inc.* [cited 2014 August 27th]; Available from: http://www.depuy.com/healthcare-professionals/product-details/agility-lp-total-ankle-system.

[86] *"Agility Ankle Primary Revision" – DePuy Orthopaedics, Inc.* [cited 2014 August 27th]; Available from: http://www.depuy.com/healthcare-professionals/product-details/agility-lp-total-ankle-system.

[87] *DePuy Orthopaedics, Inc.* [cited 2014 May 28th]; Available from: http://www.depuy.com/healthcare-professionals/product-details/agility-lp-total-ankle-system.

[88] Kofoed, H., *Cylindrical cemented ankle arthroplasty: a prospective series with long-term follow-up.* Foot Ankle Int, 1995. **16**(8): p. 474-9.

[89] *"STAR Instruments Guide" – Small Bone Innovations, Inc.* [cited 2014 January 14th]; Available from: http://www.star-ankle.com/.

[90] Anderson, T., Montgomery, F., and Carlsson, A., *Uncemented STAR total ankle prostheses. Three to eight-year follow-up of fifty-one consecutive ankles.* J Bone Joint Surg Am, 2003. **85-A**(7): p. 1321-9.

[91] Park, J.S. and Mroczek, K.J., *Total ankle arthroplasty.* Bull NYU Hosp Jt Dis, 2011. **69**(1): p. 27-35.

[92] Hintermann, B., Valderrabano, V., Dereymaeker, G., and Dick, W., *The HINTEGRA ankle: rationale and short-term results of 122 consecutive ankles.* Clin Orthop Relat Res, 2004(424): p. 57-68.

[93] Rho, J.Y., Kuhn-Spearing, L., and Zioupos, P., *Mechanical properties and the hierarchical structure of bone.* Med Eng Phys, 1998. **20**(2): p. 92-102.

[94] Doblaré, M., García, J.M., and Gómez, M.J., *Modelling bone tissue fracture and healing: a review.* Engineering Fracture Mechanics 2004. **71**: p. 1809–1840.

[95] Landis, W.J., *The strength of a calcified tissue depends in part on the molecular structure and organization of its constituent mineral crystals in their organic matrix.* Bone, 1995. **16**(5): p. 533-44.

[96] Mehta, S.S., *Analysis of the mechanical properties of bone material using nondestructive ultrasound reflectometry - Ph.D. Thesis*. 1995, University of Texas Southwestern Medical Center: Dallas.

[97] Weiner, S. and Traub, W., *Bone structure: from angstroms to microns.* FASEB J, 1992. **6**(3): p. 879-85.

[98] Weiner, S. and Wagner, H.D., *The material bone: structure-mechanical function relations.* Ann Rev Mater Sci, 1998. **28**: p. 271-98.

[99] Tortora, G. and Derrickson, B., *Principles of Anatomy and Physiology* 13th ed. 2012: Wiley.

[100] Browner, B.D., Jupiter, Levine, and Trafton, *Skeletal Trauma – Basic science, Management and Reconstruction*. 2003: Elsevier Health Sciences.

[101] Frost, H.M., *Bone remodeling dynamics.* Springfield, I.L.: Charles C. Thomas, 1963.

[102] Ronald, R., *Modeling and remodeling in bone tissue - Thesis*. 2005, Technische Universiteit Eindhoven: Eindhoven.

[103] Adachi, T., Tsubota, K., Tomita, Y., and Hollister, S.J., *Trabecular surface remodeling simulation for cancellous bone using microstructural voxel finite element models.* J Biomech Eng, 2001. **123**(5): p. 403-9.

[104] Beaupre, G.S., Orr, T.E., and Carter, D.R., *An approach for time-dependent bone modeling and remodeling-application: a preliminary remodeling simulation.* J Orthop Res, 1990. **8**(5): p. 662-70.

[105] Cowin, S.C. and Hegedus, D.H., *Bone Remodeling I: theory of adaptive elasticity.* Journal of Elasticity, 1976. **6**(3): p. 313-326.

[106] Weinans, H., Huiskes, R., and Grootenboer, H.J., *Effects of material properties of femoral hip components on bone remodeling.* J Orthop Res, 1992. **10**(6): p. 845-53.

[107] Mullender, M.G. and Huiskes, R., *Proposal for the regulatory mechanism of Wolff's law.* J Orthop Res, 1995. **13**(4): p. 503-12.

[108] Quental, C., Folgado, J., Fernandes, P.R., and Monteiro, J., *Subject-specific bone remodelling of the scapula.* Comput Methods Biomech Biomed Engin, 2012.

[109] Guedes, J.M. and Kikuchi, N., *Preprocessing and postprocessing for materials based on the homogenization method with adaptive finite element methods.* Computer methods in applied mechanics and engineering (Elsevier Science Publishers) 1990. **83**: p. 143-198.

[110] Rodrigues, H., *A Mixed Variational Formulation for Shape Optimization of Solids with Contact Conditions.* Structural Optimization, 1993. **6**: p. 19-28.

[111] Jacobs, C.R., Levenston, M.E., Beaupre, G.S., Simo, J.C., and Carter, D.R., *Numerical instabilities in bone remodeling simulations: the advantages of a node-based finite element approach.* J Biomech, 1995. **28**(4): p. 449-59.

[112] Fernandes, P. and Rodrigues, H., *Optimization models in the simulation of the bone adaptation process.* "Computational Bioengineering Current trends and applications", Cerrola, M., Dobalré, M., Martínez, G., Calvo, B., Imperial college press, 2004.

[113] Robalo, T., *Analysis of bone remodeling in the tibia after total knee prosthesis - Master Thesis*. 2011, Instituto Superior Técnico: Lisbon.

[114] Fernandes, P.R., Folgado, J., Jacobs, C., and Pellegrini, V., *A contact model with ingrowth control for bone remodelling around cementless stems.* J Biomech, 2002. **35**(2): p. 167-76.

[115] Fernandes, P.R., Folgado, J., Jacobs, C., Pellegrini, V., and Rodrigues, H., *Numerical analysis on bone remodeling and bone ingrowth in cementless total hip arthroplasty*, in *International Congress on Computational Bioengineering*. 2003.

[116] Luenberger, D.G., *Linear and Nonlinear Programming*. 2nd ed. 1989: Addison-Wesley Publishing Company.

[117] Corazza, F., O'Connor, J.J., Leardini, A., and Parenti Castelli, V., *Ligament fibre recruitment and forces for the anterior drawer test at the human ankle joint.* J Biomech, 2003. **36**(3): p. 363-72.

[118] Pankovich, A.M. and Shivaram, M.S., *Anatomical basis of variability in injuries of the medial malleolus and the deltoid ligament. I. Anatomical studies.* Acta Orthop Scand, 1979. **50**(2): p. 217-23.

[119] Cowin, S.C., *Bone Mechanics*. 1989: Boca Raton, Florida: CRC Press, Inc.

[120] Cowin, C.S., *The mechanical properties of cortical bone tissue.* In: Cowin, C.S. (Ed.), Bone Mechanics, CRC, Florida, 1991.

[121] Yamada, H., *Strength of Biological Materials.* Williams and Wilkins, Baltimore, 1970.

[122] Jensen, N.C., Hvid, I., and Kroner, K., *Strength pattern of cancellous bone at the ankle joint.* Eng Med, 1988. **17**(2): p. 71-6.

[123] Athanasiou, K.A., Liu, G.T., Lavery, L.A., Lanctot, D.R., and Schenck, R.C., Jr., *Biomechanical topography of human articular cartilage in the first metatarsophalangeal joint.* Clin Orthop Relat Res, 1998(348): p. 269-81.

[124] Serway, R.A. *Física*. 1992.

[125] *Abaqus - Theory Manual, Version 6.10.* [cited 2014 June 15th]; Available from: https://www.sharcnet.ca/Software/Abaqus610/Documentation/docs/v6.10/books/stm/default.htm.

[126] Completo, A., Rego, A., Fonseca, F., and Simões, J.A., *Modelo numérico e experimental da tíbia intacta e com componente tibial da prótese do joelho*. Universidade de Aveiro.

[127] Viceconti, M., Bellingeri, L., Cristofolini, L., and Toni, A., *A comparative study on different methods of automatic mesh generation of human femurs.* Med Eng Phys, 1998. **20**(1): p. 1-10.

[128] [cited 2014 November 25th]; Available from: http://pubs.rsna.org/doi/full/10.1148/rg.235035059.

[129] [cited 2014 November 25th]; Available from: http://www.podiatrytoday.com/managing-osteolysis-following-failed-ankle-implant.

Annex A

Algorithm for transition of the tibia and talus' densities from the intact model to the TAA+Agility™ and TAA+S.T.A.R.™

This algorithm was developed in Matllab® and starts by the analysis of the initial mesh, with corresponds to the intact bone mesh. It reads the nodes of the initial mesh, saving their data (the densities values and spatial coordinates of each node). Then, it repeats the process but for the final mesh, which corresponds to the mesh of the bone where the prosthesis were introduced, saving the spatial coordinates of its nodes. After that, the algorithm runs through every nodes of the final mesh, the one that it is desirable to transit the densities, and determines what are the closest nodes, in spatial terms, of the intact bone mesh (initial). After this determination, the algorithm operates in two possible ways, according to what it founds:

- Just one node found: it is called the closest node and its density is attributed to the corresponding final mesh node;
- More than one nodes found (initial mesh) at minimum distance of the node from the final mesh: the algorithm performs the weighted average of densities of the initial mesh nodes and gives its value to the node of the final mesh.